THESIS FOR THE DEGREE OF DOCTOR OF PHILOSOPHY (PHD)

Molecular background of acquired resistance of *BRAF^{V600E}* mutated human melanoma

by Vikas Patel

Supervisor: Prof. Dr. Margit Balazs, PHD, DSc

UNIVERSITY OF DEBRECEN

DOCTORAL SCHOOL OF HEALTH SCIENCES

DEBRECEN, 2022

TABLE OF CONTENT

TABLE OF CONTENT

Abbreviations

AKT: v-akt murine thymoma viral oncogene homolog

BRAF: v-raf murine sarcoma viral oncogene homolog B1

BRAFi: BRAF inhibitor

$BRAF^{mut}$: primary melanoma tumours harbouring BRAF mutation

$BRAF^{WT}$: primary melanoma tumours without BRAF mutation which also includes tumours with NRAS mutation

CCND1: cyclin D1

CDK: cyclin dependent kinase

CDKN2A: cyclin dependent kinase inhibitor 2A

COT/ MAP3K8: mitogen activated protein kinase kinase kinase 8

CSD: chronically sun-damaged

DMSO: dimethyl sulfoxide

ECM: extracellular matrix

EDTA: ethylenediaminetetraacetic acid

EGF/MAPK: Mitogen-activated protein kinase pathway

EGFR: epidermal growth factor receptor

ERK1-2: mitogen activated protein kinase 1-2

FBS: fetal bovine serum

FDA: US Food and Drug Administration

FDR: false discovery rate

GAPDH: glyceraldehyde 3-phosphate dehydrogenase

GF: growth factor

HRAS: v-Ha-ras Harvey rat sarcoma viral oncogene homolog

IGF: Insulin-like Growth Factor pathway

IGF-1R: insulin-like growth factor 1 receptor

IL-2: interleukin-2

KIT: v-kit Hardy-Zuckerman 4 feline sarcoma viral oncogene homolog

LOXL1: lysyl oxidase like 1

MAPK: mitogen-activated protein kinase

ABBREVIATIONS

MEK1-2: mitogen-activated protein kinase kinase 1-2

MEKi: MEK inhibitor

MITF: microphthalmia-associated transcription factor5

MM: malignant melanoma

mTOR: mechanistic target of rapamycin

nd: no data available

NF1: neurofibromin 1

NRAS: neuroblastoma RAS viral (v-ras) oncogene homolog

$NRAS^{mt}$: primary melanoma tumours harbouring NRAS mutation

OPN/SPP1: osteopontin/ secreted phosphoprotein 1

PBS: phosphate buffered saline

PERK/EIF2AK3: eukaryotic translation initiation factor 2 alpha kinase 3

PI3K: phosphatidylinositol 3-kinase

PTEN: phosphatase and tensin homolog

qRT-PCR: quantitative reverse-transcription polymerase chain reaction

RAF: v-raf murine sarcoma 3611 viral oncogene homolog (ARAF), vraf murine sarcoma viral oncogene homolog B1 (BRAF), v-raf-1

RGP: radial growth phase

RIN: RNA integrity number

RIPA: Radio-Immunoprecipitation Assay

RT: room temperature

RTKs: receptor tyrosine kinases

SAMD11: sterile alpha motif domain containing 11

SD: standard deviation

UV: ultraviolet

UVA and UVB: ultraviolet A and B

WHO: World Health Organization

WST-1: water soluble tetrazolium (salt)-1

WT: wild type

Introduction

Malignant melanoma of the skin is potentially the most serious type of skin cancer for both men and women, with an ever-increasing global occurrence [1]. Although it only accounts for 1% of all skin cancers, it is responsible for the great majority of skin cancer-related deaths. The GLOBOCAN 2020 report estimates 324,635 new melanoma cases with 57,043 deaths worldwide in 2020, produced reported by the International Agency for Research on Cancer [2]. In 2020, Australia and New Zealand had the highest incidence rates (Table 1).

Table 1. Estimated melanoma of the skin incidence and mortality rates, standardized by all ages (World) in 2020

	Males		Females	
Populations	Incidence*	Mortality*	Incidence*	Mortality*
Australia and New Zealand	41.6	3.7	30.5	1.9
Western Europe	19.4	1.9	18.9	1.2
Northern America	18.5	1.5	14.3	0.75
Northern Europe	17.4	2.4	18.4	1.4
Southern Europe	9.2	1.8	8.9	0.98
Central and Eastern Europe	5.7	2.1	5.6	1.4
Southern Africa	4.1	1.3	2.8	0.72
Polynesia	3.9	1.2	3.6	0.29
World	3.8	0.7	3	0.45
South America	3.1	1	2.7	0.61

**ASR (World) per 100 000, Source: https://gco.iarc.fr/today*

The rates of incidence differ between European nations. The greatest rates have been seen in northern and western Europe, while the lowest rates have been observed in the Mediterranean and eastern sections of the continent (Figure 1).

In men, melanoma mainly occurs on the back, while in women it is most common on the legs. The individual risk of emerging melanoma increases with fair skin, blond or red hair, blue eyes, a greater number of nevi, and freckles phenotypes [3]. Additionally, emerging evidence suggests that excessive ultraviolet-B (UVB) radiation exposure during childhood, particularly sunburns, is linked to an increased risk of developing melanoma [4]. Furthermore, the accumulation of

genetic and epigenetic alteration promotes uncontrolled cell proliferation, and escape of melanoma cells from programmed cell death in response to DNA damage that leads to melanoma [5]. In addition to this, a series of gene mutations in mitogen-activated protein kinase (MAPK) signalling molecules, results in constitutive activation of the MAPK pathway leading to uncontrolled cell proliferation [6].

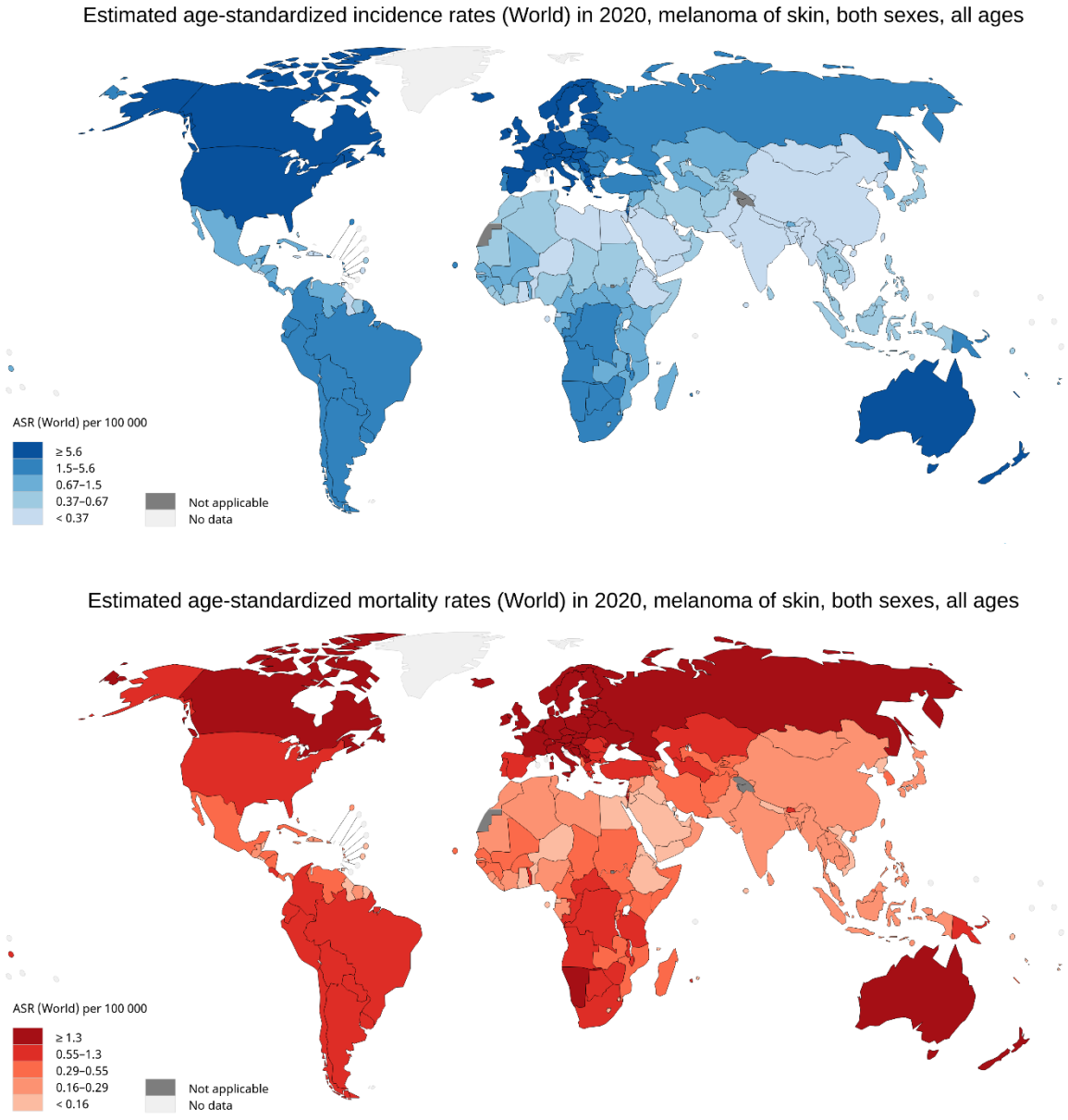

Figure 1. Estimated skin melanoma incidence and mortality rates worldwide by age group. *Data source: GLOBOCAN 2020, Graph production: IARC, World Health Organization (http://gco.iarc.fr/today).*

A number of therapies for advanced stage melanoma have been approved over the last decade by the Food and Drug Administration (FDA). The treatment options were determined based on the location of the lesions, stage, and genetic profile of the tumours. The treatment options may include the following parameters: surgical resection, radiation, chemotherapy, photodynamic therapy (PDT), targeted therapy, or immunotherapy alone or in combination. However, surgical treatment is still the primary clinical option for melanoma patients with stages I-IIIB [7,8].

The most common genetic alterations in malignant melanoma include the activating mutations in the *BRAF* oncogene, 45-60% of patients tumours carry mutations within this gene [9]. *BRAF* mutations are one of the most effective therapeutic targets for advanced stage and metastatic melanoma [10]. The most promising treatment strategy for metastatic and unresectable *BRAF*-mutated melanomas is the use of BRAF inhibitors (vemurafenib, dabrafenib, encorafenib etc.), either alone or in combination with MEK inhibitors (cobimetinib, trametinib, binimetinib etc.) [11]. Other effective therapeutic options include immune checkpoint blockade therapies such as anti-PD-1, anti-PD-L1 and anti-CTLA-4, either alone or in combination [12]. With these breakthroughs therapeutic treatment options, patients with metastatic melanoma have experienced increased median overall survival from 9 months to more than 2 years, and in some instances, have achieved long-term remission or complete response [13,14].

Despite several clinical advancements, the durability of the therapy response is a major obstacle because the development of acquired drug resistance. A hallmark of melanoma that results from acquired resistance is metastatic spread in distant organs such as the lungs, brain, bones and liver [15,16]. Because of the resistance to the initial treatment and the aggressive metastatic ability of melanoma, this disease is frequently linked with a high mortality rate. This emphasizes the need of early detection and precise diagnosis in determining the course of the disease. Therefore, a molecular understanding of drug resistance is also necessary to ensure success in the long-term survival of patients.

The major aim of this work was to develop the first three-dimensional, reproducible melanoma spheroid models using melanoma cell lines with $BRAF^{V600E}$ mutation that are sensitive and resistant to BRAF inhibitor (PLX4720 a vemurafenib analogue) and to compare the gene expression profiles of melanoma cell lines cultured under various conditions (2D and 3D) in both sensitive and resistant model systems. In addition, our study was extended by generating a panel of BRAF and MEK inhibitor resistant cell lines during combination treatment with

encorafenib (Braftovi™) plus binimetinib (Mektovi®) - (selective BRAF and MEK inhibitors, respectively), to discover alterations associated with the acquired resistance in melanoma. We compared phenotypic changes, cell proliferation, invasive potential, drug holiday effect, genomic (RNA-seq) and proteomic (proteome profiler) changes in the drug resistant and sensitive cell line models.

Molecular background of malignant melanoma

Among all tumour types, malignant melanoma is characterized by the highest mutational burden [17]. The disease is triggered by both hereditary and environmental factors (UV radiation). Melanoma development is primarily due to sporadic-, rather than inherited mutations [18]. Approximately 10% of primary melanoma cases are familial and the *CDKN2A* tumour suppressor gene is the most commonly altered gene in familial cancers [19]. Contrary to this, among all tumour types, cutaneous melanomas are characterized by a high level of somatic mutation mainly caused by exposure to ultraviolet radiation (Figure 2) [20,21].

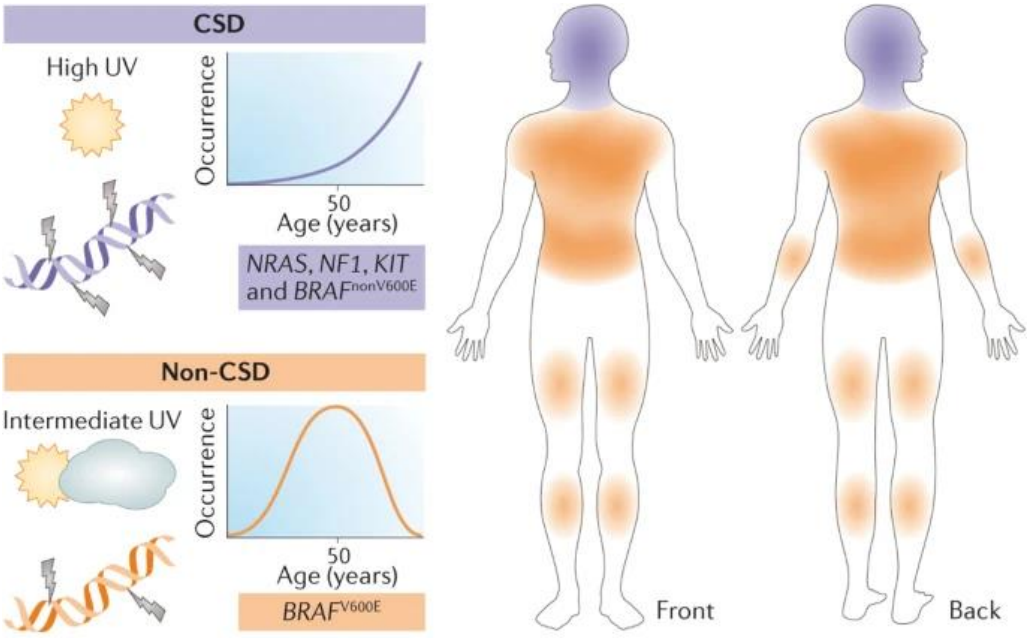

***Figure 2**. **A schematic illustration of classic UVR skin exposure and associated mutations.** Chronically sun damaged (CSD) melanomas have a greater mutations (NRAS, NF1, KIT and $BRAF^{nonV600E}$) and late age of onset. These melanomas are most common in parts of the body with the most sun exposure, such as the back and neck. In contrast, non-CSD melanomas occur earlier in life, have anatomical regions with intermediate degrees of sun exposure, are more likely to be linked with naevi, and may have lower mutation loads ($BRAF^{V600E}$). Adopted from Shain and Bastian [22].*

Using high throughput molecular technologies and bioinformatics analyses, a large amount of melanoma tissue samples has been analysed and classified into four subgroups according to activating gene mutations [23], including *BRAF*- (~50%); *N-Ras*, *K-Ras*, and *H-Ras*- (~25%); *NF1*-mutant melanomas (~15%), and triple-wild-type melanomas (~10%) [23]. Additionally, copy number alterations including amplifications of the *KIT*, *MITF*, *CCND1*, and *CDK4* genes, and deletions of the *PTEN* and *CDKN2A* tumour suppressor genes are characteristic for the triple-wild-type tumours [24,25]. Other genetic alterations include activating mutation of the promoter region of the *TERT* gene (30-80%) [26,27]. UV exposure induced molecular signatures are less likely to be found in the most commonly altered oncogenes including *BRAF* and *NRAS*, but UV molecular signatures are more likely to be associated with the alterations of tumour-suppressor genes which play important role in melanoma progression, such as *CDKN2A* and *TP53* [28]. In addition, numerous tumour suppressor genes, including *NF1*, *PTEN*, and *ARID2*, are commonly mutated in melanoma [23,29]. A study led by Wang et al. discovered 10 distinct prognostic gene signatures using a systematic bioinformatics study of the tumour microenvironment. These include *IL15*, *APOBEC3G*, *CCL8*, *GBP4*, *CLIC2*, *RARRES3*, *SAMD9L*, *IGHV1-18*, *TLR2*, and *HLA.DQB1* [30].

Signalling pathways and cell cycle regulation in melanoma

Melanoma is characterised by a high genomic heterogeneity [31]. Development of the disease is dependent on the abnormal proliferation of melanocytes, which is accomplished through constant signalling pathways that regulate the cell cycle and other events within the cells. A number of molecular signalling pathways and the complexity of their interactions are associated with disease development and cancer progression. These characteristics suggest that no single molecular alteration plays a crucial role in these processes, rather, multiple changes combined into a specific clinical and biological outcome are responsible for the development and progression of the tumours. Several signalling pathways, involving tumour suppressor genes (e.g. *PTEN*: phosphatase and tensin homolog), and oncogenes (e.g. *BRAF*, *NRAS*, *MITF* (microphthalmia-associated transcription factor), *cKIT*, *cMET*, *CCND1* or *EGFR*)) have been identified as a key regulator in melanoma progression by somatic mutations, copy number variation and expression changes including the epigenetic events of the different pathway

members [32,33]. Several biological signalling pathways are deregulated in melanoma cell including MAPK/ERK, PI3K/AKT, and CDKN2A (Figure 3) [34].

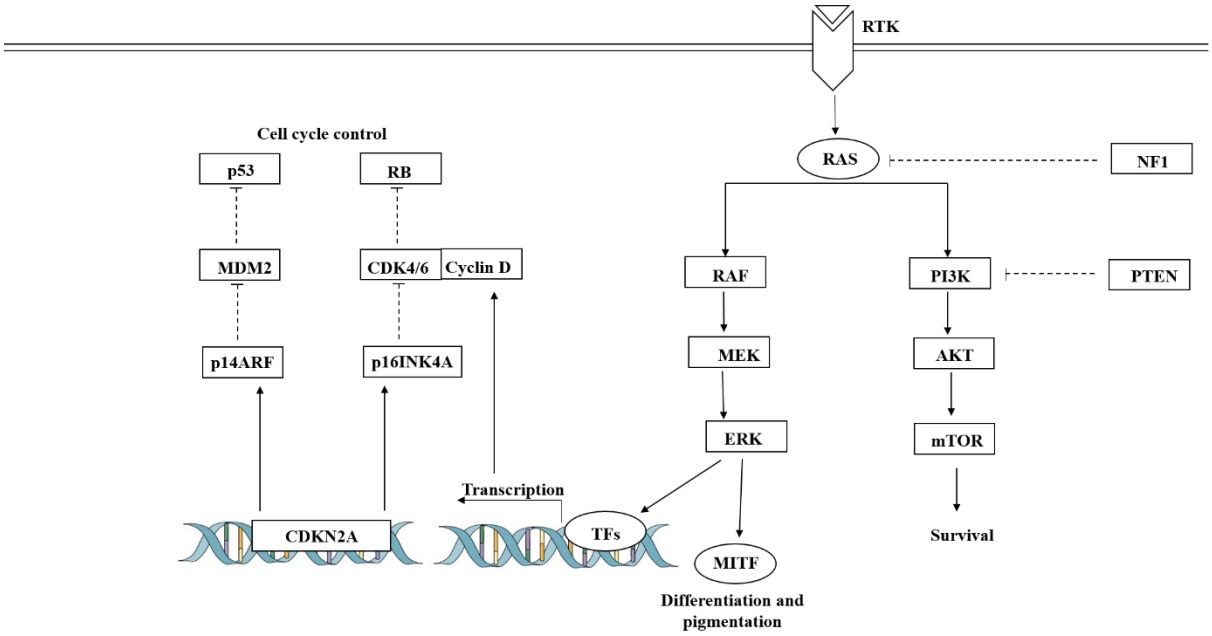

Figure 3. Deregulated signalling pathways in melanoma. *The diagram describes some of the major signalling pathways that are aberrant in melanoma and regulate growth, proliferation, and survival. Melanoma progression is accompanied by changes in components of the MAPK/ERK, PI3K/AKT, CDKN2A and p53 pathways, and the most common mutations include BRAF, NRAS, or NF1 genes. MITF, a lineage-specific oncogene, is expressed aberrantly in subsets of melanomas.*

MAPK/ERK pathway

Malignant cells emerge as a result of alterations in key signalling pathways [35]. Melanoma cell proliferation signalling is primarily mediated by MAPK pathway (Ras/Raf/MEK/ERK), which is over-activated in roughly 80–90% of cases (Figure 4). Additionally, this signalling pathway has been shown to contribute to melanoma progression such as growth, angiogenesis, invasion, and resistance to therapy [36]. Oncogenes responsible for the constant activation of MAPK pathway include *BRAF* - (40-60%) and *NRAS* - (15-30%) and *KIT* oncogenes (2–5%) [32,37]. The majority of *BRAF* mutations occur at the V600E position (Val600Glu), while in the *RAS* gene, the majority of mutations are associated with the replacement of glutamine at position 61 ($NRAS^{Q61}$) for an arginine, lysine, or leucine (Q61R/K/L), although it may also affect *HRAS* and *KRAS* [38].

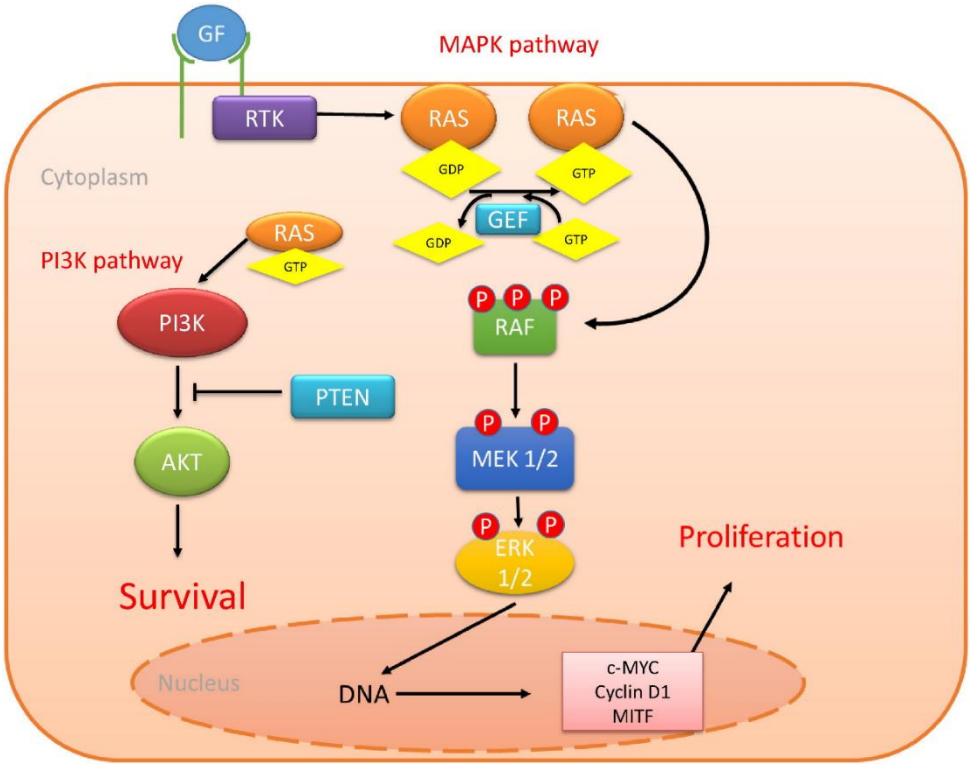

Figure 4. Schematic illustration of cellular events during MAPK signalling in melanoma. *The activation of RTKs can lead to MAPK activation by state transition of RAS from a GDP to GTP state. The active RAS phosphorylates and activates RAF, which subsequently phosphorylates and activates MEK1/2, and then ERK1/2, regulating several transcription factors in the nucleus. Adapted from Jasmina P et al. [39].*

Likely, to *RAF* and *RAS* gene mutations, *NF1* harbour loss of function mutation results in the loss of tumour suppressor activity of the gene [40,41]. Altogether, mutations in the *BRAF*, *RAS*, or *NF1* genes activate the MAPK pathway, causing in increased proliferation of cells [42]. However, it also suggests that without additional driving mutations, oncogenic *BRAF* or *NRAS* acts as initiator alterations but not enough to cause other events for melanomagenesis [43,44].

Most of the benign naevi harbour intact tumour-suppressive mechanisms to maintain a healthy proliferation rate. Moreover, oncogenic *BRAF* or *NRAS* expression causes oncogene-induced senescence (OIS) through tumour-suppressor signalling pathways such as $p16^{INK4a}$ and *p53*, which suppresses tumorigenesis and prevents neoplastic cell growth [45]. A cascade of serine/threonine protein kinases, known as the MAPK/ERK pathway, functions within the context of extracellular mitogenic stimuli and transcriptional programming in order to induce downstream signalling. The MAPK/ERK pathway is activated by receptor tyrosine kinases (RTKs), such as *EGFR* and *c-Kit*. In addition, *KIT* is frequently mutated/amplified in triple-WT

melanomas. Several sequential events trigger the MAPK pathway, such as the *RAS* phosphorylating *RAF* kinase, which subsequently phosphorylates and activates *MEK1/2*, which phosphorylates and nuclear translocate *ERK1/2*, resulting in cell cycle progression and growth. Further, MAPK/ERK- and PI3K/AKT pathways can potentially be stimulated by GTP-bound *RAS*.

PI3K/AKT pathway

Similarly to MAPK pathways, cell survival and proliferation are also regulated by the PI3K/AKT signalling pathway, which is functionally deregulated in about 55% of melanoma cases mainly because of *AKT3* amplification or loss of *PTEN* (tumour suppressor) [46]. A number of studies have revealed loss of function mutation in the *PTEN* gene in several types of tumour including melanoma [47]. Specifically, melanoma characterized by *BRAF* mutants typically exhibit *PTEN* loss while melanoma characterized by *BRAF* wild-type frequently exhibits *AKT3* amplification. Tyrosine kinases (RTKs) or other growth receptors activate PI3K signalling at the plasma membrane, which causes *PIP2* (phosphatidylinositol 4,5 bisphosphate) to be converted into *PIP3* phosphatidylinositol (3,4,5)-trisphosphate, a secondary messenger lipid resulting stimulation and activation *AKT* Ser/Thr kinases (Figure 5).

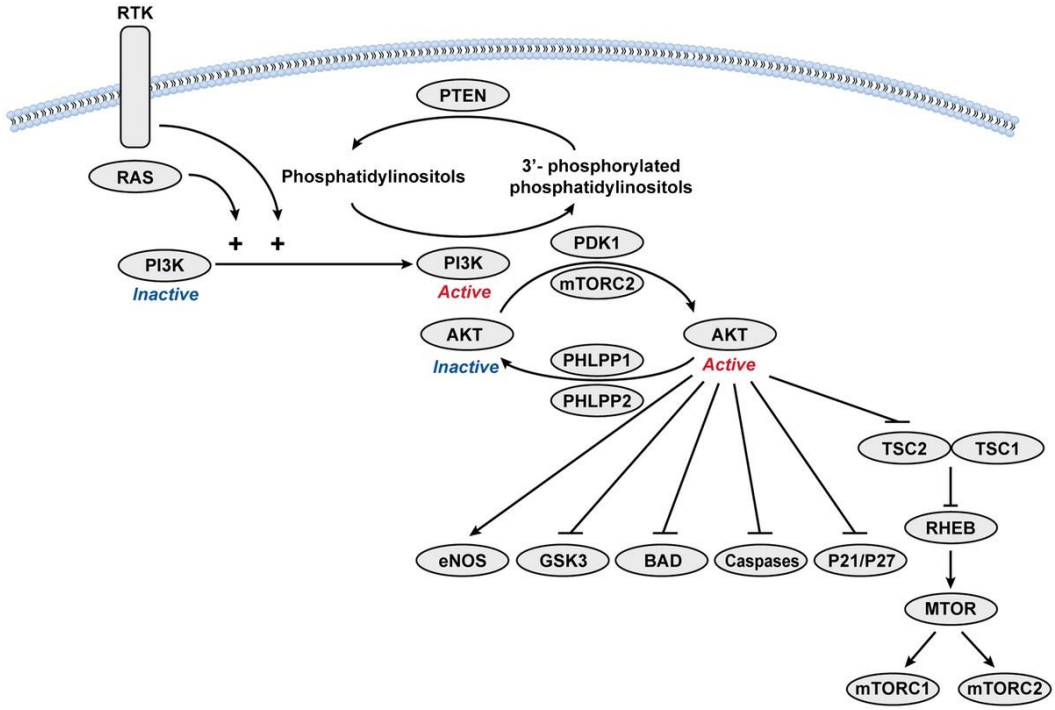

Figure 5. The PI3K/Akt/mTOR pathway. *Potential key activators, regulators, and effectors of the PI3K-AKT signalling network in melanoma. Adapted from Davies MA [46].*

AKT3 is the most prevalent isoform involved in melanoma progression by suppressing apoptosis [48]. In melanogenesis, loss of *PTEN* results in dephosphorylation of *PIP3*, preventing constitutive activation of PI3K signalling, which is also associated with $BRAF^{V600E}$ mutations [46]. Through suppression of *TSC1–TSC2*, *AKT* stimulates both protein synthesis and cell proliferation by activating *mTORC1*. Translation machinery involved in *mTORC1* is required for translation initiation and elongation.

Cell cycle

About 70% of melanomas show abnormalities in a component of the cell cycle, such as *CDKN2A/CDK4/RB*, which control the cell cycle [23]. This is usually what happens when melanoma progresses. *CDKN2A* gene plays a central role in the regulation of the cell cycle, containing two distinct proteins ($p16^{INK4A}$ and $p14^{ARF}$). The *CDKN2A* gene is altered frequently in about 60 % of sporadic and around 40 % of familial melanoma cases. The *CDK* (cyclin-dependent kinase) inhibitor $p16^{INK4a}$ inhibits *cyclin D-CDK4/6* complexes which regulate the G1-to-S phase transition in cooperation with *E2F* transcription factors (Figure 6).

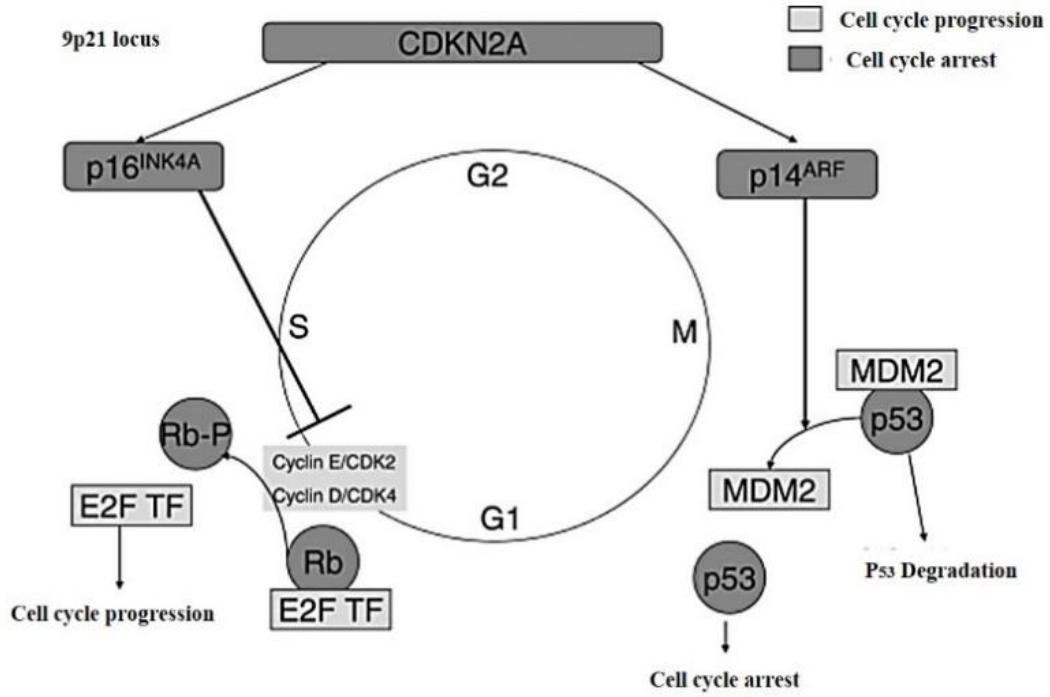

Figure 6. Cell cycle regulation by the Rb and p53 pathway. *The CDK2NA gene codes for the proteins p16 and p14. p16 prevents cyclins from phosphorylating Rb. Phosphorylated Rb is unable to bind to and inhibit the E2F transcription factor. MDM2 is regulated by p14. When p14 binds to MDM2, it cannot bind and negatively regulate p53. Adapted from Kudchadkar R [49].*

Families predisposed to melanoma have also identified with germ-line gene mutations in *CDK4*. This mutation renders *CDK4* insensitive to $p16^{INK4a}$ inhibition due to a disruption of the function of $p16^{INK4A}$. It has also been shown that *RB1* is also deficient in around 10% of *NF1* mutant melanomas. $p14^{ARF}$ inhibits *MDM2* to stop cell proliferation; *MDM2* is vital to *p53* function. *TP53* is also involved in melanoma but it is less common than other cancer.

Current and novel targeted therapies in melanoma

Because of the increasing number of the genetic alterations in melanoma, oncogenic driver mutations have gained a significant amount of interest as possible treatment targets [50]. Since our understanding of the molecular pathways and related genetic abnormalities implicated in malignant melanoma has grown, effective immunotherapies and targeted therapies for unresectable stage III and IV melanoma are now available to restore cellular homeostasis [35]. However, surgery, as the primary treatment option for localized melanoma, remains a very successful disease management approach [7,51]. Until 2011, dacarbazine chemotherapy was the "gold standard" for advanced-stage melanoma. Since 2011, the FDA has approved a variety of therapy approaches (targeted treatments and immune checkpoint inhibitors; summarized in Figure 7) that have significantly improved overall survival (OS) for patients with metastatic melanoma.

Approximately, 70% of melanoma patients have mutations in key signalling pathway genes. The oncogenic mutations may result in an aggressive melanoma phenotype and melanoma cell proliferation [52]. Following the discovery of *BRAF* mutations in numerous malignancies, including cutaneous melanoma, molecular targeted treatments were developed [53]. As a result of this breakthrough, selective BRAF inhibitors were tested as single agents in patients with metastatic melanoma and demonstrated exceptional clinical efficacy. Following the success of single-agent *BRAF* inhibition, BRAFi/MEKi combination were studied based on *BRAF* inhibition's clinical efficacy and the significance of downstream MAPK pathway signalling. Furthermore, because *BRAF* and *MEK* belong to the same signalling pathways, it appears to inhibit cell survival pathways with improved treatment outcomes and lower drug driven toxicity.

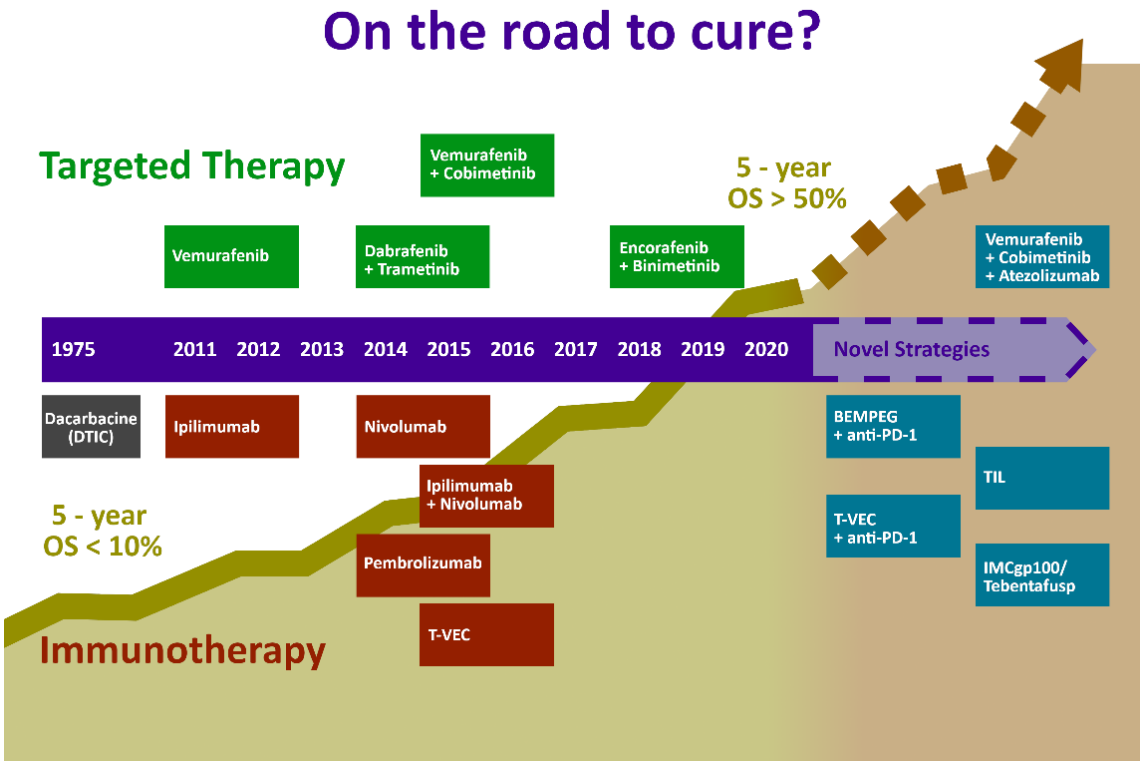

Figure 7. Systemic therapy of metastatic melanoma: on the road to cure. *The FDA approvals since 2011, the number of drugs available to treat metastatic melanoma has substantially increased. Several of these drugs were previously approved as monotherapies are currently being combined to enhance clinical outcomes. Adapted from J. Steininger et al. [54].*

Since then, a number of small molecules and antibodies have been approved by the US FDA to target these altered proteins, which are critical for cancer cell proliferation (Figure 8) [55].

Several targeted treatments have been shown to have high response rates, whereas immunotherapy has been linked to long-term responses [53]. Based on the success of targeted treatment and immunotherapy, combining these effective therapies was a reasonable next step for patients with *BRAF*-mutant melanoma.

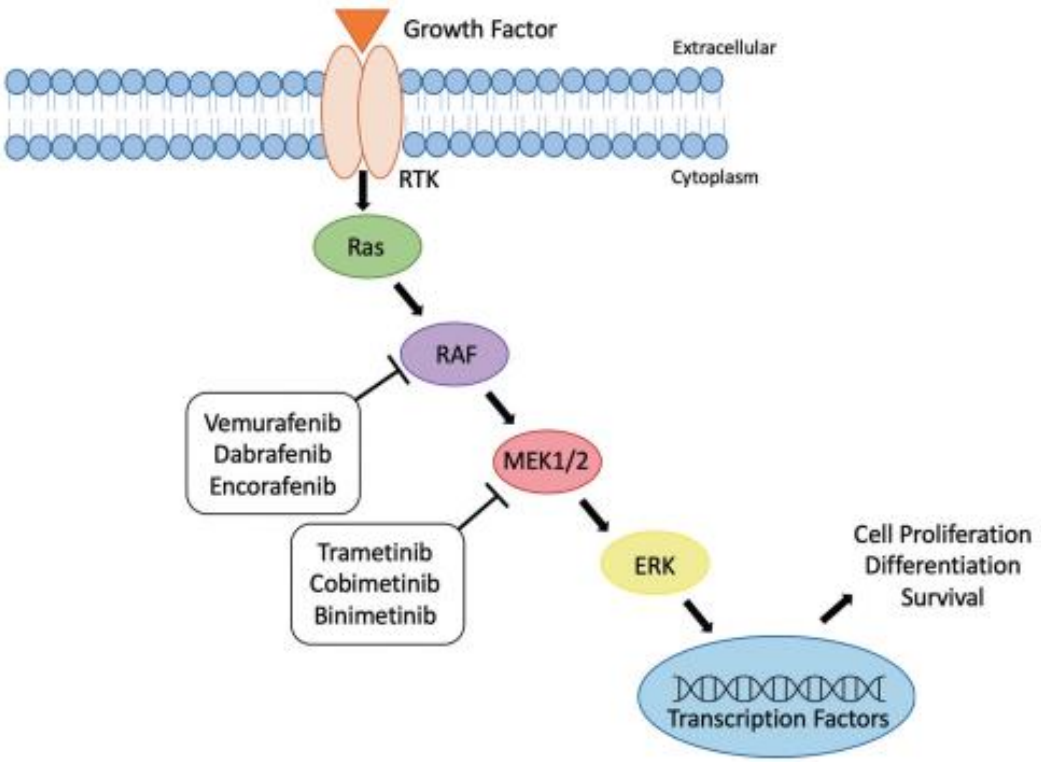

Figure 8. Schematic representation of the MAPK pathway inhibition in melanoma. *The most common therapeutic targets of the mitogen-activated protein kinase (MAPK) signalling pathway are BRAF and MEK1/2, which establish a blockage point at two separate levels, limiting oncogenic downstream signalling as well as cell differentiation and proliferation. (M. Chanda and M. S. Cohen [56].*

BRAF and MEK inhibitors

In the last two decades, the targeting of melanoma-bearing mutations has been refined through the implementation of new molecular approaches. MAPK signalling is regulated by a serine-threonine kinase known as *BRAF*, and 50% of melanomas that do not have persistent UV exposure carry a mutation in *BRAF* gene [32,57]. Mutations in the *BRAF* gene lead to increased proliferation and growth of cancer cells through activation of MAPK signalling pathway [58]. Since $BRAF^{V600E}$ is a common gene mutation, a significant driver mutation has allowed for a better understanding of melanoma cellular processes, facilitating the development of more effective targeted treatments [59].

In 2011, vemurafenib (a selective BRAF inhibitor) was approved for the treatment of unresectable metastatic melanomas with $BRAF^{V600E}$ mutations by the FDA [60]. It appears that

vemurafenib has improved the overall response in patients with $BRAF^{V600E/K}$ mutations when compared to chemotherapy. Since then, number of preclinical and clinical studies were performed evaluating the effect of vemurafenib alone, in combination with immunotherapies, and in combination with other targeted therapies [61]. In addition to vemurafenib, other BRAF inhibitor with the same mechanism of action, dabrafenib and encorafenib, was approved by the FDA for the treatment of unresectable metastatic melanomas with $BRAF^{V600E}$ mutations [57].

Using tyrosine kinases as therapeutic targets has drastically increased response rates [62]. However, the clinical response is short-lived due to acquired resistance such as *CRAF* overexpression, *COT1*, or activated mutations in the component of MAPK pathway like *N-RAS*, *BRAF*, *MEK1*, *AKT1*, or aberrant splicing of BRAF, activation of phosphatidylinositol-3-OH kinase (PI3K) via the loss of function of *PTEN* gene, and persistent activation of receptor tyrosine [63]. To overcome/delay resistance, combined therapy seem to be one of the superior options with lower drug-induced toxicity for melanoma patients [62].

Approaches that target downstream signalling of driver oncogenes are effective in overcoming resistance to BRAF inhibitors [64]. Since *MEK* is a downstream signalling component in the MAPK pathway through which *ERK1/2* is stimulated; hence, MEK inhibitors are more effective at inhibiting *NRAS*-mutant melanomas than BRAF inhibitors [65]. The FDA and the European Medicines Agency (EMA) have approved series of MEK1/2 inhibitor (trametinib, cobimetinib, and binimetinib) as monotherapy or in combination with BRAF inhibitors to treat *BRAF*-mutant advanced melanoma [66]. *MEK1/2* blockade results in a reduction of cell proliferation in tumour cells, as downstream signalling [67]. Following the first two BRAF and MEK inhibitor combination (dabrafenib+trametinib, vemurafenib+cobimetinib), FDA authorized a third BRAF and MEK inhibitor combo, encorafenib + binimetinib in 2018, for patients with unresectable or metastatic melanoma with $BRAF^{V600E/K}$ mutations [68]. The BRAF and MEK inhibitors combination shows higher response rates, longer progression-free survival, and longer survival over chemotherapy. However, a number of adverse events are associated with this class of drugs, including cutaneous, ocular, cardiac, gastrointestinal, and musculoskeletal side effect [69]. In clinical practice, the most commonly occurring and prominent adverse reactions associated with the drug use include fever (dabrafenib) and photosensitivity (vemurafenib). The following drug induced adverse reactions are less common: rash, prolonged

QTc, increased liver enzymes (vemurafenib), neutropenia (dabrafenib), anaemia, facial paresis (encorafenib) [69].

Immunotherapies

Until lately, melanoma treatment consisted on four major types of therapeutic approaches: surgery, radiation, chemotherapy, and targeted therapy [70]. Over the past decade, the cancer-immunotherapy (immuno-oncology) has emerged as therapeutic option for cancer patients including melanoma by stimulating the immune system of the body to eradicate itself the malignant cells [71]. Immunotherapy is based on the interaction between immune cell and molecules present on the surface of cancer cell. Cells of the lymphocyte family, known as cytotoxic T lymphocytes, recognize tumour-specific antigens, becoming activated, and subsequently multiply to become able to eradicate cells expressing tumour-specific antigens. Despite the activation and inhibition of the signalling pathways that govern the T-cell antitumor response, cancer cells may have an additional mechanism of escaping identification by T-cells if they do not express *B7* molecules on their surface [72]. Moreover, there is evidence that tumours and immune system of the body interact in a complex manner to encourage the spread of cancer [73]. Metastases are the major cause of death associated with cancer [74]. With the understanding that immune cells interact with cancer cells, Immunotherapy is considered as a possible therapeutic strategy for individuals with advanced-stage melanoma [75].

In order to activate T-cells, antigen-presenting cells (APCs) facilitate interaction between T-cell receptors and peptide antigens as known as major histocompatibility complex (*MHC*). Contrary to T-cell proliferation and differentiation, T cell inhibition depends on the interaction of inhibitory ligands and receptors between the APC and T cells. These costimulatory signals are also referred to as an immunological checkpoint, which are vital to T cell proliferation and differentiation. By inhibiting T cell inhibitory signals, T cells are activated indefinitely, and the antitumor effect of T cells is continuously maintained (Figure 9).

So far, several antibodies have been approved by the FDA for advance metastatic melanoma with notable improvements in overall survival, including Ipilimumab (anti-CTLA-4), nivolumab (anti-PD-1) and pembrolizumab (anti-PD-1) [76].

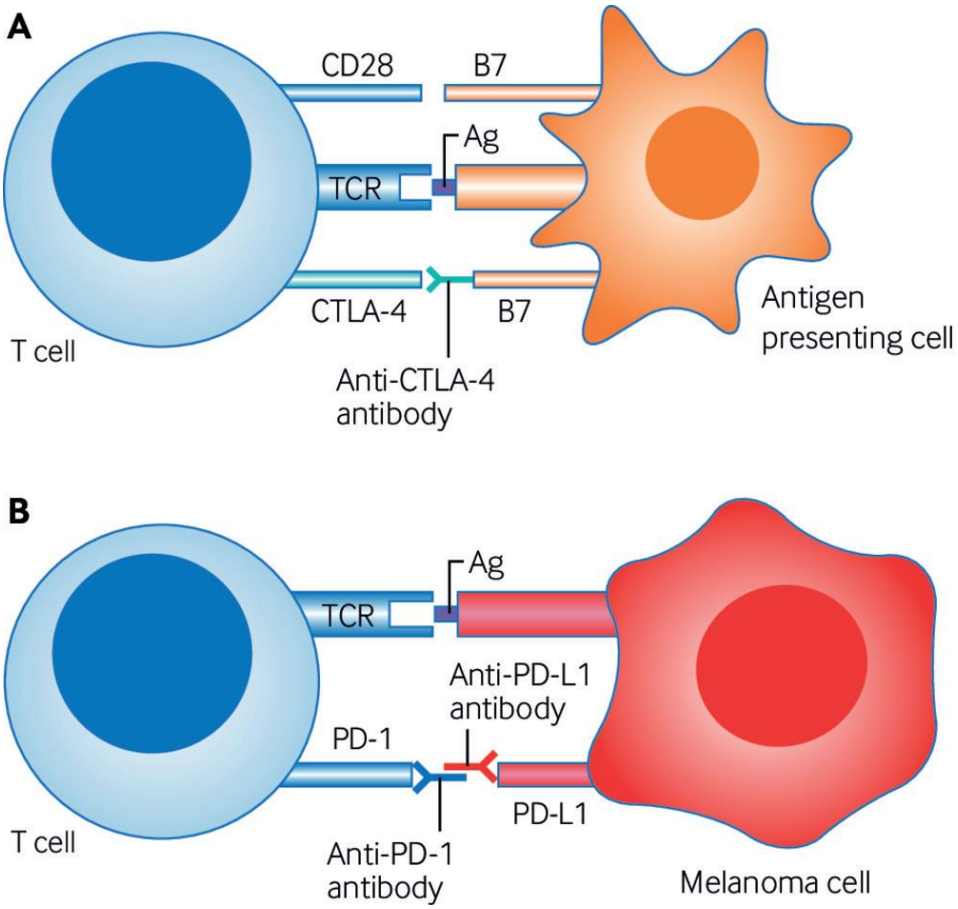

Figure 9. Immunotherapy for melanoma focusing on the immune checkpoint proteins. *A. The activated T cell expresses the CTLA-4 cell surface receptor. CTLA-4 suppresses any immune response produced by T cells when linked to a specific antigen. Using antibodies to inhibit CTLA-4 inhibits the downregulation of T cells, which improves the effectiveness of anti-tumour drugs. B. In addition, when the programmed death protein-1 (PD-1) receptor binds to PD-L1, T cell activity is reduced. The PD-L1 ligand is bound by antibodies to PD-1 and PD-L1, therefore suppressing downregulated T cells and increasing their antitumor activity. Adapted from Karimkhani C et al. [77].*

Immunocheckpoint blocking is most effective when paired with targeted therapy, either as an initial treatment or as part of a sequence combination regimen to optimize patient benefit. In support of the sequence issue, predictive biomarkers are being investigated in the treatment of melanoma [78]. *PD-1* and *CTLA-4* act through different mechanisms to attenuate T-cell activation. For instance, *CTLA-4* suppresses *CD28* by competing for shared *B7* ligands, whereas *PD-1* inhibits T-cell activation by sending inhibitory signals through interaction with *PD-L1/2*. The combination treatment may be possible due to its suppressive behaviour. By this hope, the combination of ipilimumab and nivolumab has been approved for advanced metastatic

melanoma. This combination, on the other hand, induces toxicity while increasing response rates [79].

Resistance to BRAF inhibitors

Activation of the MAPK pathway is essential for many cellular processes, such as cell growth and differentiation [11]. Furthermore, in normal cells, the physiological upstream negative feedback response inhibits sustained MAPK-pathway activation; but, in melanoma cells with *BRAF*^{V600} mutations, this mechanism is dysregulated, resulting in constitutive MAPK pathway activation [80]. Targeting *BRAF*^{V600} mutant cells by using selective BRAF inhibitor become one of the most successful treatment strategies to treat melanoma. Nonetheless, most patients develop resistance to these therapies after the first year of treatment, while a small group exhibits intrinsic resistance to them (Figure 10).

Patients that acquired BRAF inhibitor resistance were shown to have reactivation of the MAPK pathway, higher levels of *pERK*, and multiple *MEK1/2* mutations [81]. In light of this, a combination of BRAF and MEK inhibitors (BRAFi/MEKi) was selected instead of BRAFi alone since it provides more potent inhibition of the MAPK pathway with durable response and lower rates of drug-induced toxicity [82]. Unfortunately, even when combination treatment is used, the majority of patients develop resistance and tumour relapse.

An enormous amount of research has been conducted over the last several years to understand the mechanism of resistance to BRAF inhibitors, and also MEK inhibitors, in patients with *BRAF*-mutant melanoma. To date, BRAF inhibitors have been associated with a variety of resistance mechanisms, but not limited to these ones [83,84]. BRAFi resistance is primarily due to MAPK pathway activation, or activation of alternative survival and proliferation pathways. There are three main types of BRAFi resistance: intrinsic, adaptive, and acquired [85].

Intrinsic resistance to MAPK inhibitors occurs when melanoma cells have an innate ability to resist the therapeutic effect of the target inhibitor. About 20% of patients with *BRAF*-mutant melanoma demonstrate intrinsic resistance [86]. The molecular mechanisms linked to intrinsic resistance have been identified in various pre-clinical and clinical studies. These mechanisms include loss of *PTEN* and *NF1*, amplification of the *CCND1* gene, overexpression of the *COT* gene, mutations in *RAC1*, and the loss of the *USP28-FBW7* complex [85].

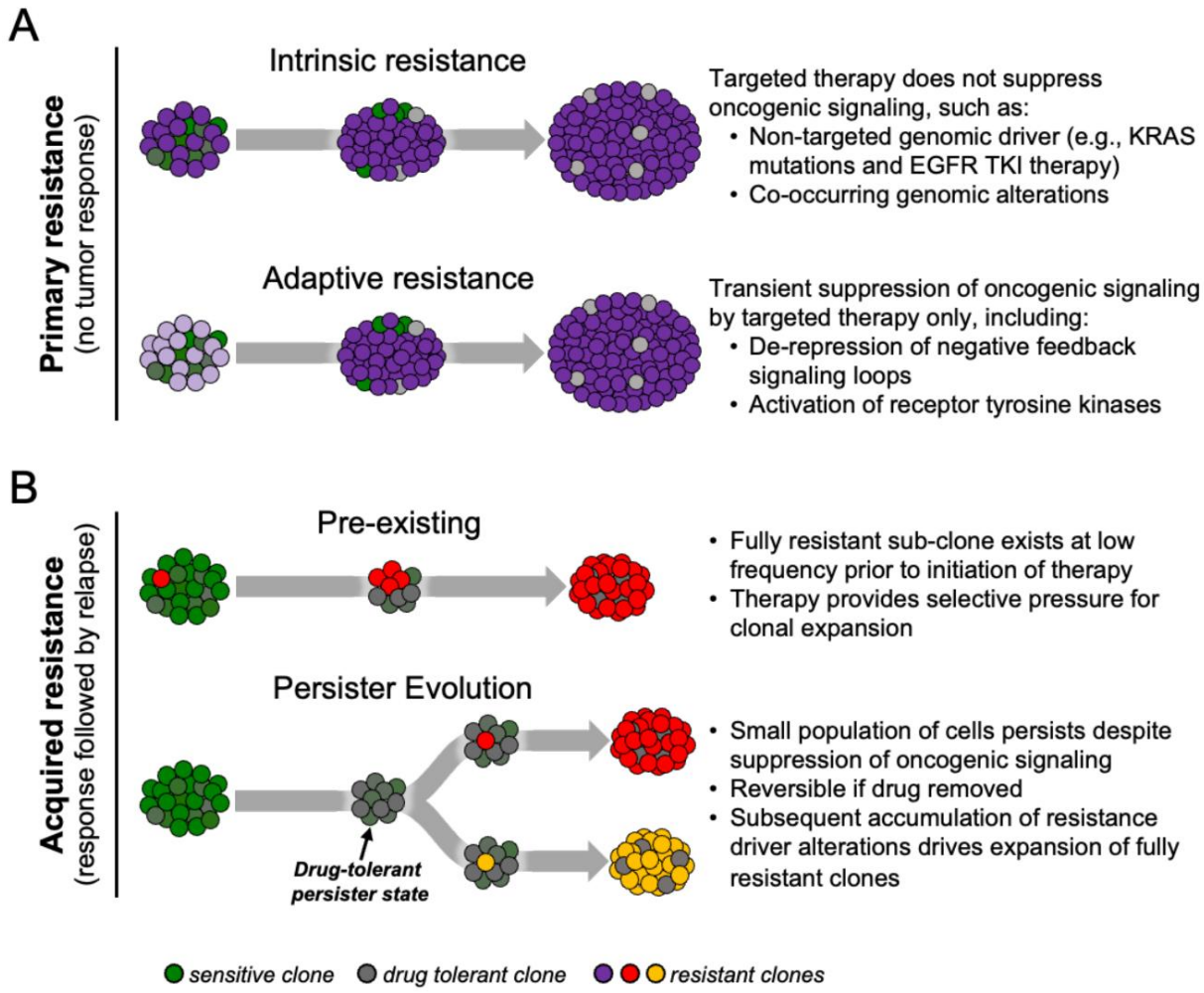

Figure 10. The biology of drug resistance in cancer. *Drug resistance might occur during or after the first response to therapy. (A) Existing drug-resistant clones may be a primary source of resistance, allowing oncogenic signalling to continue to occur. Conversely, adaptive resistance occurs when clones of resistant cells multiply following an initial therapeutic response to targeted therapy. (B) Tumour relapses may be triggered by the selection of resistant clones that existed prior to treatment and can develop a variety of different resistance mechanisms to escape drug-induced suppression. Adapted from Cabanos HF, Hata AN [87].*

The emergence of adaptive resistance occurs during the early phase of inhibitor treatment, particularly during the first 24 to 48 hours. This provides sufficient time for alternative mutations to develop in melanoma cells during the early stages of treatment. The adaptive resistance to BRAF inhibitors adversely affects the success of targeted therapies. A number of molecular mechanisms have been identified as contributing to adaptive resistance, such as the

upregulation of RTKs (*EGFR*, *ERBB3*, *PDGFR*, and *FGFR*), upregulation of *MITF*, the paradoxical role of *SOX10*, and metabolic rewiring [88]. In response to BRAF inhibition, these molecular changes stimulate cell proliferation and inhibit cell death.

In patients with metastatic melanoma treated with long-term BRAFi, reactivation of the MAPK/ERK downstream pathway and the emergence of new mutations ultimately lead to acquired resistance. This mechanism may also involve the activation of the PI3K/AKT/mTOR pathway. A number of investigations have shown that the molecular changes involved in acquired resistance include *RAS* mutations, dimerization of RAF proteins and RAF paradox, *BRAF* gene amplification and splicing, *MEK1/2* mutations, *RTK* hyperactivation, PI3K-AKT pathway aberrations, YAP/TAZ pathway activation, downregulation of *DUSPs* and *STAG2* or *STAG3* and *RNF125* expression [85,89]. Regardless, a significant amount of research has been undertaken on resistance mechanisms. However, around 40% of resistant tumours fail to demonstrate these alterations, and the underlying mechanism of resistance remains unclear.

Importance of 3D cell culture

The tumour infiltrating cells and tumour types are exceedingly diverse, adding to the complexity of the disease [90]. As a result, developing novel therapies is a persistent, critical, and difficult process. *In vitro* drug screening is a low-cost, commonly used method for identifying and selecting drugs of greater therapeutic potential. Two-dimensional (2D) flat monolayer cell culture is currently the most commonly used method for cell-based assay analysis because it is easy and convenient. There is a fundamental problem with most drug tests; they are done in 2D *in vitro* cultures. These cultures do not accurately mimic tumour complexity or human physiology. In 2D cell culture, cells developed more contact space with the plastic surface than neighbouring cells, resulting in decreased cell-to-cell interaction and cell to extracellular matrix interaction [91]. In addition, cells grown in a 2D environment experience unrestricted access to nutrients, drug and gases exchanges (Figure 11) [92]. The irrelevant 2D environment can generate misleading results when it comes to cancer cell predicted responses to anticancer drugs [93]. Several anticancer drugs fail as they enter the animal testing stage due to an unphysiological 2D environment.

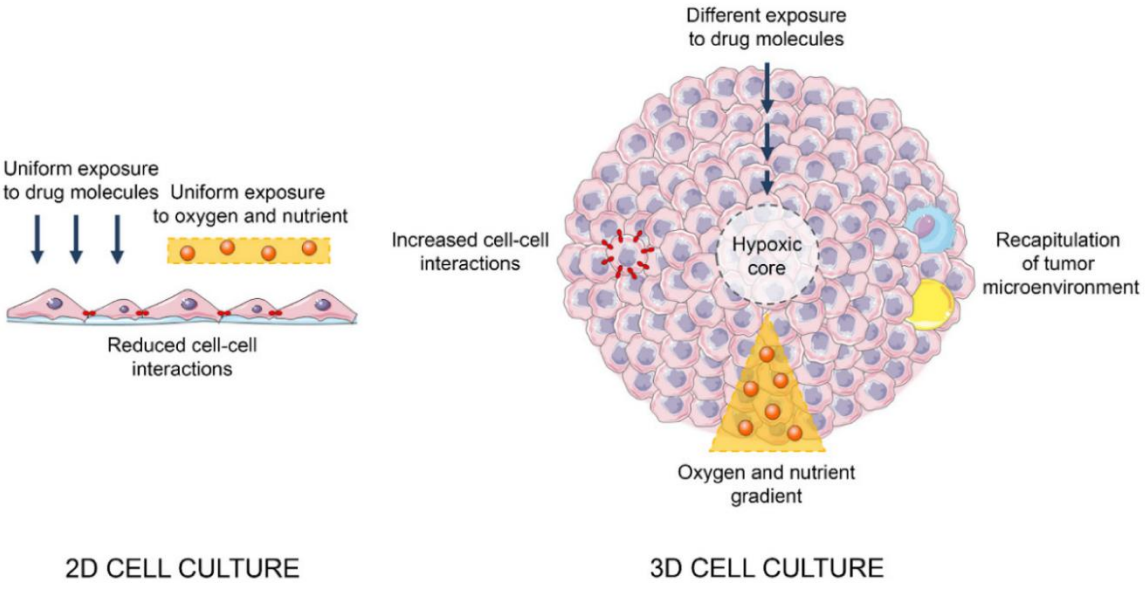

Figure 11. The primary disparities between 2D and 3D cell cultures. *This figure emphasizes the biological importance of 3D cell culture in comparison to 2D cell culture. Three-dimensional (3D) cells behave more like tissue in terms of gaseous exchange and nutrient distribution than two-dimensional (2D) cell culture. Adapted from Fabrizio et al. [92].*

The primary limitation of conventional 2D cell culture systems led to the development of 3D cell culture systems, which promise to reduce inconsistency between cell-based assays and *in vivo* drug screening [94]. Three-dimensional (3D) culture systems are becoming more common due to their potential to replicate tissue-like structures more efficiently than monolayer cultures [94]. The use of 3D cultures especially spheroid provides a more accurate physiologically relevant model for *in vitro* cancer cell cultures and drug screening [95]. This approach helps cells to expand and communicate with their surroundings. It also enables consistently reliable results compared to cells that grow on the flat plastic surface [23]. The cells are grown under 3D cell culture methods exhibit various tumour features such as similar morphology to *in vivo* tumours, proliferation, differentiation, cell to cell interaction, signal transduction, and drug response [23,90]. Julia C et al. observed that 3D cultured cells are more insensitive to cytotoxic agents, and their gene transcripts are more consistent with the results *in vivo* tumours than in 2D monolayers [90]. Taken together, it has the potential to minimise the gap between conventional 2D culture and animal research, and it is critical for future tumour biology studies. In comparison to 2D cell culture, spheroid culture clearly provides a better model for studying cellular physiology and drug screening. There are some other 3D models, such as 3D skin

reconstruct and organoids, but they have limitations because of their *ex vivo* nature [96]. The other possibility is to use patient-derived xenografts (PDXs) isolated from patients and xenotransplanted into immune-suppressed mice. PDXs can be used preclinically, such as for anti-tumour drug testing, or for analysis in an *in vivo* environment [97]. The advantage of using patient-derived xenografts in mice is the possibility to analyze the unchanged tumour itself as well as to test drugs and drug resistance *in vivo* and it allows to analyze the complexity of cancer cells within a tumour. The development of spheroid model has decreased the gap between *in vitro* and *in vivo* testing but not bridged. Despite being close to the *in vivo* setting, 3D model system especially spheroids has some advantages and disadvantages when compared to the tumour xenograft model, such as failing to mimic the full architecture of *in vivo* tissues, such as vasculature and interstitial fluid flow. Below I summarized the advantages and disadvantages of 3D spheroids compared to tumour xenograft models.

Tumour Microenvironment: The microenvironment of the tumour is critical to its survival and development [98]. Cancer cells become invasive and spread from the originating location to distant regions via a complicated and multistep metastatic cascade involving interactions between the tumour microenvironment's cellular and structural components. Tumour microenvironment is inadequately developed in the spheroid culture compared to the tumour xenograft model, resulting in a poor comprehension of cancer cells' spreading potential.

Maintenance of in vivo structure and viability and genetic profile: It has been demonstrated that the tumour xenograft model preserve 92–97% of the genetic mutations seen in the parental patient tumours, as well as providing a comparable structure to the tumour’s natural environment to some extent. However, it should be emphasized that the gene expression of the xenograft model might be host specific. On the other hand, in the spheroid, the structure and genetic composition of the spheroid are most likely different due to the unnatural artificial environment, weak gaseous exchange system, and absence of other cell types such as immune cells, which also play an important role in tumour cell stability.

Potential of high-throughput studies: Cancer-derived xenograft models allow for the identification of potential drugs for individual patients as well as the understanding of how cancer cells develop treatment resistance [99]. Despite their great reproducibility, xenograft-based models have numerous technical drawbacks, including a long engraftment period, high expenses, restricted statistical power, and a limited possibility for use in high-throughput

experiments [100]. On the other hand, spheroid culture is cost effective, convenient, short engraftment time and, high potential cell characterisation, allowing for characteristic-based findings.

The reason to adopting 3D cell culture over animal studies is based on various additional factors such as expense, documentation related to the safety and efficacy of a treatment in a living organism, which is time and resource intensive.

Objectives

Despite intensive research efforts, which have significantly improved melanoma patient survival, therapy resistance to the targeted mono- and combined therapies remains unsolved problems. The major focus of our study was to investigate molecular alterations associated with acquired resistance in malignant melanoma cell line models.

Because majority of currently available data on drug resistance have been obtained from 2D *in vitro* cell cultures we aimed to:

- develop reproducible three-dimensional melanoma spheroid models from *BRAF*^{V600E} mutant melanoma cell lines that are sensitive and resistant to a BRAF inhibitor (BRAFi)
- compare the gene expression signature of the sensitive and resistant melanoma cell lines grown under 2D and 3D cell culture conditions,
- define genes that are differently expressed between differently cultures cells.

In parallel, our aim was to explore the molecular background associated with acquired resistance of melanoma cells during combinatory treatment using BRAF and MEK inhibitors:

- in order to reach our goal we established human melanoma cell lines resistant to encorafenib (BRAF inhibitor) plus binimetinib (MEK inhibitor),
- evaluated the invasive properties of drug-sensitive and drug-resistant cell lines,
- studied the effect of “drug holiday” on cell proliferation and protein expression in the drug sensitive and resistant cell lines,
- investigated and compared the gene expression pattern of BRAFi/MEKi resistance using RNAseq analyses,
- defined the biological functions of the differently expressed genes linked to the development of resistance.

Materials and methods

Cell lines and culture conditions

A total of 9 human melanoma cell lines were included into our study. These cells were purchased from the Coriell Institute for Medical Research (Camden, New Jersey, USA). All cell lines were cultured at 37°C in a humidified incubator with 5% CO_2 and 95% air using RPMI 1640 (Lonza Group Ltd, Basel, Switzerland) supplemented with 10% of foetal bovine serum (FBS) (Gibco, Carlsbad, California, USA), 2 mmol/l glutamine, and 50 mg/ml gentamycin sulphate. Once the cells had reached 70% confluence, they were passaged with trypsin (IITD PAN, Wroclaw, Poland) in standard 25 cm^2 flasks. The clinical and pathological characteristics of cell lines are presented in Table 2. The WM1366 cell line was wild-type for the $BRAF^{V600E}$, but exhibited the *NRAS* mutation, while the WM3211 cell line was wild-type for both gene.

Table 2. Characteristics of human melanoma cell lines

Cell line	Sex/age (years)	Origin[a]	Growth phase[b]	Histologic type[c]	BRAF mutation status[d]	*NRAS* status mutation status[e]
WM983A[p1]	Male/54	Primary	VGP	NM	V600E	wt
WM983B[m1]	-	Metastasis	-	-	V600E	Wt
WM278 [p1]	Female/62	Primary	VGP	NM	V600E	wt
WM1617 [m1]	Female/62	Metastasis	-	-	V600E	wt
WM902B	Female	Primary	VGP	SSM	V600E	wt
WM793B	Male/37	Primary	RGP/VGP	SSM	V600E	wt
WM35	Female/24	Primary	RGP/VGP	SSM	V600E	wt
WM1366	Male/79	Primary	VGP	-	wt	61L
WM3211	Male/74	Primary	RGP	SSM	wt	wt

[a]tumor type of melanomas which the cell lines were derived from, [b]VGP: vertical growth phase, [c]NM: nodular melanoma, [d]V: valine, E: glutamic acid, [e]wt: wild type, [p]primary tumour derived cell line with metastatic pair from the same patient, [m]metastatic pair of primary derived cell line

Development of BRAFi (PLX4720) resistant cell lines under 2D and 3D cell culture conditions

BRAFi (PLX4720) resistant cell lines were established using two cell lines (WM983A and WM983B) as described before, by continuously increasing the concentration of a vemurafenib analogue PLX4720 [101]. In brief, WM983A, WM983B cell lines were seeded at low densities in T/25 flasks until cell confluence reached about 80%. Then, the cells were switched to medium containing 5 μM PLX4720 and cultured. The surviving cells were treated with PLX4720 (5 μM) every 3 days until cells reached 80% confluence (~10 weeks). The resistant cell lines were designated as $WM983A^{RES}$ and $WM983B^{RES}$.

To develop spheroids, BRAFi sensitive and resistant cells were seeded using $1.8x10^4$ cells/well into Corning® Costar® Ultra-Low Attachment (6 well) plates containing RPMI-1640 supplemented with 2 mmol/l glutamine and 50 mg/ml penicillin and streptomycin. After 72 hours the medium was supplemented with 10%, FBS. The cells were grown for one week, then the visible spheroids were transferred into a cell culture flask (T/25) and leaved to attach (~ 6 hours). After attachment, the spheroids were washed, cell debris were removed using 1xPBS. Spheroids were assigned as $WM983A^{SPH}$, $WM983B^{SPH}$, $WM983A^{RES\text{-}SPH}$ and $WM983B^{RES\text{-}SPH}$.

Development of BRAFi (encorafenib) + MEKi (binimetinib) resistant cell lines

Nine melanoma cell lines (WM983A, WM983B, WM278, WM1617, WM902B, WM793B, WM35, WM1366 and WM3211) were treated in combination with encorafenib (BRAFi: ENCO) + binimetinib (MEKi: BINI). Resistant cell lines were generated through long-term high-dose treatment from six cell lines using increasing concentrations of ENCO+BINI as described [102]. Briefly, cells were cultured in a humidified incubator (5% CO_2 and 95% air at 37°C) until they achieved 70% confluence in a T/25 culture flask. Then, the medium was switched to growth medium containing the combination of ENCO+BINI and allowed to grow for three months. The concentration of the drug combination at the beginning of treatment was 1 nmol/l for each cell line and increased up to 200 nmol/l. Depending on the sensitivity of the cell line, to reach the maximum concentration of the drug combination, the time frame varied between three and five months. Unless otherwise indicated, the resistant cells were maintained in complete medium supplemented with 200 nmol/l inhibitor mixture to prevent resistance loss. Comparisons of the different parameters (cell viability, invasive potential, protein expression,

and transcriptome profile) between the sensitive and resistant cells were performed at the same passage number. Inhibitors (Encorafenib (LGX818), Binimetinib (MEK162), and PLX4720) were purchased from Selleck Chemicals LLC (Houston, TX/USA). Stock solutions were prepared in dimethyl sulfoxide (DMSO) and kept in aliquots at -20°C/-80°C, according to the manufacturer's instructions.

Cell proliferation assay

To assess the viability of cells, WST-1 assay (2-(4-iodophenyl)-3-(4-nitrophenyl)-5-(2,4-disulfophenyl)-2H-tetrazolium) (Sigma-Aldrich Inc., St Louis, Missouri, USA) were used in accordance with the manufacturer's instructions. In brief, 5 x 10^3 cells were seeded in triplicate on 96-well plates and grown in 100 µL growth medium for 24 hours. On the following day, the medium was replaced with fresh growth medium enriched with the combination of 1 µmol/l of ENCO + BINI for 72 hours. DMSO was used during the control experiment. Then, 10 µL WST-1 reagent was directly added to each well, and cells were incubated at 37°C for three hours. Absorbance at 440 nm was measured using an Epoch™ Microplate Spectrophotometer (BioTek Instruments, Winooski, Vermont, USA), reference absorbance was set to 650 nm. The viability of the cells was defined as follows: dividing the absorbance of the ENCO+BINI treated cells by that of the DMSO-treated control cells (the absorbance of control cells was defined as 100%).

Drug holiday experiment

Drug holiday experiment was performed as we published [102]. Shortly, resistant cells (5×10^3 cells/well/100 µL medium) were seeded into 96-well plates in triplicate containing combination of 200 nmol/l ENCO + BINI in each well for 24 hours. The next day, cells were divided into two groups: the first half of each cell line was switched to growth medium enriched with drug for 72 hours, while the other half was retained in growth medium containing the DMSO (0.5 %) for 72 hours. Then, 10 µL of WST-1 reagent was directly added to each well, and the cells were incubated at 37°C for the following three hours. Absorbance was measured as described above. Percentage of viable cells was calculated from relative absorbance.

In-vitro invasion assay

The invasive potential of the inhibitor (ENCO+BINI)-sensitive and -resistant melanoma cells was evaluated using BioCoat Matrigel Invasion Chambers (BD Biosciences, Bedford, Massachusetts, USA) as described before [103]. Shortly, for BRAFi/MEKi-sensitive cells, the upper part of the invasion chamber was filled with a serum-free cell suspension (500 µL), and growth medium with 10% FBS was used (as a chemoattractant) in the lower chamber. For BRAFi/MEKi-resistant cells, we filled the upper chamber with 500 µL of the melanoma cells (cells were kept in serum-free medium containing a 200 nmol/l combination of the inhibitors). The culture medium in the lower chamber was supplemented with 10% FBS (as a chemoattractant) and a 200 nmol/l combination of ENCO+BINI. The invaded cells were fixed with ice-cold methanol after 24-h incubation and stained with haematoxylin-eosin. Invasive cells were counted under microscope (200x magnification) in seven different areas, and cell numbers are displayed as the mean ± SD of three independent experiments.

Protein expression analysis

Protein expression analyses were performed as described in detail before by Szász et al. [101] Shortly, ENCO+BINI sensitive and resistant cells were cultured at approx. 80% confluence and washed gently (2x) using ice-cold PBS. One ml of RIPA Lysis and Extraction Buffer (Thermo Fisher Scientific Inc., Waltham, MA, USA) containing 20 µL protease and phosphatase inhibitor cocktail (Thermo Fisher Scientific Inc., Waltham, MA, USA) was added to each cell culture, and cells were removed from the tissue culture flask by applying a cell scraper blade (Thermo Fisher Scientific Inc., Waltham, MA, USA). Cell lysates were transported to microtubes, incubated on a rocking shaker (30 min, 4 °C), and centrifuged (13,000 rpm, 30 min, at 4 °C). The supernatants were transferred into new Eppendorf tubes, and the protein concentration was determined using the Bradford Protein Assay (Bio-Rad Hungary Ltd., Budapest, Hungary) as described in the supplier's instruction. The Proteome Profiler™ Human XL Oncology Array Kit was obtained from R&D Systems (R&D Systems, Inc., Minneapolis, Minnesota, USA). Preparation of all the necessary reagents and the array procedure was performed according to the manufacturer's detailed protocol. The labelled proteins were detected and visualized using Chemi Reagent Mix (R&D Systems Inc., Minneapolis, Minnesota, USA). The protein expressions (labelled spots on the membrane) were exposed using the Azure c300 Chemiluminescent Imaging System (Dublin, CA, USA) and were

analysed using AzureSpot (Vesion: 2.2.167) software. The intensity of the positive control (reference spot) was considered 100%.

RNA Isolation and Microarray Hybridization

RNeasy Mini Kit (Qiagen GmbH, Hilden, Germany) was used for total RNA isolation. Concentration of RNA was measured using NanoDrop ND-1000 UV-Vis spectrophotometer. Only samples with ratios >1.8 (measured at 260/280 nm) were included in further analysis. An Agilent 2100 Bioanalyzer was used to evaluate sample quality before RNA sequencing (Agilent Technologies Inc., Santa Clara, CA, USA).

RNA sequencing and RNA-seq data analyses

RNA-Seq and data analyses were performed as described previously [104]. To obtain global transcriptome data, high throughput mRNA sequencing analysis was performed on an Illumina sequencing platform. An Agilent BioAnalyzer with Eukaryotic Total RNA Nano Kit (Agilent Technologies, Waldbronn, Germany) was used for checking RNA integrity (RIN). RNA samples with integrity number >7 were accepted for the library preparation process. mRNA-Seq libraries were prepared from total RNA using an Ultra II RNA Sample Prep kit (New England BioLabs Inc., Ipswich, MA, USA) according to the manufacturer's protocol. Briefly, oligo-dT conjugated magnetic beads were used for mRNA enrichment, and then mRNAs were eluted and fragmented at 94 Celsius. Fragmented mRNAs were reverse-transcribed to single-stranded cDNA using random primers, and then double stranded cDNAs were generated. After end repair, A-tailing and the adapter ligation steps of the library preparation process were finished by amplification of adapter ligated fragments. Sequencing was performed on an Illumina NextSeq 500 instrument using single-end 75-cycle sequencing. The HISAT2 algorithm was used for alignment of raw sequencing reads to human reference genome version GRCh38. StrandNGS software (www.strand-ngs.com) was used for further statistical analysis. Aligned data were normalized using the DESeq algorithm, and then differentially expressed genes were determined by a moderated T-test with Bejamini-Hochberg FDR for multiple testing correction. A p-value of 0.05 was considered significant. Library preparations, sequencing, and primary data analysis were performed at Genomic Medicine and Bioinformatics Core Facility of the University of Debrecen, Hungary.

Gene Expression Analysis of Melanoma Cells Cultured Under 2D and 3D Cell Culture Conditions

Analysis of gene expression microarray data was carried out as described previously [105]. After background correction, log2 transformation and normalization, intensity data were inserted to Bioconductor BRB-Array Tools 4.6.0 Richard Simon and Amy Peng Lam (National Cancer Institute, Bethesda, USA). After normalization, quality control, and filtering steps of the data, 9,653 genes were used in further analyses. To reveal the differentially expressed genes between cells growing in 2D and 3D, paired t-tests with a random variance model were applied, considering a P-value 0.01 or less to be statistically significant. The microarray data were deposited in the Gene Expression Omnibus repository (http://www.ncbi.nlm.nih.gov/gds) under accession number GSE114443 and GSE148638.

Gene Expression Analysis of ENCO+BINI sensitive and resistant cell lines

Analysis of differentially expressed genes was carried out as described by Ahn et al. [106]. The following criteria were applied to determine significantly expressed genes in each sample: fold change ≥2 and p-value ≤0.05. The RNA-Seq data were deposited into the Gene Expression Omnibus (GEO) repository (http://www.ncbi.nlm.nih.gov/gds) under accession number GSE186108.

Gene Ontology Functional Analysis and Gene Set Enrichment Analysis (GSEA)

To gain mechanistic insight into the gene lists generated from the RNA-Seq data, a functional enrichment analysis was performed to identify the biological pathways more enriched in a gene list than would be expected by chance. The ToppFun tool ToppGene suite (https://toppgene.cchmc.org/) was applied to find the functional enrichment of genes with at least a 2-fold change difference between the treated (resistant to BRAFi/MEKi) and control groups (sensitive to BRAFi/MEKi) based on GO pathways under default settings and a p-value cut-off of 0.05.

To identify gene sets from the Molecular Signatures Database (MSigDB) v7.2 (c5.all.v7.2.symbols.gmt), GSEA version 4.1.0 was used, which summarizes and represents specific well-defined biological states or processes and displays coherent expression values (www.gsea-msigdb.org).

Pathway Analysis

Significant pathways associated with specific gene expression signatures were identified using the EnrichR web-based application (http://amp.pharm.mssm.edu/Enrichr/#). Only significantly altered signalling pathways (p-value ≤0.05) were included in the analyses. Benjamini-Hochberg adjustment (FDR <0.05) was applied as a cut-off, and pathways with ≥5 significantly differentially expressed genes were considered and used to define molecular pathways associated with the differentially expressed genes.

Quantitative Real-Time PCR

Quantitative real-time PCR (qRT-PCR) was used to define the relative mRNA expression of selected genes in five melanoma cell lines (WM983A, WM983B, WM278, WM1617, and WM902B and their BRAFi/MEKi resistant pairs) using a Light Cycler 480 Real-Time PCR System (Roche Diagnostics GmbH, Mannheim, Germany). cDNA synthesis was performed applying High-Capacity cDNA Reverse Transcription Kit (Life Technologies (Applied Biosystems, USA)) with random primers as described in the supplier's protocol; 600 ng of total RNA for each reaction was used. SYBR Premix Ex Taq (Takara Holding Inc., Kyoto, Japan) was applied to carry out the qRT-PCR reaction. GAPDH (glyceralde-hyde-3-phosphate dehydrogenase: Hs9999 9905_m1) was used as a reference gene, and the Livak method (2^-ddCT equation) was applied for the qRT-PCR data analyses. The primer sequences for the selected genes are summarized ***in Supplementary Table 1A*** (validation of Affymetrix data) and ***Supplementary Table 1B*** (validation of RNAseq data) (see Appendix). Environmental contamination was evaluated by including no template control (NTC) reactions.

Statistical Analysis

Statistical analysis was performed using SPSS (IBM SPSS 19.0, SPSS Inc., Chicago, IL, USA) and Graph Pad Prism 9 (Graph Pad Software Inc., San Diego, CA, USA) software. Pearson's correlation coefficient was calculated to correlate the RNA-seq and qRT-PCR data. The cellular parameters were statistically analysed using the Mann–Whitney–Wilcoxon test. Only a p-value <0.05 was considered statistically significant. Data are presented as the average ± standard deviation (±SD) of at least three independent experiments. Error bars on the figures represent ±SD.

Results

Development and characterization of BRAF inhibitor resistant melanoma cell lines growing under traditional and 3D cell culture conditions

Morphology of melanoma cells grown under 2D and 3D conditions

Melanoma cell lines are effective *in vitro* models for obtaining an overview of the molecular alterations involved in cancer development and progression. Adherent cell culture is frequently used in these studies. Melanoma cells grow in monolayer which differs considerably from the conditions *in vivo*. Our aim was to develop 3D melanoma cell culture of BRAFi sensitive and resistant cells and compare the gene expression signatures of cells growing under the different cell culture conditions. As described under the Materials and Methods section, we successfully developed melanoma cells growing as spheroids from the WM983A and WM983B cell lines. WM983A cells are originated from a primary melanoma tumor and WM983B is originated from the same patient's metastatic lesion. The development of resitant melanoma speroids from both cell lines were also successful (WM98A$^{\text{RES-SPH}}$ and WM983B$^{\text{RES SPH}}$). Figure 12. shows the morphology of the WM983A cells growing as adherent cells (Figure 12a) and as spheroids (Figure12b).

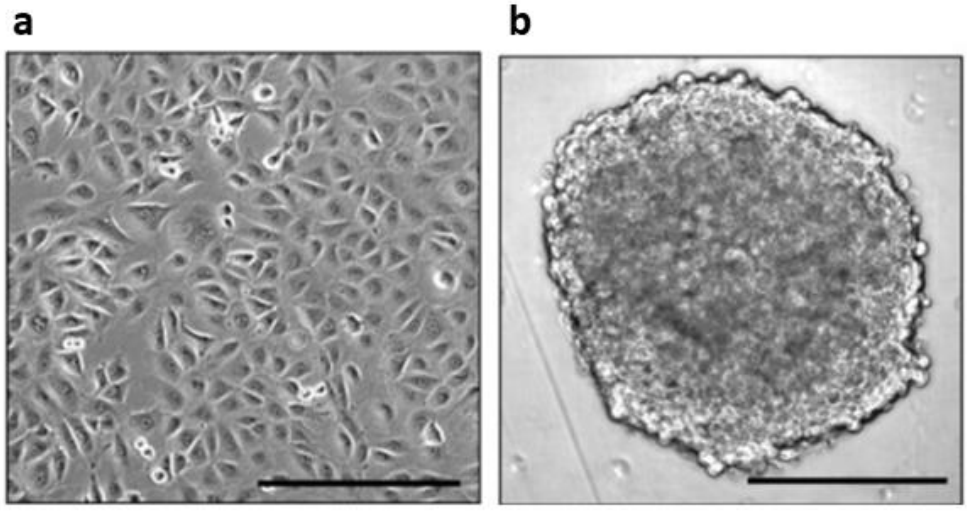

Figure 12. Morphology of the WM983A melanoma cells. *a) cells growing under traditional 2D cell culture condition and b) under 3D cell culture conditions. Both images were captured at 100x magnification.*

Gene expression profiles of BRAFi (PLX4720) sensitive melanoma cell lines cultured under 2D and in 3D conditions

Gene expression profiles of BRAFi sensitive (2D cell culture designated as WM983A and WM983B; 3D cell culture designated as WM98A^{SPH} and WM983B^{SPH}) melanoma cell lines were compared (data obtained by using the Affymetrix Human Gene 1.0 microarray). This analysis resulted in 1049 differently expressed genes between the two types of cell culture conditions. Among the 1049 genes 562 were overexpressed) and 487 downregulated (*Supplementary Table 2:* attached as separate file). After hierarchical clustering the gene expression data, the generated heat map (Figure 13a) clearly showed the expression differences between the adherent and spheroid cell cultures for both cell lines.

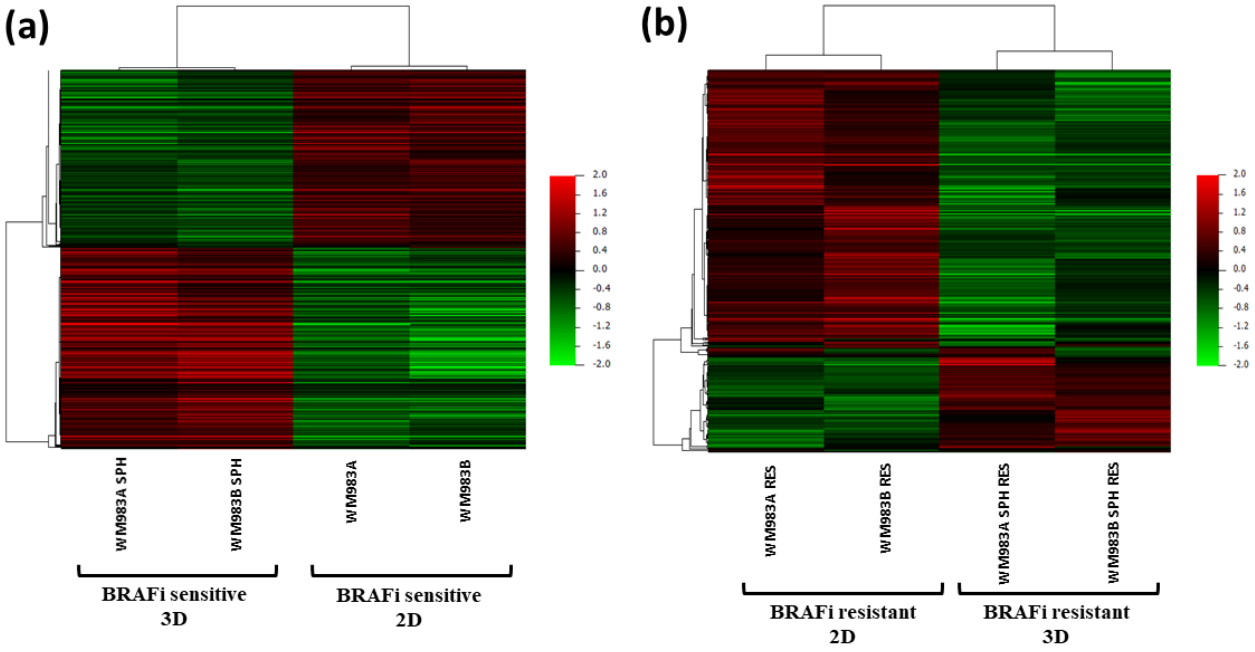

Figure 13. *Unsupervised hierarchical clustering of genes that were differentially expressed in BRAFi sensitive and resistant melanoma cell lines cultured under 2D and 3D conditions. (**A**) Hierarchical cluster analysis was performed on 1,049 differently expressed genes that were in BRAFi sensitive adherent cells (WM983A and WM983B) and spheroids (WM983A^{SPH} and WM983B^{SPH}). (**B**) Hierarchical cluster analysis of 297 significantly altered genes in BRAFi resistant spheroids (WM983A$^{SPH-RES}$ and WM983B$^{SPH-RES}$) compared to the resistant 2D cultured cells (WM983^{RES} and WM983B^{RES}). Cell lines are displayed horizontally, and genes displayed vertically. The colour of each cell represents the median-adjusted expression value of each gene. Red colour indicates increased expression and green colour represents decreased expression.*

In order, to determine the functional and biological significance of the differentially expressed 1,049 genes in the BRAFi-sensitive cells, we performed pathway enrichment analysis. This analysis revealed that the upregulated genes are involved in a variety of biological pathways

mainly in the regulation of cell cycle, G2/M checkpoints, p53 signalling pathway, DNA replication, Rho GTP-ase signalling, DNA repair, cellular senesce and other cancer-related signalling pathways (Figure 14. and Supplementary Table 3. see as attached file).

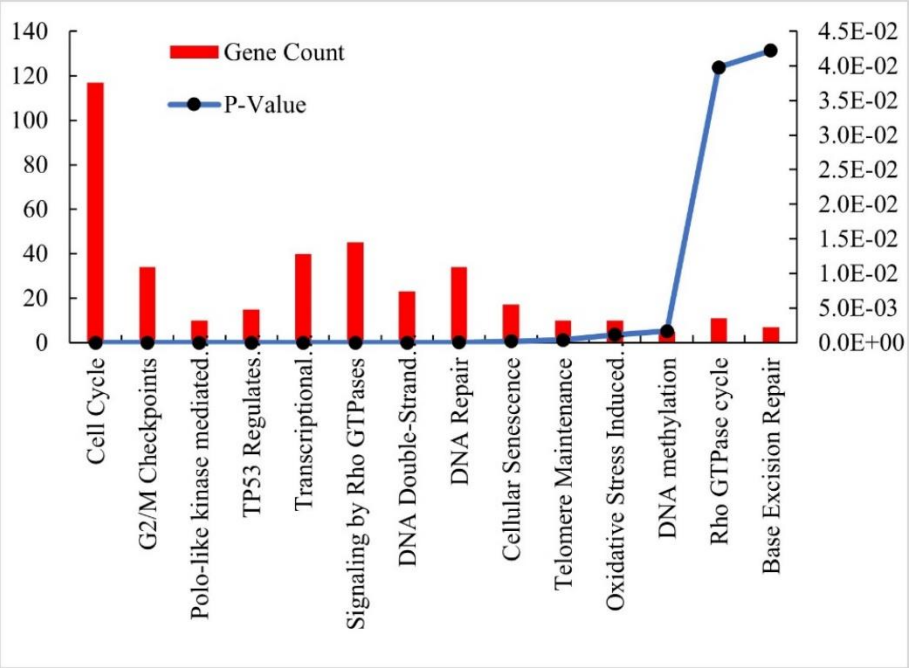

Figure 14.

Pathway enrichment analysis of the significantly upregulated genes in sensitive melanoma spheroid cells compared to the sensitive adherent cells. *The selection criteria included altered molecular pathways with at least five observations.*

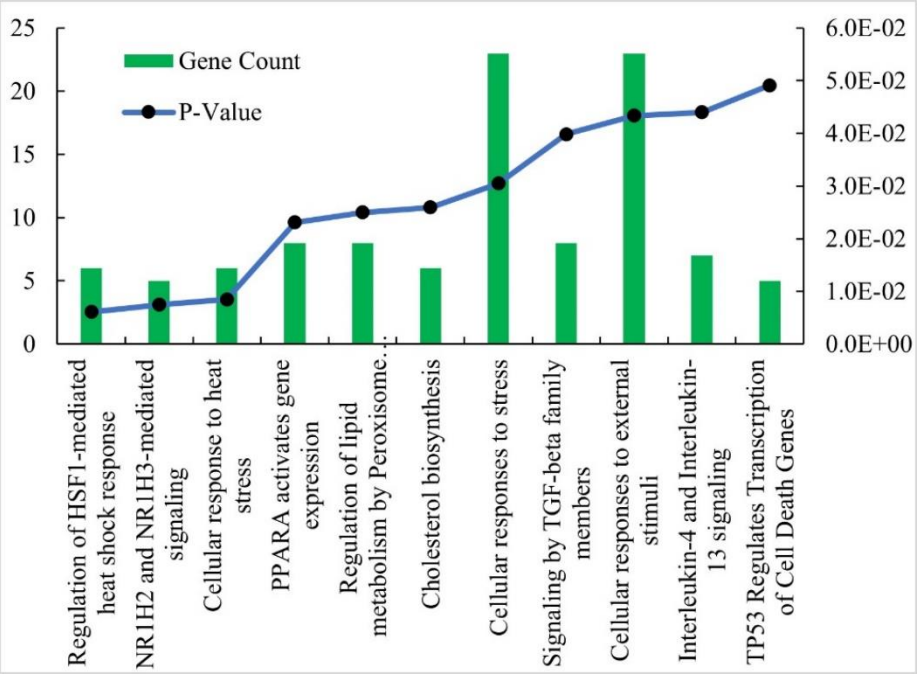

Figure 15.

Pathway analysis of the significantly downregulated genes in sensitive melanoma spheroid cells compared to the sensitive adherent cells. *The selection criteria included altered molecular pathways with at least five observations.*

The functional role of downregulated genes were clustered into the following pathways: cellular responses to external stimuli and stress, regulations of lipid metabolism by peroxisome proliferator-activated receptor alpha signalling by TGF-beta family members, interleukin-4 and interleukin-13 signalling, TP53 regulated transcription of cell death, and other cancer related pathways (Figure 15. and Supplementary Table 4. see in the Appendix).

The functional involvement of differently expressed genes between the sensitive adherent and spheroid cells was validated by using the web-accessible program: Database for Annotation, Visualization and Integrated Discovery (DAVID) https://david.ncifcrf.gov/.

Gene expression profiles of PLX4720 resistant melanoma cell lines cultured under 2D and in 3D conditions

BRAFi resistant melanoma cell lines were developed from the PLX4720 sensitive cell lines. The morphology of the resistant cell lines (Figure 16.) were different from the sensitive cells under 2D cell culturing conditions, showing elongated, fibroblast-like shape. The resistant cell lines grow similarly such as the sensitive cells during the spheroid formation.

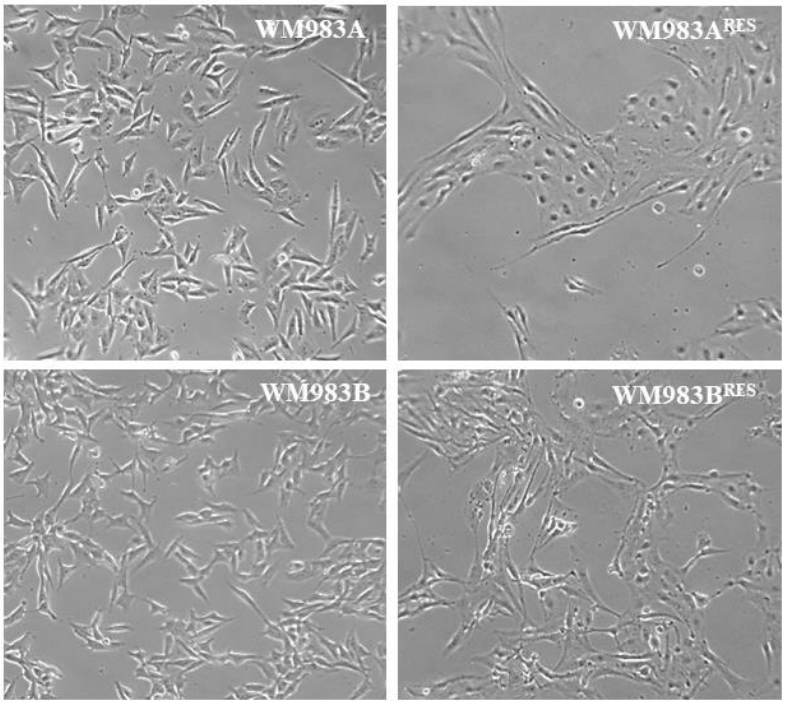

Figure 16. Microscopic images of the BRAFi (PLX4721) sensitive and resistant melanoma cell lines. *(100X magnification).*

Gene expression of the differently cultured BRAFi resistant cells was analysed using using the Affymetrix Human Gene 1.0 microarray. Gene expression analysis of the resistant adherent

melanoma cell lines (WM983A^{RES} and WM983B^{RES}) and their corresponding spheroids (WM983A$^{RES\text{-}SPH}$ and WM983B$^{RES\text{-}SPH}$) revealed 297 significantly differentially expressed genes (Supplementary Table 5. see in the Appendix). Unsupervised hierarchical cluster analysis of the resistant cell lines shows clear differences between the gene expression of the adherent cells and cells growing in the spheroids (Figure 13B)**.** Based on the analysis 72 genes were upregulated and 225 genes were downregulated in the resistant spheroids compared to the resistant adherent cells. Pathway analysis of the differentially downregulated genes revealed that these genes are mainly involved in cellular and mitochondrial translation, axon guidance pathway, ROBO receptor regulation and signalling, G2/M checkpoints, and other cancer related pathways (Figure 17.; downregulated genes are listed in Supplementary Table 6. see in the Appendix).

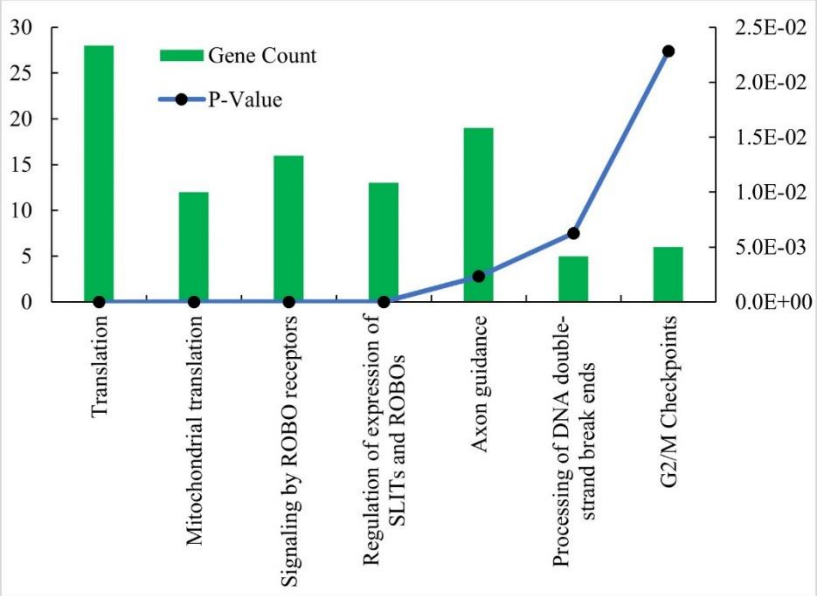

Figure 17. Pathway analysis of the significantly downregulated genes (*n = 225****) in resistant melanoma spheroid cells compared to the resistant adherent cells.*** *The selection criteria included altered molecular pathways with at least five observations.*

Upregulated genes in the resistant spheroids were not significantly enriched in any pathway according to our criteria.

Comparison of the gene expression signature of the BRAFi sensitive and resistant cell lines during spheroid formation

In order to describe similarities and differences of gene expression between the sensitive and resistant cell lines associated with spheroid formation, we compared the expression patterns of overexpressed

and downregulated genes of the WM983A and WM983B cell lines. Based on these data, we found 447 genes which were downregulated only in the sensitive- and 185 genes only in the resistant spheroids, respectively. The number of upregulated genes in the BRAFi sensitive spheroids was 556, while 66 genes were detected in the resistant spheroids. Using Venn diagram, we were able to identify 46 genes that were commonly altered in both types of spheroids (BRAFi sensitive and resistant) (Figure 18). The list of the 46 genes are summarized in Supplementary Table 7 (see in the Appendix). Forty shared genes were downregulated including *MMP16*, *IGF1R*, *FLOT1* and *CEP19* and the 6 commonly upregulated genes included the followings: *HIST1H2BM*, *DDAH1*, *UCP2*, *MBD3L5*, *DEFB124* and *MLF2*.

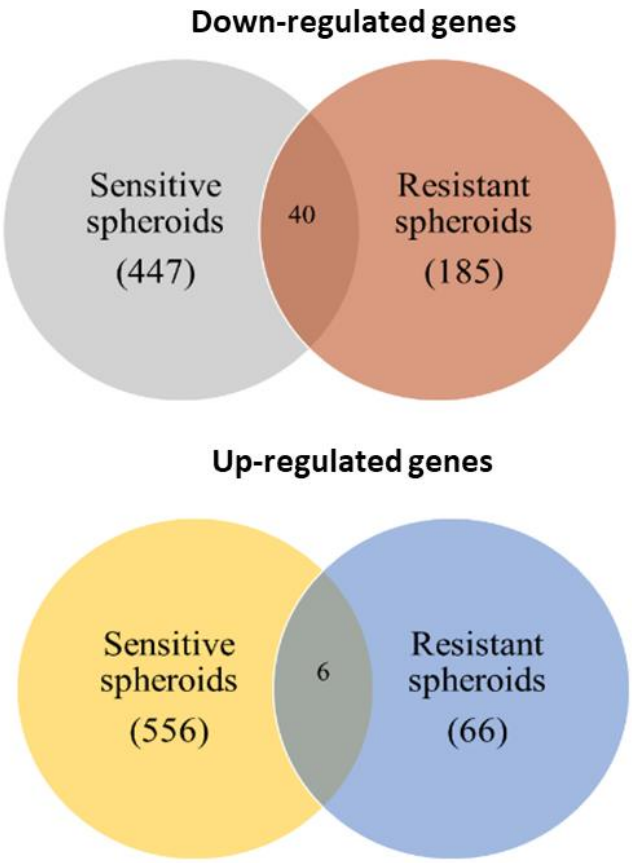

Figure 18. Differentially expressed genes in the BRAFi sensitive and resistant spheroids. *Venn diagrams showing the number of genes differentially expressed by the PLX4720 resistant spheroids (WM983A$^{RES\text{-}SPH}$ and WM983B$^{RES\text{-}SPH}$, compared to the corresponding sensitive spheroids: WM983A^{SPH} and WM983B^{SPH}). The diagram also shows the number of commonly upregulated (6) and downregulated (40) genes between the sensitive and resistant spheroids.*

Furthermore, we discovered an inverse gene expression trend for several genes when compared the gene expression differences between sensitive and resistant spheroids. Ten of the 712 genes that were upregulated in resistant spheroids were downregulated in sensitive spheroids but

upregulated in resistant ones (**Table 3**). In contrast, the expression of three genes (*SCN8A*, *RING1*, and *ABHD4*) was downregulated in sensitive spheroids while upregulated in resistant ones. Surprisingly, inversely expressed genes seem to be involved in the cell cycle (*CENPF*, *LOXL2*, and *BNIP3*) and epigenetic gene regulation (*HIST1H2BB*).

Table 3. Gene expression differences between sensitive and resistant spheroid formation of melanoma cells

No.	Gene symbol	Fold-change in sensitive spheroids[1]	P-value	Fold-change in resistant spheroid[2]	P-value
1	***HIST1H2BB***	**6.3**	0.035	**0.51**	0.030
2	***CENPF***	**4.37**	0.024	**0.54**	0.019
2	***LOXL2***	**4.36**	0.028	**0.62**	0.046
4	***BNIP3***	**1.91**	0.032	**0.32**	0.007
5	***DCUN1D1***	**1.89**	0.019	**0.47**	0.025
6	***CMSS1***	**1.68**	0.018	**0.59**	0.034
7	***SMC3***	**1.64**	0.007	**0.62**	0.042
8	***ZNF639***	**1.62**	0.023	**0.58**	0.030
9	***IKBIP***	**1.49**	0.046	**0.52**	0.048
10	***IFT57***	**1.4**	0.029	**0.61**	0.043
11	***SCN8A***	0.63	0.001	2.66	0.012
12	***RING1***	0.45	0.032	2.17	0.029
13	***ABHD4***	0.45	0.044	1.89	0.037

[1]*Comparison of gene expression between sensitive spheroids and sensitive monolayer cultures.*
[2]*Comparison of gene expression between resistant spheroids and resistant monolayer cultures.*
Red colour represents upregulated genes; green colour represents downregulated genes.

Validation of microarray data

To confirm gene expression changes, the Affymetrix microarray data were validated using quantitative real-time PCR (qRT-PCR) analysis. This study included eight genes (*ABHD4, HIST1H2BB, SCN8A, CMSS1, DCUN1D1, IKBIP, SMC3* and *ZNF639*). The primer sequences of the genes are listed in Supplementary Table 1A (see Appendix). Two of the selected genes were upregulated in the BRAFi sensitive spheroids and six were downregulated, the expression

of these genes were the opposite in the resistant 3D growing cells. The QRT-PCR data are summarized in Table 4**.**

Table 4. Relative mRNA expression of BRAFi sensitive and resistant cell lines cultured in 2D and 3D method detected by qRT-PCR

	WM983A (sensitive)		**WM983B (sensitive)**		**WM983A (resistant)**		**WM983B (resistant)**	
Genes	**2D**	**3D**	**2D**	**3D**	**2D**	**3D**	**2D**	**3D**
ABHD4	0.007	0.018	0.010	0.006	0.026	0.039	0.007	0.069
HIST1H2BB	0.196	0.167	0.184	0.211	0.112	0.013	0.038	0.025
SCN8A	0.000	0.000	0.000	0.006	0.009	0.012	0.004	0.011
CMSS1	0.057	0.045	0.030	0.055	0.027	0.010	0.009	0.021
DCUN1D1	0.062	0.068	0.105	0.112	0.033	0.019	0.020	0.032
IKBIP	0.015	0.033	0.038	0.011	0.015	0.012	0.012	0.023
SMC3	0.053	0.045	0.023	0.089	0.011	0.011	0.005	0.018
ZNF639	0.031	0.037	0.027	0.085	0.021	0.019	0.010	0.029

PCR data were analysed using Livak method with GAPDH as a reference gene.

Comparing the fold change gene expression levels that were generated using the Affymetrix microarray analysis with the qRT-PCR results, we found that five out of the eight genes tested (*DCUN1D1, CMSS1, ZNF639, ABHD4, and HIST1H2BB*) showed the same direction of gene expression changes in the sensitive- and in the resistant spheroids. In addition, we observed a strong correlation between the Affymetrix array and qRT-PCR expression data in case of the *ABHD4* and *SCN8A* genes ($R > 0.7$; P-value < 0.05).

Molecular alterations associated with acquired resistance during combined treatment of BRAF and MEK inhibitors on BRAFV600E mutated melanoma cell lines

The effect of BRAF and MEK inhibitor treatment on viability of melanoma cell lines

To investigate the effect of ENCO+BINI treatment on melanoma cell viability we used nine cell lines: 7 were carrying the $BRAF^{V600E}$ mutation, one had mutated $NRAS^{Q61L}$ (WM1366), and one (WM3211) was wild type for both oncogenes (**Table 2**). All cell cultures were treated with the combination of 1 μmol/l drug mixture for 72 hours. Only melanoma cells with BRAF mutations showed significant ($p < 0.05$) decrease in cell viability during the treatment (Figure 19).

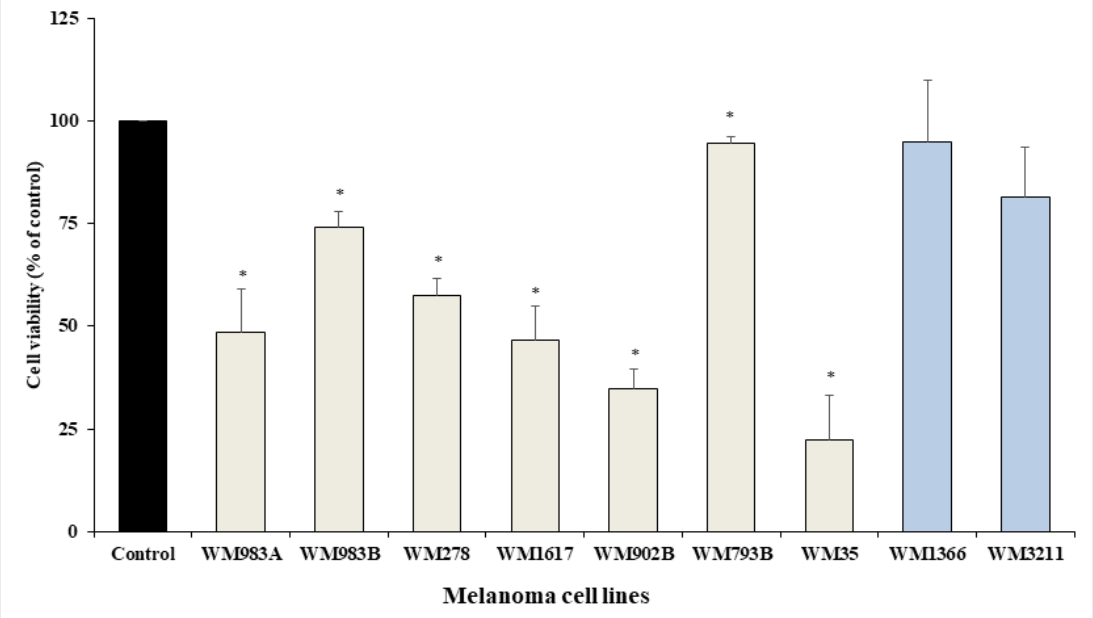

Figure 19. Growth-inhibitory effect of the combination treatment (ENCO+BINI) on melanoma cell lines. *Melanoma cell lines were treated with a 1 μmol/l drug mixture. After 72 hours of incubation, cell viability was measured using a WST-1 assay. Grey columns: BRAF mutated cells; blue columns wild-type for BRAF mutation. Control cells (black column) were treated with the vehicle of the drug mixture. The data are presented as the mean ± SD of three independent experiments. The asterisks indicate statistically significant differences (Mann–Whitney–Wilcoxon test; * p<0.05).*

The decrease of cell viability was not uniform within the *BRAF* mutated cell lines. More than 30% decrease was observed in five cell lines (WM35, WM902B, WM1617, WM983A and WM278). WM793B cells were also sensitive to the treatment, but the viability of these cells decreased by less than 10%. In contrast, we did not detect significant changes in cell viability

in the WM1366 *(NRAS^{Q61L}* mutant) and WM3211 (*BRAF/NRAS* wild-type) melanoma cell lines.

Establishment of ENCO+BINI resistant melanoma cell lines

To establish resistant cell line variants during combination treatment with BRAFi/MEKi, cells were treated continuously with increasing concentrations of ENCO+BINI mixture for 3-5 months starting at 1 nmol/l and the drug concentration was increased during every passage up to 200 nmol/l. First, we started with a lower concentration (1 nmol/l) to allow cells to develop resistance, which supports the maintenance of heterogeneity, and give enough time to adapt to the drug. During the establishment of the resistant cell lines, we observed that the cells originally showed no change at the starting concentration (1 nmol/l), cells stopped dividing only when the drug concentration was increased. After a few days, cells began to divide, and we observed that the morphology of the drug-sensitive cells differed from that of the ENCO/BINI-resistant cells. Similarly, to the PLX4720 treatment (see above) the resistant cells mainly displayed elongated phenotype (**Figure 20.**).

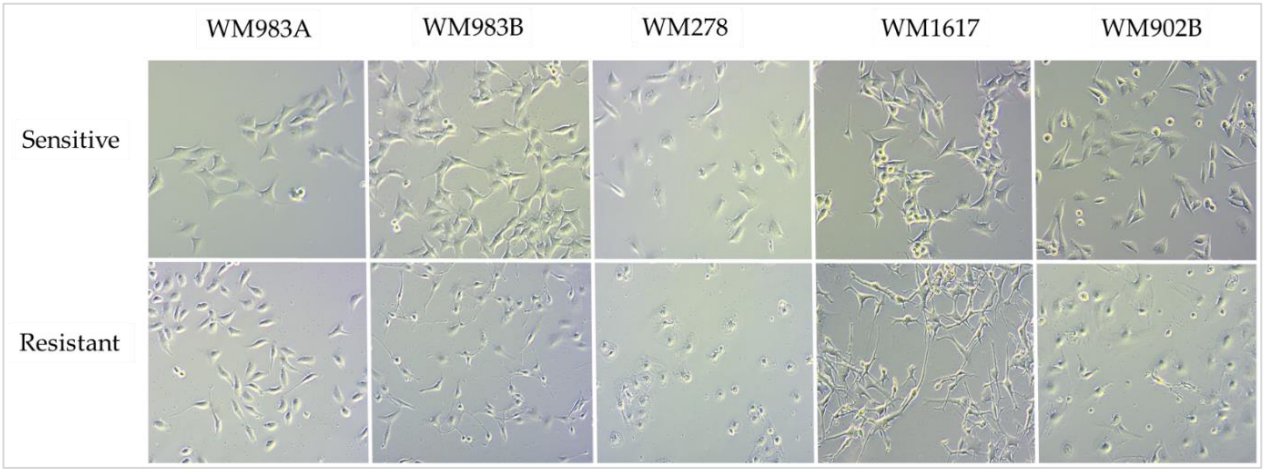

Figure 20. Photomicrographs of the ENCO+BINI-sensitive and resistant melanoma cell lines.
All images were captured at 100x magnification.

Because morphological changes frequently associated with the changes of cell invasiveness, and the resistant cells often show epithelial-mesenchymal transition (EMT), we determined the invasive characteristics of cell lines using a Matrigel invasion assay. Based on this experiment we observed that the WM983A^{E+BRes}, WM278^{E+BRes}, and WM902B^{E+BRes} cell lines had

significantly enhanced invasive properties compared to the corresponding sensitive cell lines (**Figure 21**).

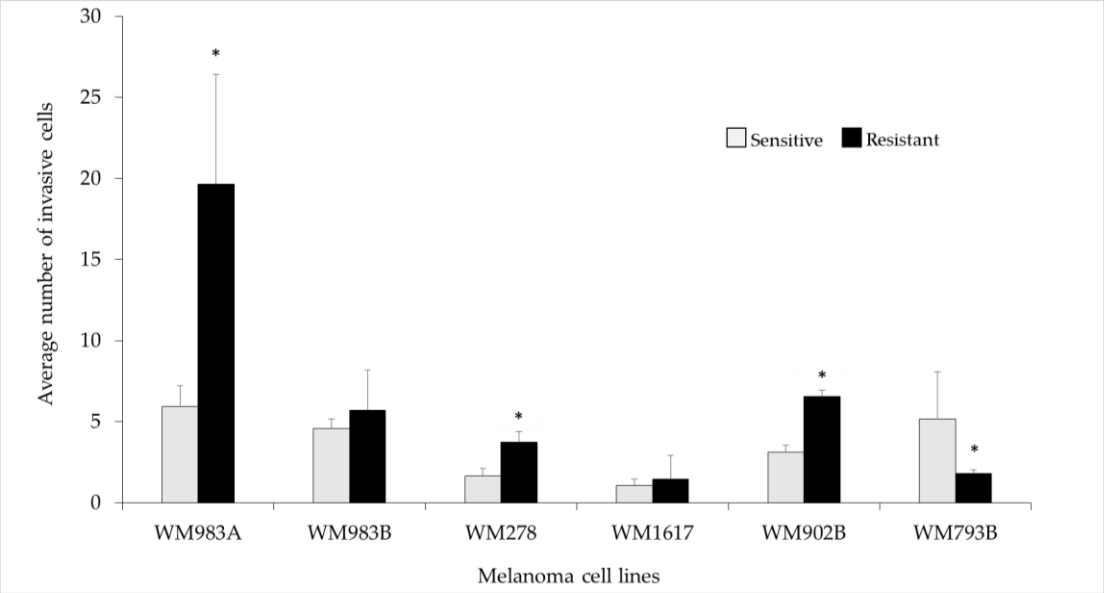

Figure 21. Invasive potential of the ENCO+BINI-resistant cell lines*. Light grey columns correspond to the sensitive, and black columns represent the inhibitor resistant cell lines. The asterisks indicates a statistically significant difference (Mann–Whitney–Wilcoxon test; * p<0.05).*

The invasive properties of two cell lines: WM983B^{E+BRes} and WM1617^{E+BRes} did not change significantly, both were originated from melanoma patient's metastatic lesion. We also observed, that the WM793B^{E+BRes} cells behaved differentially, these cells showed significantly decreased invasive potential compared to the sensitive cells.

Alterations of cancer related proteins associated with the development of acquired resistance during BRAFi/MEKi treatment

Protein expression changes during the development of the combined drug resistance were determined using Proteome Profiler Human XL Oncology Array. This array detects the expression of 84 cancer related proteins that have been spotted in duplicate on nitrocellulose membranes. These analyses showed a number of differentially expressed proteins in the resistant cell lines when compared to the drug sensitive pairs. Analysing the protein expressions, we did not observed similar trend among the drug resistant cell lines (WM983A, WM983B, WM278, WM1617, and WM902B). Proteins with detectable differences (>10%) in at least one cell line revealed 17 differentially expressed proteins in the resistant cell lines, data are summarized in **Figure 22**.

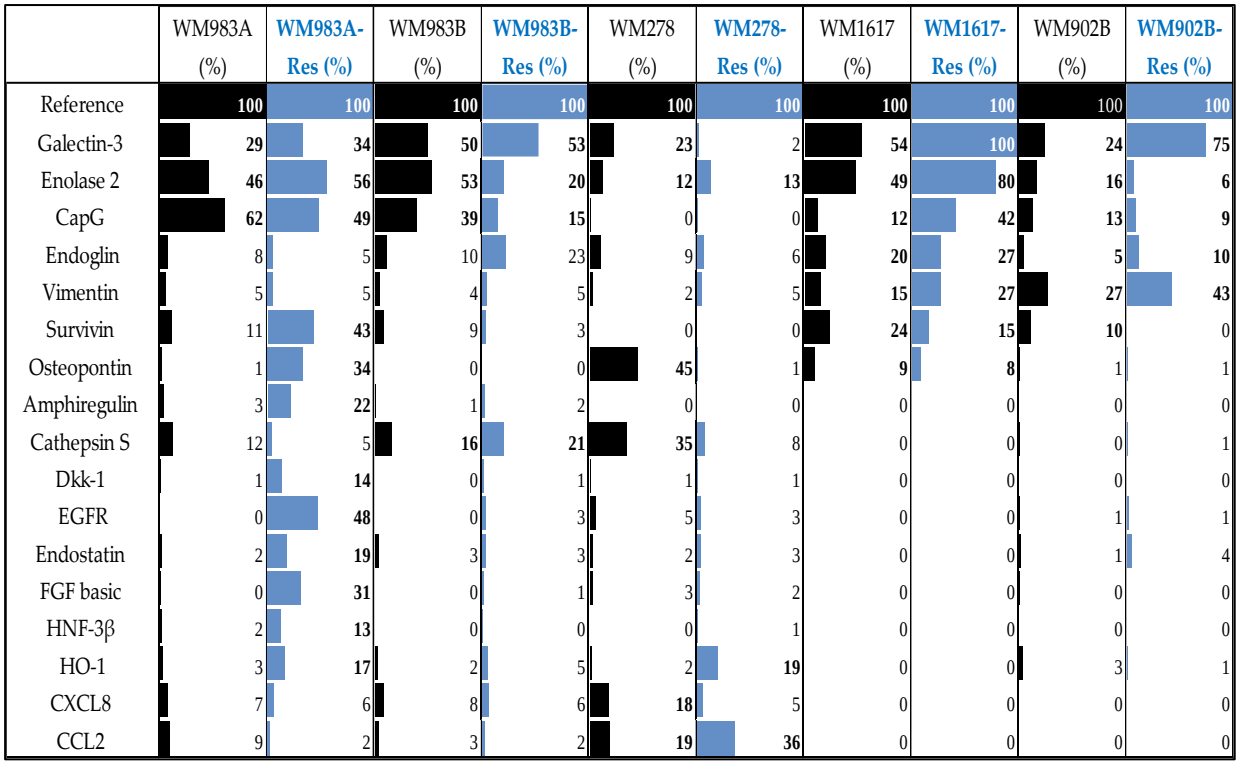

	WM983A (%)	WM983A-Res (%)	WM983B (%)	WM983B-Res (%)	WM278 (%)	WM278-Res (%)	WM1617 (%)	WM1617-Res (%)	WM902B (%)	WM902B-Res (%)
Reference	100	100	100	100	100	100	100	100	100	100
Galectin-3	29	34	50	53	23	2	54	100	24	75
Enolase 2	46	56	53	20	12	13	49	80	16	6
CapG	62	49	39	15	0	0	12	42	13	9
Endoglin	8	5	10	23	9	6	20	27	5	10
Vimentin	5	5	4	5	2	5	15	27	27	43
Survivin	11	43	9	3	0	0	24	15	10	0
Osteopontin	1	34	0	0	45	1	9	8	1	1
Amphiregulin	3	22	1	2	0	0	0	0	0	0
Cathepsin S	12	5	16	21	35	8	0	0	0	1
Dkk-1	1	14	0	1	1	1	0	0	0	0
EGFR	0	48	0	3	5	3	0	0	1	1
Endostatin	2	19	3	3	2	3	0	0	1	4
FGF basic	0	31	0	1	3	2	0	0	0	0
HNF-3β	2	13	0	0	0	1	0	0	0	0
HO-1	3	17	2	5	2	19	0	0	3	1
CXCL8	7	6	8	6	18	5	0	0	0	0
CCL2	9	2	3	2	19	36	0	0	0	0

Figure 22. Protein expression of BRAFi/MEKi sensitive (black columns) and resistant (blue columns) melanoma cell lines*. Proteins with detectable differences (>10%) in at least one cell line are shown. Protein expressions were analysed using the Proteome Profiler Human XL Oncology Array. Numbers next to the columns indicate the protein expression as a percentage of the intensity of the reference on the array. The intensity of the reference (added only the solvent of the drug) is displayed as 100%.*

The expression of the seventeen proteins were not uniform within the cell lines. Relatively high expression was seen for three proteins: Galectin, Enolase and CapG in the WM983A and WM983B drug-sensitive cell lines, the expression of these proteins were still high in the corresponding BRAFi/MEKi resistant cells. The largest number (twelve proteins) of differentially expressed proteins were recognized in the WM983A^{E+BRes} cells, compared to the sensitive ones. These proteins included Survivin, Osteopontin, Amphiregulin, EGFR, FGF and HO-1. Interestingly the expression of Galectin increased in four cell lines (between 34-100%) being the highest in the WM1617^{E+BRes} cells.

Effect of drug withdrawal on the viability and protein expression on ENCO/BINI resistant melanoma cell lines

Because drug-dependency is frequently observed during the development of acquired resistance, we cultured the resistant cell lines without the drug mixture, replacing the ENCO/BINI with DMSO (solvent of the drugs) and let the cells to grow for 72 hours. Surprisingly, the cell proliferation did not decrease significantly, and we did not observe significant cell death after 72 hours of the "drug holiday" in five cell lines (WM983A, WM983B, WM278, WM902B, and WM793B) compared to the control cell lines that were treated continuously with 200 nmol/l ENCO/BINI. These experiments clearly show that these *BRAF* mutated cell lines are not addictive to BRAFi/MEKi treatment (**Figure 23.**).

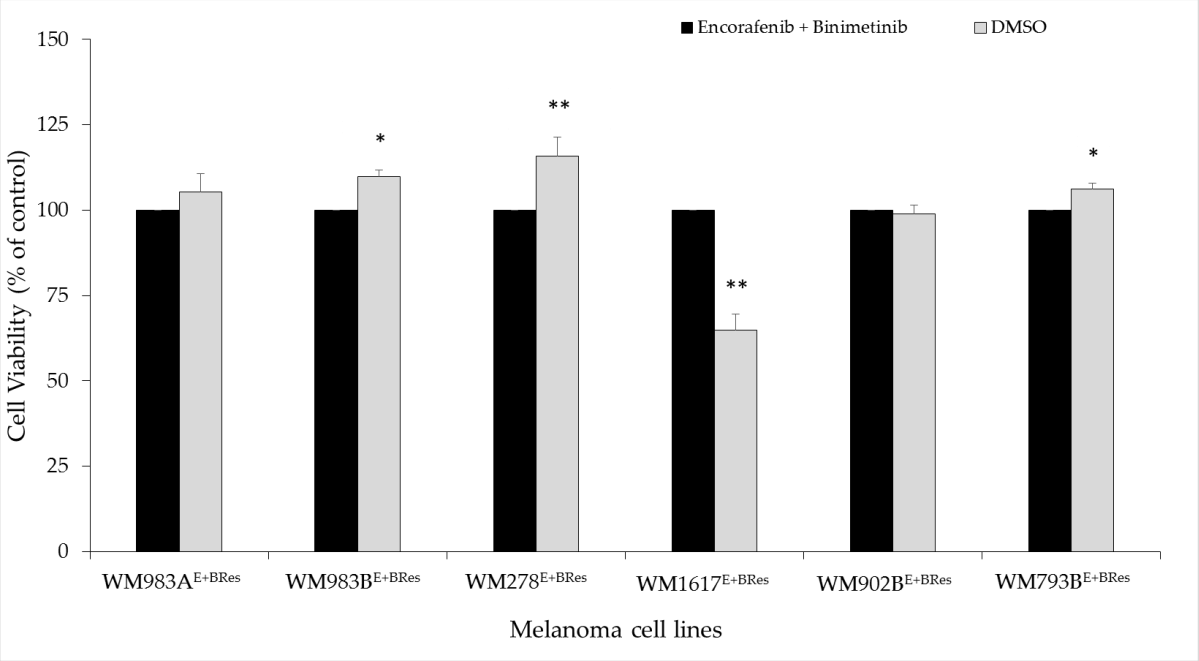

***Figure 23. Effect of drug withdrawal on the viability of ENCO/BINI resistant melanoma cell lines**. The viability of the resistant cells after drug withdrawal (grey columns) was compared to cells that were treated continuously with the drugs (cells grown in the presence of 200 nmol/l ENCO+BINI: black columns). The data are presented as the mean ± SD of three independent experiments. The asterisk indicates a statistically significant difference (Mann–Whitney–Wilcoxon test; * $p<0.05$, ** $p<0.001$).*

Moreover, the cell proliferation of 3 cell lines ($WM983B^{E+BRes}$, $WM278^{E+BRes}$, $WM793B^{E+BRes}$) increased significantly ($p<0.05$, $p<0.001$) during the "drug holiday", which indicates that these cells still experienced drug pressure. In contrast, opposite effect was detected in the

WM1617^{E+BRes} cell line, cells behaved differently and showed significantly reduced cell proliferation**.**

We selected three resistant cell lines (WM983A^{E+BRes}, WM983B^{E+BRes}, and WM1617^{E+BRes}) and cultured the cells in the absence of the drug combination for 10 days, then measured the cell viability and protein expression changes and compared to the control resistant cells (cells were continuously treated with the inhibitor mixture).

The drug holiday results are summarized on **Figure 24.**, which demonstrates noticeably that 3 days drug withdrawal significantly increased the cell viability in the resistant WM983B^{E+BRes} cells, and a slight increase was observed in the WM983A^{E+BRes} cells. The viability of cells did not decrease in these two cell lines even after 10 days of drug withdrawal, the viability of cells was above the continuously (control) drug treated cells. In contrast, the WM1617^{E+BRes} behaved differentially during this experiment, the viability of the cells decreased below 85% after 3 days drug removal and the decrease was significant after 10 days of days drug withdrawal compared to the control cells (**Figure 24**.).

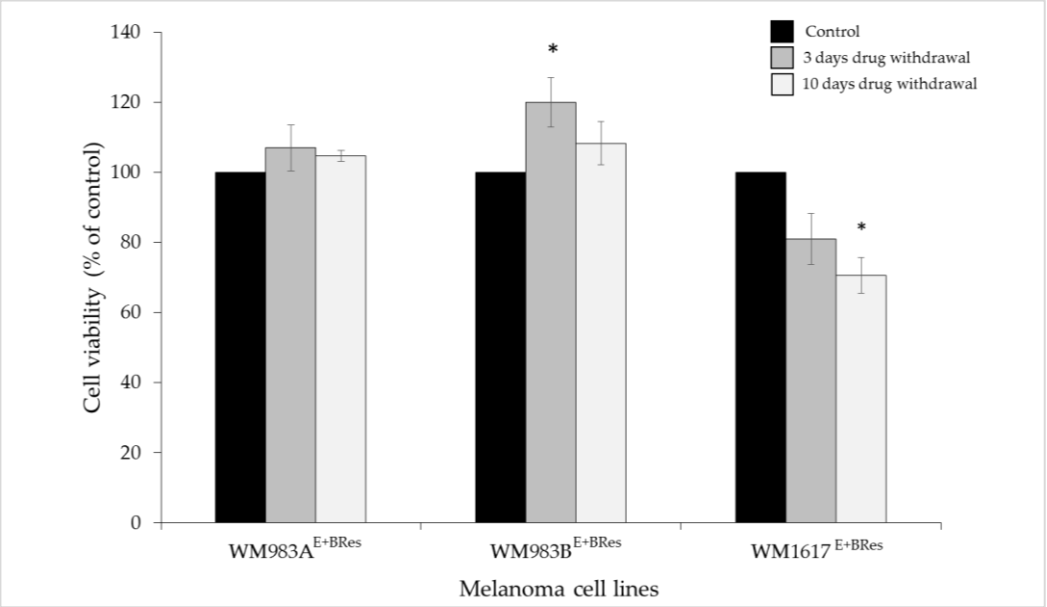

Figure 24. The effect of drug withdrawal on the viability of the resistant melanoma cell lines. *Control cells were grown in the presence of 200 nmol/l ENCO+BINI (black columns). Three days drug withdrawal (cells grown in the presence DMSO for 3 days: dark grey columns), 10 days drug withdrawal (cells grown in the presence DMSO for 10 days: light grey columns). The data are displayed as the mean ± SD of three independent experiments. The asterisk indicates statistically significant difference (Mann–Whitney–Wilcoxon test; * p<0.05).*

Protein expression changes of the resistant cell lines was investigated after the drug holiday using the same Proteome Profiler (Proteome Profiler Human XL Oncology Array) as we used before.

Drug withdrawal resulted in changes of seven proteins (CapG, Enolase 2, Galectin-3, HO-1/HMOX1, OPN, Survivin, and Vimentin) in all the resistant cell lines (**Figure 25**.).

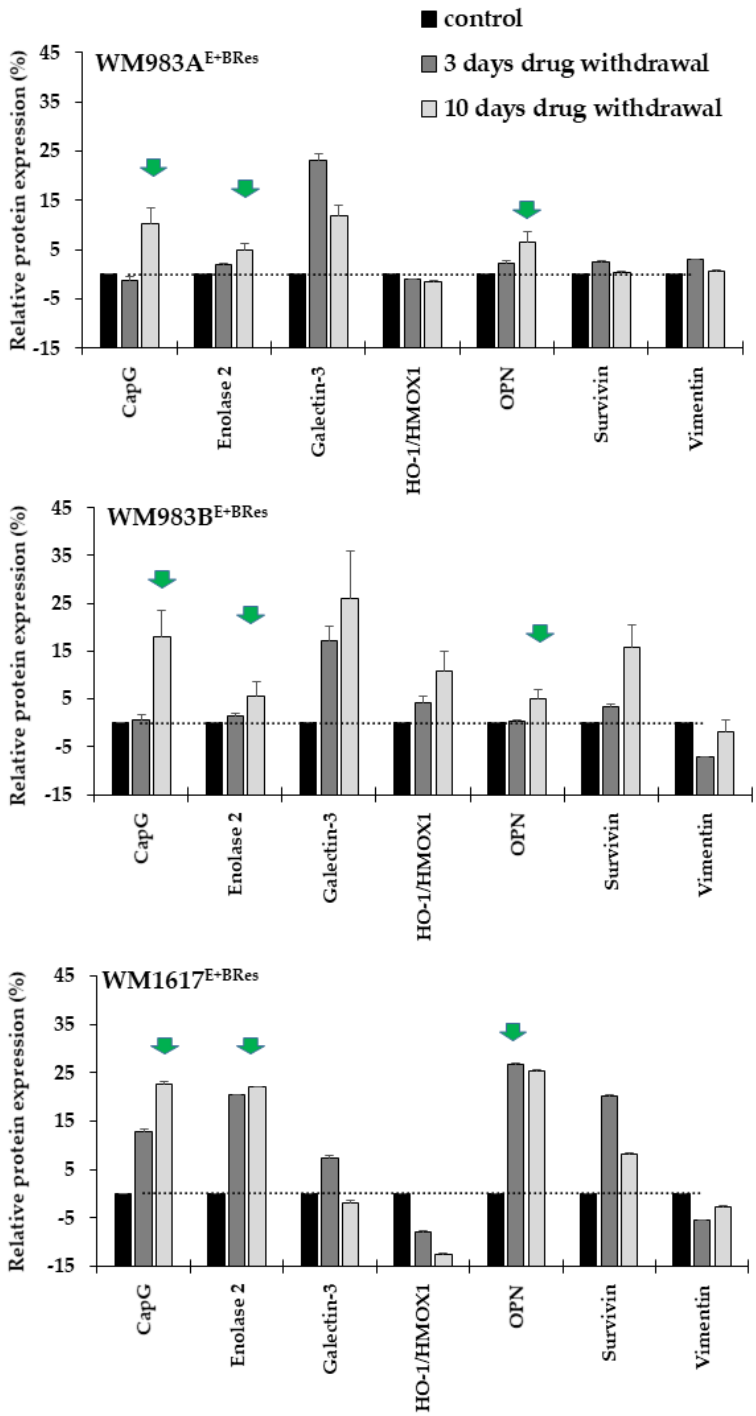

Figure 25. Protein expression changes of the BRAFi/MEKi resistant melanoma cell lines. *Control cells were grown in the presence of 200 nmol/l inhibitor mixture (black columns). Drug withdrawal for 3 days (cells grown in the presence DMSO: dark grey columns), drug withdrawal for 10 days' drug withdrawal (cells grown in the presence DMSO: light grey columns). Green arrows indicate uniform changes of 3 proteins.*

Ten days of "drug holiday" resulted in extensive changes in protein expression. The most uniform alterations were detected the increase expression of three proteins: CapG, Enolase 2 and OPN in all cell lines (green arrows on Figure 25.). Noticeable increase of galectin-3 were seen in the WM983A^{E+BRes} and WM983B^{E+BRes} cell lines. The expression of the vimentin protein did not changed after 10 days of drug withdrawal in any of the cell lines. Survivin expression was variable. It should be noted that in addition to the co-expressed proteins, several other proteins were also highly expressed, e.g. cathepsin S, EGFR, endoglin CXCL8, and CCL20 in the WM983B^{E+BRes} cells, and the HIF-1α, endoglin, P53, snail in the WM1617^{E+BRes} cells (***Supplementary Figure 1. see Appendix***).

Identification of differentially expressed genes in resistant melanoma cell lines using RNA-Seq analysis

We performed RNA-Seq analyses to determine gene expression patterns in five ENCO/BINI-sensitive and the corresponding resistant melanoma cell lines. The number of differentially expressed genes were 1591 (fold change ≥ 2, p-value ≤ 0.05). Majority of the genes were upregulated (n=1024), the number of downregulated transcripts was 567 in the resistant cell lines (Supplementary Table 8. added in separate files). The top 10 up-and downregulated genes are listed in **Table 5**.

Table 5. Top 10 differentially expressed genes in BRAFi/MEKi resistant melanoma cell lines

Upregulated genes			**Downregulated genes**		
Gene symbol	**Fold change**	**P-value**	**Gene symbol**	**Fold change**	**P-value**
CXCL12	73.055	0.030	*DMRT2*	-36.360	0.004
COL5A1	45.342	0.009	*MRGPRX4*	-26.686	0.002
ALPK2	37.803	0.005	*TRIM51*	-23.160	0.003
ABCC3	22.176	0.005	*CTD-2207A17.1*	-23.002	0.049
CHST15	21.430	0.021	*RP4-718J7.4*	-21.898	0.018
RP11-326A19.5	21.394	0.033	*VEPH1*	-20.866	0.000
LAMA5	21.264	0.010	*RP11-459E5.1*	-20.773	0.011
SAMD11	20.976	0.003	*GJB1*	-20.765	0.028
RP11-54O7.3	20.856	0.004	*ART3*	-20.169	0.015
HHIPL2	20.509	0.004	*FABP7*	-19.772	0.022

The fold changes of the 10 most highly expressed genes were above 20-fold, being the highest for *CXCL12*, *COL5A1* and *ALPK2* genes. While the most downregulated genes included *DMRT2*, *MRGPRX4*, *TRIM51* and *CTD-2207A17.1* genes.

Unsupervised hierarchical clustering of the differentially expressed genes (n=1591) distinguished between the BRAFi/MEKi-sensitive and resistant melanoma cell lines (**Figure 26**.). The drug-sensitive and the resistant cell lines were grouped together. The gene expression patterns of the sensitive cell lines were similar in all cell lines, but in case of one resistant cell ($WM1617^{E+BRes}$) we observed different pattern. Interestingly most of the genes that were downregulated in the inhibitor-sensitive cell lines became upregulated during acquiring the resistant phenotype, and the upregulated genes turned downregulated. A number of the upregulated genes did not change during the development of the drug resistance in the $WM1617^{E+BSen}$ cell line.

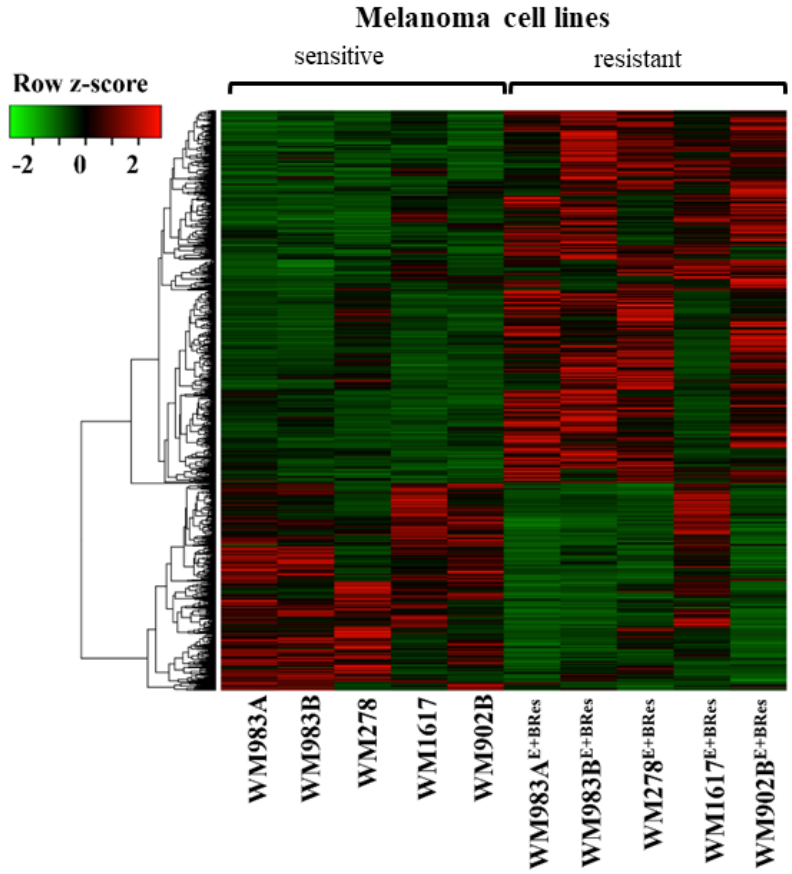

Figure 26. Unsupervised hierarchical clustering of the differentially expressed genes in BRAFi/MEKi-sensitive and resistant melanoma cell lines. *Cell lines are displayed horizontally, and genes vertically. The colour of each cell represents the median-adjusted expression value of each gene. Red represents increased gene expression, and green represents decreased gene expression.*

The top 30 downregulated genes are listed in ***Supplementary Table 10*** (see in the Appendix) and the top 30 upregulated are listed in ***Supplementary Table 11*** (see in the Appendix) for each cell line.

We validated the RNA-seq data by qRT-PCR in case of ten genes (upregulated genes: CXCL12, COL5A1, ALPK2, ABCC3, CHST15 and downregulated genes DMRT2, MRGPRX4, TRIM51, VEPH1 and GJB1). Seven of the ten genes examined (CXCL12, COL5A1, ABCC3, CHST15, DMRT2, MRGPRX4, and VEPH1) exhibited the same direction of gene expression in the parental and resistant cell lines.

Gene Set Enrichment Analysis of the differentially expressed genes

GSE analysis of the differentially expressed genes allowed us to define groups of genes that were significantly enriched and associated with common biological functions. Those included: regulation of cell proliferation, biological adhesion, regulation of cell death, response to drug, vasculature development, protein kinase activity, regulation of cell development, and regulation of chromosome organization ($p \leq 0.05$). The gene sets that correlated with drug resistance are summarized in **Table 6**.

Table 6. Gene sets correlated with the resistant phenotype

Name	ES	P-value
REGULATION OF CELL POPULATION PROLIFERATION[a]	0.219	0.013
BIOLOGICAL ADHESION[a]	0.190	0.027
APOPTOTIC PROCESS[a]	0.205	0.027
REGULATION OF CELL DEATH[a]	0.204	0.030
RESPONSE TO DRUG[a]	0.408	0.002
RESPONSE TO OXYGEN LEVELS[a]	0.367	0.008
VASCULATURE DEVELOPMENT[a]	0.251	0.010
PROTEIN KINASE ACTIVITY[a]	0.350	0.005
REGULATION OF CELL DEVELOPMENT[b]	-0.202	0.016
REGULATION OF CHROMOSOME ORGANIZATION[b]	-0.343	0.035
REGENERATION[b]	-0.365	0.039
GLIAL CELL DIFFERENTIATION[b]	-0.304	0.049

ES – Enrichment score, a – positive correlation (light grey rows), b – negative correlation (dark grey rows)

We performed Gene Ontology (GO) analysis of the differentially expressed genes and found numerous significantly (p-value ≤ 0.001) enriched GO terms grouped into biological processes (n=194), molecular functions (n = 9), and cellular components (n = 6). The biological processes included cell adhesion, cell migration, axon guidance, response to drug, regulation of cell differentiation, and drug transport. Molecular functions included DNA-binding transcription activator activity, MAPK cascade, MAP kinase tyrosine/serine/threonine phosphatase activity and the cellular component was associated intrinsic component of plasma membrane, extracellular matrix (**Figure 27**).

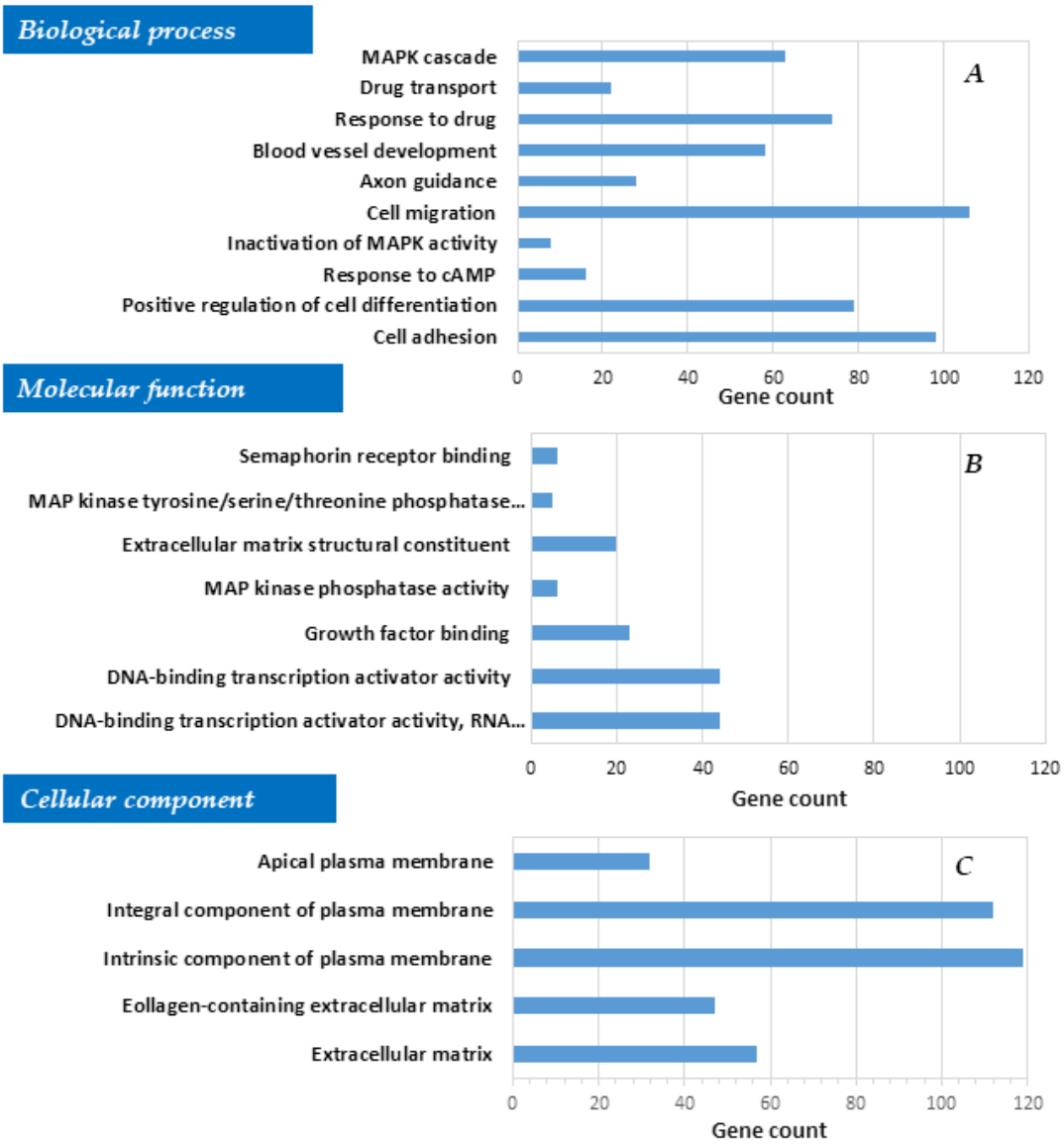

Figure 27. Gene Ontology analysis of differentially expressed genes in ENCO+BINI-resistant cell lines. *Significant differentially expressed genes with a fold change ≥ 2 and p-value ≤ 0.05 were analysed to determine the enriched Gene Ontology terms. A number of genes enriched are plotted for A) biological processes, B) molecular functions, and C) cellular components.*

Pathway analysis of differentially expressed genes

We performed pathway analysis of the differentially expressed gene in order to further understand the biological functions of genes during the development of drug-resistance. Pathway analyses were performed using the Molecular Signatures Database (MSigDB version 7.5.1.; *http://www.gsea-msigdb.org/gsea/msigdb/*). The results of this analysis highlighted that the differentially expressed genes were associated with different molecular pathways. The significantly altered pathways (including at least 5 upregulated genes) were functionally associated with ATF-2 and AP-1 transcription factor networks, extra cellular matrix, TNF-alpha signalling via NF-kβ, epithelial mesenchymal transition, KRAS signalling and reactive oxygen species pathway and are summarized in the upper part of **Table 7.**

Table 7. Involvement of differentially expressed genes in molecular pathways

Molecular pathway	P-value	Genes included
ATF-2 transcription factor network[a]	1.71E-06	*JDP2, MMP2, FOS, ATF3, SOCS3, JUN, JUNB, JUND, DUSP1, DUSP8*
Ensemble of genes encoding extracellular matrix and extracellular matrix-associated proteins[a]	3.14E-06	*A2M, FSTL3, ADAM8, CCL26, SVEP1, FBLN1, SPON2, AGT, MMP2, MMP11, VEGFD, LTBP4, CXCL12, AMBP, NID2, SEMA4B, SEMA3C, SFRP4, SEMA4G, POSTN, MUC1, BDNF, C1QL1, MMP24, GPC1, NTF4, ARTN, MMP25, COL18A1, OVGP1, PCSK6, ANXA8L1, WNT4, NTN5, COL1A1, COL5A1, WNT6, TSKU, CSF1, IGFBP5, IGFBP6, SRGN, EGLN3, PLXDC1, LAMA5, HTRA3, EDIL3, LGALS9, MMRN2*
AP-1 transcription factor network[a]	8.49E-06	*AGT, FOS, FOSB, ATF3, HLA-A, JUN, JUNB, JUND, BCL2L11, DUSP1*
LPA receptor-mediated events[a]	2.01E-04	*MAPT, MMP2, FOS, SRC, LPAR2, SLC9A3R2, JUN, LPAR1*
Epithelial mesenchymal transition[a]	6.13E-04	*IL32, OXTR, JUN, TAGLN, POSTN, NNMT, MAGEE1, GADD45B, BDNF, MMP2, TPM1, FBLN1, NID2, MYLK, FSTL3, COL1A1, SFRP4, CXCL12, COL5A1, BASP1, GPC1, EDIL3*
Reactive oxygen species pathway[a]	1.18E-02	*PDLIM1, G6PD, ABCC1, GPX3, TXNRD1, JUNB, FTL*
TNF-alpha signalling via NF-kB[a]	1.46E-02	*JUN, SMAD3, GADD45B, CSF1, CEBPD, DUSP1, TNFRSF9, FOS, SOCS3, ZFP36, NFIL3, NINJ1, BCL3, FOSB, MAP3K8, JUNB, ATF3*
KRAS signalling[b]	6.06E-04	*ST6GAL1, MAP3K1, CCL20, IL10RA, RGS16, LIF, EMP1, PLAT, ETV1, ETV4, DUSP6, ETV5, PCSK1N, TSPAN13, C3AR1*
IL-2/STAT5 signalling[b]	1.68E-03	*CD83, S100A1, IL10RA, RGS16, LIF, EMP1, ETV4, TIAM1, MAFF, BCL2, CTLA4, ITGA6, ICOS, SMPDL3A*
TNF-alpha signalling via NF-kB[b]	1.20E-02	*DUSP4, NR4A1, DUSP2, CD83, NR4A3, BCL2A1, CCL20, SPHK1, MAFF, LIF, TNC, PHLDA2*
Coagulation[b]	1.69E-02	*ACOX2, S100A1, MAFF, S100A13, PLAT, CTSE, DUSP6, MBL2, CPN1*
Oestrogen response [b]	2.78E-02	*TIAM1, MREG, INPP5F, ELOVL2, MYB, TFF3, BCL2, HR, RAB17, NBL1, SLC19A2*

a - molecular pathways linked to upregulated genes; b - molecular pathways linked to downregulated genes

The pathway analyses underlined that the upregulated genes were significantly associated with epithelial-mesenchymal transition, which promotes metastasis and is often associated with drug resistance. The downregulated genes listed in the lower part of **Table 7** and were associated with KRAS signalling, TNF-alpha signalling via NF-kB, inflammatory response, IL-2/STAT5 signalling, coagulation, and early oestrogen response. In order to identify the connection between the molecular pathways, we used a web-based visual analytics platform (NetworkAnalyst 3.0; *https://www.networkanalyst.ca*). **Figure 28.** displays that the upregulated genes are linked to cancer-related pathways including TNF signalling pathways, oestrogen signalling, breast cancer, as well as MAPK signalling pathways.

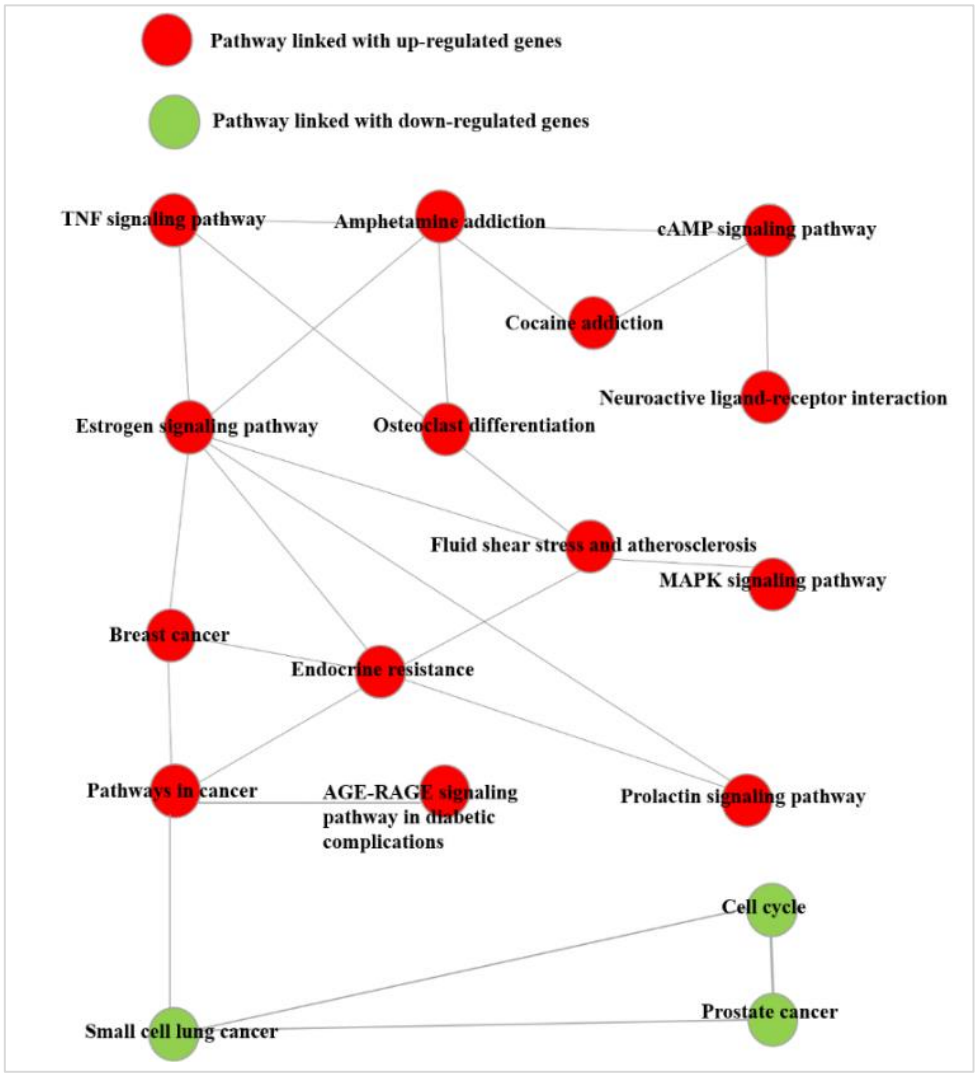

Figure 28. Interactions between the different signalling pathways associated with the development of acquired resistance (NetworkAnalyst 3.0). *Red dots represent upregulated pathways, and green dots represent downregulated pathways.*

In contrast, cell cycle pathway was downregulated. Both pathway linked with up-regulated genes and pathways linked with down-regulated genes are interconnected with signalling pathways related to cancer. Our data indicate that integrated pathway and network analysis of differentially expressed genes can help to understand the molecular mechanism underlying the development of acquired resistance, and might provide effective targets for the development of target specific successful treatment of melanoma.

Discussion

Despite several advancement and options in the treatment of malignant melanoma, the disease is still the leading cause of skin cancer associated death Majority of cutaneous melanoma are characterized with the dysregulation of the MAPK pathway (also known as the Ras/Raf/MEK/ERK pathway) due to activating mutations in the *B-RAF* and *RAS* genes and other genetic or epigenetic alterations [32,57]. Approximately 40-60 % of melanomas harbour activating mutations ($BRAF^{V600E}$ and $BRAF^{V600K}$) in the *BRAF* oncogene [23]. $BRAF^{V600E}$ mutation can achieve ~500-fold enhancement in the kinase activity to downstream mitogen-activated protein kinase signalling, which controls key cellular events, including proliferation, differentiation, migration, survival, and angiogenesis [107]. Targeted inhibition of the mutant protein is the most promising therapy option for melanoma patients with advanced disease [108]. Pre-clinical and clinical studies show that targeting *BRAF* using RAF-selective inhibitors results in remarkable tumour shrinkage in $BRAF^{V600E}$ mutant melanomas. A panel of BRAF inhibitors (vemurafenib, dabrafenib, encorafenib, etc.) and a series of MEK inhibitors (cobimetinib, trametinib, binimetinib, etc.) has revolutionized the treatment of melanoma patients [109], and recently combination of a BRAF and MEK inhibitor (Encorafenib: Braftovi™ + Binimetinib: Mektovi®) was approved by the FDA for melanoma patients with $BRAF^{V600E/K}$ mutation [110,111]. The combination of the small molecule inhibitors showed not only a high response rate, but a favourable toxicity profile and impressive progression-free survival (~16.9 months compared to the ~ 9 month BRAFi monotherapy) in patients with $BRAF^{V600E}$ mutation [110,112]. Unfortunately, even the high success of the different targeted therapies, acquired resistance develops in a large number of melanoma patients [113,114]. Despite many studies have addressed to clarify the molecular background of acquired drug-resistance and to identify new therapeutic target molecules to improve patient survival, the mechanism of resistance remains unclear. Antibodies targeting immune checkpoint inhibitors, including cytotoxic T-lymphocyte-associated antigen 4 (CTLA-4), programmed cell death (PD)-1, and PD-ligand 1 (PD-L1), has expanded dramatically [108,115,116]. A combination of BRAFi/MEKi and anti-PD-1 treatments (vemurafenib + cobimetinib + atezolizumab) was introduced for unresectable or metastatic melanoma with the $BRAF^{V600}$ mutation to improve survival and prevent resistance (approved by FDA in 2020) [108].

DISCUSSION

Cell culture is a widely used *in vitro* tool to reveal the molecular background of new anti-cancer drugs [117,118]. Most of the studies is based on conventional 2D cell cultures which have several limitations when compared to 3D tumour tissues, including differences in cellular communication, cell morphology, cell and extracellular medium interactions responsible for differentiation, proliferation, gene and protein expression, responsiveness to stimuli, drug metabolism and other cellular functions [119]. It has been observed that the gene expression pattern of cells is altered during conventional cell culturing due to the unlimited access to oxygen, metabolites, nutrients, and signalling molecules [119-122]. 3D spheroid cultures are improved cellular models that provide more contact surface for mechanical inputs for cell adhesion, accurate atmosphere for cell migration, differentiation, survival, and growth, variable access to oxygen, nutrients, metabolites, and signalling molecules [123,124]. Spheroid cell culture also reflects growth kinetics, metabolic activity and resistance to radiotherapy and chemotherapy more similar to tumour cells *in vivo* [125]. Structural modifications of the architecture of melanoma cells significantly effect gene expression of several genes, these genes play a role in melanoma progression and during the metastatic processes as described by [126].

One aims of our study was to generate reproducible three-dimensional melanoma spheroid models from BRAF inhibitor sensitive and resistant melanoma cell lines. Simultaneously, we aimed to compare the gene expression signature of the adherent and the spheroid cell lines in both drug-sensitive and drug-resistant model systems. This type of studies has not been performed before. During our study, we successfully developed spheroids from BRAF inhibitor (PLX4720) sensitive and resistant primary WM983A and metastatic WM983B tumour originated cell lines obtained from the same patient.

In parallel, we aimed to explore molecular alterations associated with acquired resistance during combinatorial treatment of $BRAF^{V600E}$ mutant melanoma cell lines using BRAF and MEK inhibitors. We established six human melanoma cell lines that became resistant during encorafenib (BRAF inhibitor) and binimetinib (MEK inhibitor) treatment and evaluated the invasive properties, studied the effect of "drug holiday" on cell proliferation and protein expression in the drug-sensitive and drug-resistant cell lines, investigated the gene expression characteristics underlying BRAFi/MEKi resistance using RNAseq analyses and defined the biological functions of the differently expressed genes associated with the development of acquired resistance. Development of 3D models for *in vitro* anti-cancer drug testing can give new insights into the behaviour and molecular alterations of cancer cells associated with

acquired resistance during drug treatment [127,128]. Breslin et al. have studied the applicability of 3D as well as monolayer cell cultures to drug sensitivity and resistance in breast cancer and concluded that the biological information represented by 3D and 2D cell cultures are considerably different [129]. Spheroids reveal higher innate resistance to anti-cancer drugs compared to cells cultured under standard 2D conditions. Ryabaya et al. reported that metformin increases anti-tumour activity of MEK inhibitor (binimetinib) in both conventional monolayer (2D) cultures and 3D models of human metastatic melanoma cells [130].

Several studies have reported differentially expressed genes associated with BRAF inhibitor resistance in melanoma cell lines, however, most of these studies are based on monolayer cell cultures [131]. The successful development of melanoma spheroids allowed us to compare gene expressions of the inhibitor sensitive and resistant 2D and 3D melanoma cell models. The expression profiles of the two BRAFi sensitive cell line models were highly different. The differently expressed genes in the sensitive spheroids included 562 upregulated and 487 downregulated genes. Among the top 10 overexpressed genes, we identified 4 genes (*SPC25, CCL2, CCNE2* and *PLK1*) that were previously described to have functional roles in cell migration and metastasis formation, in addition, these genes are all involved in cell cycle regulation through different pathways [132-134]. The *SPC5* gene encodes a protein that may be involved in kinetochore-microtubule interaction and spindle checkpoint activity, the *CCL2* gene is one of several cytokine genes clustered on the long arm of chromosome 17 and the related pathways include G-protein signalling Ras family GTPases in kinase cascades and ERK signalling. Vergani et al., using a panel of $BRAF^{V600E}$ mutant melanoma cell lines, patients plasma and tumours, have showed that *CCL2* (chemokine monocyte chemoattractant protein-1) production by melanoma cells is involved in resistance to a BRAF inhibitor PLX4032 and its inhibition may restore drug sensitivity [135]. The *CCNE2* and *PLK1*genes are immune evasion-related genes, *CCNE2* is essential for cell cycle regulation and responsible for promoting the G1/S phase transition as well as the progression through the G1 phase [136]. Recently, Su et al. observed a synergistic anti-proliferative response of combined treatment with the inhibition of PLK1 and NOTCH in human melanoma cells [137].

The top 10 downregulated genes are involved in various signalling pathways, such as the *CHN2* gene in the regulation of RAC1 activity, the *FOS* gene in EGFR signalling, *ITGA7* in integrin pathways and Akt signalling, and in tumour initiation and progression [138-140].

DISCUSSION

Our BRAFi resistant spheroid cells exhibited 297 differentially expressed genes compared to the adherent resistant cells. Downregulated genes (n=225) are mainly involved in different translation pathways including axon guidance pathway, ROBO receptor signalling, G2/M checkpoints and other cancer related pathways. It was described by Argast et al. that genes involved in axon guidance are inhibited by oncogenic B-Raf/MKK/ERK signalling in melanoma [141]. Genes of the axon guidance signalling pathway, including plexin B1 and semaphorin 3D genes, as well as R-RAS were down-regulated in resistant spheroids. Several studies have shown that plexin B1 is associated with tumour progression and emerging as clinical biomarker [142,143]. In contrast, a significant loss of the ROBO receptors was published in melanoma by Denk et al., these receptors are best known for mediating axon guidance through attraction or repulsion of growth cones, and their expression is known to correlate with tumour angiogenesis [144].

When we compared the gene expression between the sensitive and resistant spheroids we identified a set of genes that were differentially expressed in the resistant and sensitive spheroids of both cell lines. A certain group of genes were down- or upregulated only in the sensitive and resistant spheroids, respectively. We could identify 46 genes that were altered in both type of spheroids. Most of the common genes (n = 40) including *MMP16, IGF1R, FLOT1* and *CEP19* were downregulated and functionally involved in several types of cancers including melanoma [141,144,145]. Upregulated genes involved only six genes: *HIST1H2BM, DDAH1, UCP2, MBD3L5, DEFB124* and *MLF2*, these genes have roles in interleukin-2 signalling pathway and negative regulation of cell proliferation. Published data indicate that approximately 80% of melanoma cell lines express elevated levels of DDAH-1 protein, suggesting that *DDAH-1* may be a potential target for regulating nitric oxide production in melanoma cells [146]. *UCP2* plays a critical role in molecular mechanisms involved in carcinogenesis by altering cell proliferation. Furthermore, *UCP2* stimulates the cellular response to programmed cell death protein-1 blockade treatment in melanomas and contributes to effective anti-tumour responses [147]. *MLF2* (myeloid leukaemia factor 2) is a critical component of tumour initiation and metastasis formation in breast cancer [145]. Additionally, suppression of S-phase histone *HIST1H2BB* can improve treatment outcome in melanoma cells [148]. Three of the commonly downregulated genes *(MMP16, IGF1R*, and *FLOT1)* in our resistant spheroids are associated with the aggressive behaviour of melanoma [149,150]. Since these genes were found to be commonly altered in both sensitive and resistant spheroids, our

findings might point out that these genes are crucial for the development of melanoma spheroids.

During our analysis we discovered an inverse gene expression signature between the sensitive and resistant spheroids. The expression of three genes (*SCN8A, RING1 and ABHD4*) was downregulated in sensitive spheroids but elevated in the resistant cells. In contrast upregulation of 10 genes (*HIST1H2BB, CENPF*, *LOXL2*, *BNIP3*, *DCUN1D1*, *CMSS1*, *SMC3*, *ZNF639*, *IKBIP*, and *IFT57*) was detected in the sensitive spheroids, while downregulation of the same genes was detected in the resistant spheroids. The *SCN8A* gene (which encodes type VIII alpha subunit of voltage gated sodium channel) expression is considerably lower in COLORECTAL tumour tissue compared to the corresponding normal tissue [151] and only a limited information is available for melanoma, Carrithers et al. data suggest that intracellular sodium release mediated may regulate cellular invasion of melanoma cells [152]. Similar to the *SCN8A, RING1* gene (ring finger protein-1) was also inversely expressed between the sensitive and resistant spheroids. The *RING1* has been identified as a differentially expressed gene that plays an important role in epigenetic regulation in cancer [153]. Additionally, the transcriptional activity of this gene is implicated in the aggressive phenotypes of melanoma [154]. We also observed that the *ABHD4* gene was upregulated the in the BRAFi resistant and down-regulated in the sensitive spheroids. This gene was identified as a potential regulator of anoikis sensitivity (an endogenous death program) that is one of the primary events of tumour metastasis. Anoikis resistance is a critical feature of tumour cells that enables tumour cells to survive in foreign environment and to promote metastatic dissemination [155].

The ten genes that were upregulated in the sensitive and downregulated in the resistant spheroids are involved in tumour initiation and progression, but no detailed study was published yet in case of melanoma. According to the cBioPortal Cancer Genomics database, 17 canonical histone *H2B* genes, such as *HIST1H2B* and *HIST1H2BM*, contribute to cancer progression [148], notwithstanding the direct function of these genes have not yet been recognized, and the direct role of the genes has not yet been described. According to Kruiswijk et al., *CENPF* may function as a cancer driver gene and play a role in cancer tumorigenesis [156]. *LOXL2* (Lysyl oxidase-like 2) plays an integral role in epithelial-mesenchymal transition by stabilizing *SNAI1* transcription factor, and it serves as a tumour promoter in human melanoma cells by increasing invasiveness, evasion of apoptosis, and proliferation [157]. There is also evidence that *LOXL2* overexpression can occur in primary and metastatic melanoma and in other types of cancer, and

it assumed that might have important role *in vivo* in the development of drug resistance [157]. Overexpression of hypoxia responsive protein *BNIP3* in cancerous cells is highly controversial as it has been reported to be associated with promoting cell death, as well as tumour suppression while simultaneously promoting tumour development [158,159]. The ubiquitin-like ligase, *DCUN1D1* represents a potential cancer driver gene that causes malignant transformation of squamous cells [160]. The study of Sarogni et al., have shown associations between *SMC3* gene expression and a number of cancers, including acute myeloid leukaemia and bladder cancer [161]. *ZNF639* (zinc-finger protein amplified in squamous cancer) gene are associated with oesophageal squamous cell carcinomas and *IFT57* (Intraflagellar Transport 57) was described lung cancer [162,163]. These differently expressed genes require more attention during the future experiments. Generally, these results underline the gene expression signature of spheroid formation and highlight important molecular pathways that are different between 2D and 3D cell culture.

Over the past few years, melanoma research has put an emphasis on the characterization of acquired resistance at the molecular level. These findings indicate significant gene expression changes in melanoma cells that may help to explain the emergence of acquired resistance to BRAFi. [164]. Genetic and epigenetic factors are both involved in the development of the resistance [57,165]. During the last decades, a number of new drugs have been developed, including BRAF antagonists, anti-cytotoxic T-lymphocyte-associated antigen 4 (CTLA-4), programmed cell death protein 1 (PD-1) antibodies and programmed cell death ligand 1 (PD-L1) [108,166]. The FDA has approved a new therapeutic treatment option for advanced stage melanoma patients with $BRAF^{V600}$ mutations combining anti-PD-1/anti-PD-L1 with anti-BRAF and anti-MEK. This combinatorial triple therapy includes atezolizumab (PD-L1 inhibitor) along with cobimetinib and vemurafenib [167].

Treatment of $BRAF^{V600}$ mutant advanced melanoma using the combination of BRAF (encorafenib) and MEK (binimetinib) inhibitors was introduced into the clinic in 2018 [116]. The combination of the dual-targeted inhibitors provides inspiring treatment options as a targeted therapy for patients with $BRAF^{V600}$-mutated melanoma with improved overall response [168,169]. However, despite impressive clinical successes, many patients are diagnosed with tumour recurrence and experience a more aggressive melanoma tumour after the initial response limiting the long-term therapeutic benefits. Unfortunately, acquired resistance to most of the drugs or drug combinations limits the number of patients with long-lasting responses.

DISCUSSION

Recently, a large number of studies has focused on identifying the underlying molecular mechanisms leading to the development of drug resistance, however, the molecular alterations in this process remain unclear. There is a very urgent need to identify common, resistance associated molecular targets in melanoma cells which would help to discover more effective treatment possibilities for this aggressive cancer. The novelty of our study is that we were able to develop encorafenib plus binimetinib resistant melanoma cell lines after continuous BRAFi/MEKi treatment and compare the gene and protein expression differences between the drug-sensitive and drug-resistant melanoma cells. Our results highlight a number of molecular changes that arise during the evolution of acquired resistance. In contrast to the monotherapy associated BRAFi resistance development [101], we also observed that intermittent dosing of the drug combination (ENCO+BINI) might not be beneficial for melanoma patients with a $BRAF^{V600E}$ mutation, this observation probably has clinical relevance.

In addition to molecular alterations, we detected morphological changes during the development of the resistant cells. BRAFi/MEKi resistant cells displayed elongated and spindle-shaped phenotype. Interestingly, one of the resistant cell lines ($WM1617^{E+BRes}$) displayed a unique morphology different from the others and this cell line behaved differently during the whole study. Morphological changes during the development of drug resistance was also described by others [101,170]. It has been observed that, in addition to altered morphology, drug-resistant cells frequently exhibit greater invasive potential. Similar to published data, we found that the invasive potential of the resistant cells was higher than that of the sensitive cells, with one exception ($WM793B^{E+BRes}$). In addition, using transcriptome analysis, we observed that numerous invasive markers, including MMP2, were substantially elevated (fold change = 3.135, p-value = 0.009) [171,172].

From a clinical point of view, discontinuation of targeted therapy is one of the most successful approaches to prevent or delay the acquisition of drug resistance. Several preclinical and clinical studies have suggested that periodic drug dosage may be clinically beneficial [101,173,174]. However, recently published experimental and clinical investigations have failed to establish the clinical benefits of interrupted drug dosing, and “drug holiday” has become highly controversial in terms of therapeutic improvement [174,175]. In a good agreement with these findings, our data show that ENCO + BINI drug-resistant cells are not drug-addicted and do not show considerably enhanced lethality following a "drug holiday" [176]. In summary, our data point out that intermittent treatment unlikely to increase the effectiveness of the combined

BRAFi/MEKi treatment, further research is needed to better understand intermittent drug dosing.

A number of molecular changes related to drug resistance have already been identified, including overexpression of *EGFR*, *PDGFR*, *HGF*, *IGF*, *CRAF*, *COT*, and *MITF* and downregulation of *STAG2* or *STAG3* genes [166,177]. We have previously published that BRAFi (PLX4720) resistance is associated with certain cancer-related proteins, as detected using the Proteome Profiler Human XL Oncology Array [101]. During the combination treatment, we extended our proteome profiler study to identify and compare the protein expression patterns associated with acquired resistance during BRAFi/MEKi treatment. Our protein expression analysis revealed several differentially expressed proteins in the double targeted resistant cell lines compared to their sensitive counterparts. These proteins clustered in a unique pattern; no similar expression signature was observed in the resistant cell lines.

Galectin expression was detected in all BRAFi/MEKi sensitive cell lines, and increased expression was seen in four of the five resistant cell lines. The expression of this protein was decreased in one line, and its expression was the highest in the WM1617^{E+BRes} cells, followed by the WM902B^{E+BRes} cells. Galectin-3 has many cancer related function, including cell adhesion, cell activation, cell cycle, apoptosis, cell growth and differentiation [178] and the expression of the protein is positively correlats with the metastatic potential of human melanoma cells and plays an important role in cell–matrix adhesion during melanoma progression [179]. The protein galectin-3, which acts as an anti-apoptotic agent, is implicated in the development of resistance to chemotherapeutics in breast cancer and in the development of acquired resistance in malignant melanomas [180]. Enolase was expressed in all sensitive and resistant cell lines, but the direction of expression changes was not uniform. The expression of this protein increased in two resistant lines (WM983B^{E+BRes} and WM1617^{E+BRes}) and decreased in the other three. Furthermore, Enolase 2 (Gamma-enolase) and CapG were expressed in at least two cell lines and the expression of these proteins varied greatly between cell lines. Interestingly, Enolase 2 and CapG are used as diagnostic tumour markers in the diagnosis and prognosis of many cancer types, and both proteins have been associated with cell proliferation, invasion, migration, and metastatic capacity in several types of cancer, including melanoma [181,182]. The high variability of protein expression between the resistant cell lines indicates the necessity for more personalized (patient-specific) treatment.

DISCUSSION

EMT is a complex mechanism that facilitates the switch of tumor cells from the epithelial to the mesenchymal phenotype, and this transition allows cells to migrate from the primary site [183]. The vimentin protein, which controls actin organization and is a well-known marker of EMT, was differentially expressed in four resistant cell lines, and noticeably high expression were detected in two cell lines (WM1617^{E+BRes} and WM902^{E+BRes}) in which galectin-3 was also highly expressed. The enhanced expression of the vimentin protein in our resistant cell lines was consistent with the findings of Molnár et al. [184].

Several pre-clinical studies have shown that discontinuation of treatment after the development of resistance may lead to tumour regression and, in many cases, can restore sensitivity to therapy [185]. This phenomenon is based on the concept that drug addiction in the absence of the drug causes a selection disadvantage in the resistant population. Indeed, in preclinical melanoma models, periodic treatment with BRAF inhibitors results in a longer-lasting therapeutic response compared to continuous therapy [173]. Recent clinical results, however, tend to show that intermittent BRAF inhibitor therapy is inferior to continuous targeted therapy, emphasizing the difficulty of translating dose and treatment regimens from animal model to patients [174]. Furthermore, different clinical studies suggest different treatment strategies for intermittent dosing and continuous treatment. On the one hand, intermittent dosing effectively manages vemurafenib-induced toxicities, improving drug tolerance and achieving or maintaining tumour shrinkage, while reduced dose continuous therapy is not [186]. The benefits of continuous versus intermittent drug dosing for patient survival are still controversial, it is not clear which molecular pathways are dominant in this phenomenon [175,187,188]. To explore the molecular changes associated with intermittent drug treatment, we first determined the viability of resistant cells removing the inhibitor combination, and analysed the protein expression alterations. We observed typical drug dependence in one cell line (WM1617^{E+BRes}) with significantly decreased cell viability after 10 days of drug withdrawal. Termination of the drug was associated with significantly decreased cell proliferation, indicating that the cells become addicted to the combination of BRAF and MEK inhibitors, exposing potential therapeutic vulnerabilities and points out that “drug withdrawal” could potentially be beneficial for therapeutic gains for melanoma patients [189] and can lead to improved survival rates and tumour regression [190]. In contrast, the other two resistant cell lines (WM983A^{E+BRes} and WM983B^{E+BRes}) exhibited increased proliferation following the “drug holiday”. Drug withdrawal resulted in protein expression changes in all three cell lines. Proteome profiler

analyses revealed seven proteins (CapG, enolase 2, galectin-3, HO-1/HMOX1, OPN, survivin, and vimentin) with altered expression after the removal of BRAFi/MEKi, some of those are well-known players in drug resistance [101,180,191-193]. However, this is the first study to shed light on the co-expression changes of proteins related to "drug holiday" in BRAFi/MEKi resistant melanoma cells.

Over the last decade, a number of studies have reported differentially expressed genes between drug-sensitive and drug-resistant cells after monotherapy using BRAF inhibitors [106,194]. Nevertheless, relatively little is known about molecular mechanisms involved in the development of acquired resistance to BRAFi/MEKi combinatorial treatment. Our RNA-seq analysis revealed almost 1600 differentially expressed genes that are probably linked to the development of BRAFi/MEKi resistance. Majority of the transcripts (n=1024) were overexpressed, the downregulated genes included 567 genes. Our pathway analysis has revealed significant correlations between upregulated genes and biological pathways such as the ATF-2 transcription factor network, the epithelial-mesenchymal transition, and the TNF-alpha signalling pathways. Within the top 10 overexpressed genes, the *COL5A1* gene (an ECM component) has been already reported to contribute to BRAFi resistance in melanoma cells during the treatment with PLX4720 BRAF inhibitor [195], and probably has a dominant role in the development of drug resistance. The other overexpressed genes are also associated with tumour progression and metastasis formation through different signalling pathways. For example, *ALPK2* is known to influence cell cycle as well as DNA repair mechanisms and acts as a tumour promoter in malignant cells [196], while *HHIPL2* is linked to gastric malignancies via hedgehog signalling [197]. Furthermore, *SAMD11* expression was linked to radio-resistance in oesophageal cancer cells [198]. The *ABCC3* (ATP Binding Cassette Subfamily C Member 3) was characterized as one of the significantly upregulated gene in our resistant cells compared to their sensitive counterparts. The ATP-binding cassette (ABC) superfamily of active transporters is a well-known marker and potential target for multidrug-resistant cancers and is upregulated in drug-resistant cell lines [199]. However, until now, these upregulated genes have not been linked to BRAFi/MEKi resistance, which enhances the novelty of the present study.

The downregulated genes were associated with KRAS and IL-2/STAT5 signalling. Previously it was reported that some of the downregulated genes play a significant role in cell migration and tumour metastasis initiation and progression and all have been involved in tumorigenesis through different pathways; for example, *DMRT* and *FABP7* play important role in epithelial-

mesenchymal transition [200,201], while *VEPH1* suppresses vascularization by inhibiting AKT activation [202]. Hao Feng et al. found that downregulation of VEPH1 regulates the progression of melanoma cells with involvement in the TGF-β signalling pathway [200,201,203]. This signalling pathway is considered to act as a double-edged sword in cancer and TGF-β signalling may be a key factor in the development of resistance to chemotherapy, targeted therapy and immunotherapy [204].

In agreement with published data, we found novel long noncoding RNA transcripts (lncRNA), including *RP11-326A19.5, RP11-459E5.1,* and *RP4-718J7,* which support that lncRNA expression is associated with cancer in humans [205]. Through various molecular mechanisms, lncRNAs regulate a variety of biological processes in cancers and may serve as biomarkers of response to treatment. The *RP11-326A19.5* transcript was upregulated along with *RP11-459E5.1* and *RP4-718J7.4* transcripts in the sensitive cells which were downregulated in the resistant cell lines. Furthermore, it was reported previously that, several lncRNAs (*RP11-326A19.5* and *RP11-459E5.1*) have been linked to tumorigenesis and drug response [206,207]. In addition, *RP4-718J7.4* is associated with inflammation [208] and antibiotic resistance [209]. However, these transcripts are not well documented in BRAFi resistance at the field of melanoma. The present study is the first to suggest that several long non-coding gene transcripts might play a role in the development of BRAFi/MEKi resistance.

Even a large amount of data is published, it is hard to describe how to prevent drug resistance at this moment. Many different studies are going on to explore the most effective possible treatment combinations. We believe that the sequence of immunotherapy and combination of BRAF/MEK inhibitors would be the most effective option. One of the future directions is to explore the underlying mechanisms of acquired drug resistance and strategies for the different drug combinations. Probably the most beneficial approach will be to discover key molecules and molecular pathways that are differentially expressed between sensitive and resistant cells to prevent drug resistance and develop targeted drugs against the functionally relevant molecules.

Another prospective way to prevent drug resistance might be to combine chemotherapy with BRAF inhibitors, which is currently under preclinical development [210]. However, we believe that to expand this approach - by incorporating the other treatment strategies (synthetic lethal drug combinations, sequential drug treatment, alternate dosing, and intermittent dosing) would be more beneficial. The preclinical investigation demonstrates that these treatment strategies

provide promising results. It is likely that the BRAF+MEK inhibitor and chemotherapy combination should be utilized in an alternate manner, or chemotherapy drugs should be used during the "drug holiday" of BRAF+MEK inhibitor treatment. This proposed treatment strategy is based on the idea that chemotherapeutic drugs cause DNA damage, which is frequently impaired by DNA-damage repair (DDR) mechanisms, rendering chemotherapy treatments ineffective. The BRAF+MEK inhibitor combination, on the other hand, limits activation of the DNA-damage response, resulting in synergistic impact of the chemotherapeutic drugs. Furthermore, this approach may offer significant promise in terms of lowering drug-induced adverse effects and prolonging progression-free survival. Both drugs have been studied and are well tolerated by patients.

There are already several proposed treatment methods which can lead to long-lasting responses, such as synthetic lethal drug combinations, sequential drug treatment, alternating dosing, multiple low doses, treating reversible resistance, and bystander effect. Among these, certain strategies have progressed to the clinical stage and are showing encouraging success. Once patients progressed following BRAF+MEK inhibitor treatment, a second-line treatment option is used, that is immunotherapy with an immune checkpoint inhibitor [211]. Probably a triple combination of BRAF, MEK, and ERK inhibitors at extremely low concentrations might be effective in preventing resistance. Low concentrations will restrict drug-induced toxicity, avoid parallel pathway activation, and diminish drug-induced mutation. Several current randomized clinical trials are being conducted to evaluate the most effective treatment sequence and drug dosage of immuno-oncology agents and targeted therapy for molecular target-defined subgroups of patients with *BRAF*-mutant melanoma [212]. The SECOMBIT study (Sequential Combo Immuno and Target Therapy) was intended to establish the greatest sequential method with ipilimumab plus nivolumab and encorafenib plus binimetinib. Another potential strategy is to use small interfering RNA to inhibit the expression of particular genes responsible for drug resistance (siRNA) [213]. However, the therapeutic implementation of this method is complicated by challenges in delivering siRNA into the cytoplasm of tumour cells without the use of viral vectors, which might induce immunological activation, mutation, or inflammation [214]. One potential technique to prevent resistance is alternating dosing. Biochemical investigations have shown that resistance to BRAF inhibitors in melanoma is associated with a significant increase in sensitivity to histone deacetylase (HDAC) inhibitors. A pilot trial in

patients with BRAF inhibitor–resistant melanoma indicated that short therapy with HDAC inhibitors eradicated the drug-resistant cell population [215].

In summary, our data provide the first insight into differently expressed genes that might be involved in spheroid formation in BRAFi sensitive and resistant melanoma cells. Generally, the results underline the molecular background of spheroid formation and highlight important molecular pathways that are different between traditional monolayer/adherent and 3D cell culture. The current data on the development of acquired resistance using combination of BRAF and MEK inhibitors, offer the first understanding into differentially expressed genes and provide protein expression patterns associated with a BRAFi/MEKi-resistant phenotype in melanoma cells. Our findings contribute to a better understanding of the complex mechanisms leading to acquired resistance during combined treatment of *BRAF*-mutant melanoma. However, further studies are needed to identify the key molecules and signalling pathways responsible for therapeutic escape during BRAFi/MEKi treatment and to prevent the initiation of acquired drug resistance in melanoma.

Summary

Despite intensive research efforts, which have significantly improved melanoma patient survival, therapy resistance to the targeted mono- and combined therapies remains unsolved problems. The major focus of our study was to investigate molecular alterations associated with acquired resistance in malignant melanoma cell line models. It has been observed that the gene expression pattern of cells is altered during conventional cell culturing due to the unlimited access to oxygen, metabolites, nutrients, and signalling molecules. One aims of our study was to generate reproducible three-dimensional melanoma spheroid models from BRAF inhibitor sensitive and resistant melanoma cell lines and compare the gene expression signatures of the differently cultured melanoma cells. Using Affymetrix Human Gene arrays, we determined the gene expression pattern of melanoma cell lines. We found a large number of differentially expressed genes between drug-sensitive cells grown under different cell cultures. Pathway analysis showed that the differently expressed genes were mainly associated with cell cycle, p53, and other cancer-related pathways. Drug-resistant cells grown under 2D and 3D cell culture conditions exhibited 297 differentially expressed genes (72 up- and 225 downregulated) and were linked to various pathways including cellular translation, axon guidance, and IGF1R signalling. In addition, 13 genes, including *DCUN1D1*, *CMSS1*, *ZNF639*, *ABHD4*, and *HIST1H2BB*, exhibited inverse expression between sensitive- and resistant spheroid, with functional role in anoikis resistance and cell cycle regulation.

In parallel, we explored molecular alterations associated with acquired resistance during combinatorial treatment of $BRAF^{V600E}$ mutant melanoma cell lines using BRAF and MEK inhibitors. After establishing six melanoma cell lines that became resistant during encorafenib (BRAFi) and binimetinib (MEKi) treatment we evaluated the invasive properties, studied the effect of “drug holiday” on cell proliferation and protein expression in the drug-sensitive and resistant cell lines, investigated the gene expression characteristics underlying BRAFi/MEKi resistance using RNAseq analyses and defined the biological functions of the differently expressed genes associated with the development of acquired resistance. We found that resistant cells changed their phenotype and had a higher invasive potential than sensitive cells. We observed that resistant cells did not develop drug dependency, which is in agreement with a recently published clinical study that suggests intermittent dosing might not be as beneficial as regular treatment. Using the Proteome Profiler Oncology Array, we identified cancer-related proteins that were differently expressed across sensitive and resistant cell lines, with no similar

pattern among the cell lines. Furthermore, transcriptome analysis revealed that the 1591 differentially expressed genes (1024 up- and 567 down-regulated genes) are functionally linked to a variety of biological functions, including epithelial-mesenchymal transition, and KRAS signalling, that may lead to resistance.

In summary, our data provide the first insight into differently expressed genes that might be involved in spheroid formation in BRAFi sensitive and resistant melanoma cells. The current data on the development of acquired resistance using combination of BRAF and MEK inhibitors, offer the first understanding into differentially expressed genes and provide protein expression patterns associated with a BRAFi/MEKi-resistant phenotype in melanoma cells. Our findings contribute to a better understanding of the complex mechanisms leading to acquired resistance during combined treatment of *BRAF*-mutant melanoma. However, further studies are needed to identify the key molecules and signalling pathways responsible for therapeutic escape during BRAFi/MEKi treatment and to prevent the initiation of acquired drug resistance in melanoma.

Main findings and results

This study aimed to investigate the effect of BRAFi (PLX4720) and BRAFi/MEKi (ENCO/BINI) on human melanoma cell lines.

I. Development and characterization of BRAF inhibitor resistant melanoma cell lines growing under traditional and 3D cell culture conditions

Generation of PLX4720 resistant cell lines and spheroid culture

- We successfully developed reproducible three-dimensional melanoma spheroid models from *BRAF*^{V600E} mutant melanoma cell lines that are sensitive and resistant to BRAFi.

Gene expression patterns of *BRAFi-sensitive cells* cultured in 2D and 3D conditions

- We found a total of 1049 significantly differentially expressed genes (562 upregulated and 487 downregulated) between 2D and 3D cultured BRAFi sensitive cells.
- These differentially expressed genes were involved in a variety of biological pathways, mainly in the regulation of cell cycle, G2/M checkpoints, p53 signalling pathway, cellular responses to external stimuli and stress, interleukin-4 and interleukin-13 signalling and other cancer-related signalling pathways.

Gene expression patterns of *BRAFi-resistant cells* cultured in 2D and 3D conditions

- We found the drug-resistant cells grown under 2D and 3D cell culture conditions exhibited 297 differentially expressed genes (72 upregulated and 225 downregulated).
- These differentially expressed genes were mainly involved in cellular and mitochondrial translation, axon guidance pathway, ROBO receptor regulation and signalling.

Gene expression patterns of *BRAFi sensitive-and resistant spheroid*

- We found that only 1% of genes expressing upregulations and 5.6% of genes expressing downregulations were commonly expressed between drug-sensitive and drug-resistant cells cultured in 3D environment.
- Furthermore, 13 genes (*HIST1H2BB, CENPF, LOXL2, BNIP3, DCUN1D1, CMSS1, SMC3, ZNF639, IKBIP, IFT57, SCN8A, RING1*, and *ABHD4*) with functional relevance in anoikis resistance and cell cycle regulation exhibited inverse expression between sensitive and resistant spheroid.

II. Molecular alterations associated with acquired resistance during combined treatment of BRAF and MEK inhibitors on BRAFV600E mutated melanoma cell lines

Characterisation of BRAFi/MEKi (ENCO/BINI) resistance cells

- We successfully developed the ENCO/BINI resistant melanoma cell lines.
- Drug-resistant melanoma cells had a higher invasive potential and acquired a spindle-like structure.

The effect of ENCO/BINI inhibitor treatment on viability of melanoma cell lines

- ENCO/BINI combination significantly inhibit the cell viability in only *BRAF*-mutant cell lines, but not in wild type cell lines.
- We also observed that the resistant cells behaved differently after the withdrawal of the inhibitors; five out of six were not drug addicted at all and did not exhibit significantly increased lethality. Additionally, one resistant cell line ($WM1617^{E+BRes}$) showed significantly decreased viability, indicating drug addiction.

Gene expression patterns of ENCO/BINI sensitive and resistant cell lines

- We found 1591 significantly differentially expressed genes (1024 upregulated and 567 downregulated) with functional in role cancer related pathways including ATF-2 and AP-1 transcription factor networks, extra cellular matrix, TNF-alpha signalling via NF-kβ, epithelial mesenchymal transition, KRAS signalling.

Protein array analysis of the ENCO/BINI sensitive and resistant melanoma cell lines

- We found several differentially expressed proteins, with no similar pattern among the cell lines. Furthermore, high expression of Galectin was observed in four resistant cell lines (WM983A, WM983B, WM1617, and WM902B) and decreased in counterpart drug-sensitive cells.
- Following drug withdrawal, Enolase 2, CapG, and OPN showed a consistent increase in expression following the 10 days of drug holiday.

Main key points of the study:

			Inhibitor treatment
	Sensitive Spheroid	**Resistant Spheroid**	**BRAFi (PLX4720)**
Comparison	Only 1% of upregulated- and 5.7% of down-regulated genes were commonly altered.		
	Sensitive and resistant spheroid following different molecular mechanism to form spheroid.		
	ABHD4, RING1 and SCN8A (Downregulated)	ABHD4, RING1 and SCN8A (Upregulated)	
Pathways analysis	Differently expressed genes were linked to cell cycle regulation.		
	Sensitive cells	**Resistant cell**	**BRAFi+MEKi (ENCO+BINI)**
Comparison	Less invasive	More invasive	
Effect of drug withdrawal	No drug addiction observed in resistant cell.		
	Consistent increase in protein expression of CapG, Enolase 2 and OPN following drug withdrawal in resistant cell		
Gene expression analysis	Top 5 downregulated genes (DMRT2, MRGPRX4, TRIM51, VEPH1 and GJB1).	Top 5 upregulated genes (CXCL12 COL5A1, ALPK2, ABCC3, and CHST15).	
Pathways analysis	Differently expressed gens were linked to EMT, TNF and KRAS signalling.		

All of the changes indicated in the table were detected in the resistant group as compared to the sensitive group. BRAFi - BRAF inhibitor, MEKi - MEK inhibitor, ENCO - Encorafenib, and BINI - Binimetinib.

References

1. Godar, D.E. Worldwide increasing incidences of cutaneous malignant melanoma. *J Skin Cancer* **2011**, *2011*, 858425, doi:10.1155/2011/858425.

2. Sung, H.; Ferlay, J.; Siegel, R.L.; Laversanne, M.; Soerjomataram, I.; Jemal, A.; Bray, F. Global cancer statistics 2020: GLOBOCAN estimates of incidence and mortality worldwide for 36 cancers in 185 countries. *CA: a cancer journal for clinicians* **2021**, doi:10.3322/caac.21660.

3. Leiter, U.; Keim, U.; Garbe, C. Epidemiology of Skin Cancer: Update 2019. *Adv Exp Med Biol* **2020**, *1268*, 123-139, doi:10.1007/978-3-030-46227-7_6.

4. Sample, A.; He, Y.-Y. Mechanisms and prevention of UV-induced melanoma. **2018**, *34*, 13-24, doi:https://doi.org/10.1111/phpp.12329.

5. Bennett, D.C. Genetics of melanoma progression: the rise and fall of cell senescence. *Pigment Cell Melanoma Res* **2016**, *29*, 122-140, doi:10.1111/pcmr.12422.

6. Hartman, M.L.; Sztiller-Sikorska, M.; Gajos-Michniewicz, A.; Czyz, M. Dissecting Mechanisms of Melanoma Resistance to BRAF and MEK Inhibitors Revealed Genetic and Non-Genetic Patient- and Drug-Specific Alterations and Remarkable Phenotypic Plasticity. *Cells* **2020**, *9*, doi:10.3390/cells9010142.

7. van Zeijl, M.C.; van den Eertwegh, A.J.; Haanen, J.B.; Wouters, M.W. (Neo)adjuvant systemic therapy for melanoma. *Eur J Surg Oncol* **2017**, *43*, 534-543, doi:10.1016/j.ejso.2016.07.001.

8. Batus, M.; Waheed, S.; Ruby, C.; Petersen, L.; Bines, S.D.; Kaufman, H.L. Optimal management of metastatic melanoma: current strategies and future directions. *Am J Clin Dermatol* **2013**, *14*, 179-194, doi:10.1007/s40257-013-0025-9.

9. Villanueva, M.T. Blocking BRAF to the BRIM. *Nature Reviews Clinical Oncology* **2014**, *11*, 179-179, doi:10.1038/nrclinonc.2014.32.

10. Halle, B.R.; Johnson, D.B. Defining and Targeting BRAF Mutations in Solid Tumors. *Curr Treat Options Oncol* **2021**, *22*, 30, doi:10.1007/s11864-021-00827-2.

11. Subbiah, V.; Baik, C.; Kirkwood, J.M. Clinical Development of BRAF plus MEK Inhibitor Combinations. *Trends Cancer* **2020**, *6*, 797-810, doi:10.1016/j.trecan.2020.05.009.

12. Steininger, J.; Gellrich, F.F.; Schulz, A.; Westphal, D.; Beissert, S.; Meier, F. Systemic Therapy of Metastatic Melanoma: On the Road to Cure. *Cancers* **2021**, *13*, 1430.

13. Warburton, L.; Meniawy, T.M.; Calapre, L.; Pereira, M.; McEvoy, A.; Ziman, M.; Gray, E.S.; Millward, M. Stopping targeted therapy for complete responders in advanced BRAF mutant melanoma. *Sci Rep* **2020**, *10*, 18878, doi:10.1038/s41598-020-75837-5.

14. Kiniwa, Y.; Okuyama, R. Recent advances in molecular targeted therapy for unresectable and metastatic BRAF-mutated melanoma. *Jpn J Clin Oncol* **2021**, *51*, 315-320, doi:10.1093/jjco/hyaa222.

15. Tas, F. Metastatic behavior in melanoma: timing, pattern, survival, and influencing factors. *J Oncol* **2012**, *2012*, 647684, doi:10.1155/2012/647684.

16. Damsky, W.E.; Rosenbaum, L.E.; Bosenberg, M. Decoding melanoma metastasis. *Cancers (Basel)* **2010**, *3*, 126-163, doi:10.3390/cancers3010126.

17. Davis, E.J.; Johnson, D.B.; Sosman, J.A.; Chandra, S. Melanoma: What do all the mutations mean? *Cancer* **2018**, *124*, 3490-3499, doi:10.1002/cncr.31345.

18. Reddy, B.Y.; Miller, D.M.; Tsao, H. Somatic driver mutations in melanoma. *Cancer* **2017**, *123*, 2104-2117, doi:10.1002/cncr.30593.

19. Potrony, M.; Badenas, C.; Aguilera, P.; Puig-Butille, J.A.; Carrera, C.; Malvehy, J.; Puig, S. Update in genetic susceptibility in melanoma. *Annals of translational medicine* **2015**, *3*, 210, doi:10.3978/j.issn.2305-5839.2015.08.11.

20. Alexandrov, L.B.; Nik-Zainal, S.; Wedge, D.C.; Aparicio, S.A.; Behjati, S.; Biankin, A.V.; Bignell, G.R.; Bolli, N.; Borg, A.; Borresen-Dale, A.L.; et al. Signatures of mutational processes in human cancer. *Nature* **2013**, *500*, 415-421, doi:10.1038/nature12477.

21. Craig, S.; Earnshaw, C.H.; Viros, A. Ultraviolet light and melanoma. *J Pathol* **2018**, *244*, 578-585, doi:10.1002/path.5039.

22. Shain, A.H.; Bastian, B.C. From melanocytes to melanomas. *Nat Rev Cancer* **2016**, *16*, 345-358, doi:10.1038/nrc.2016.37.

23. Antoni, D.; Burckel, H.; Josset, E.; Noel, G. Three-dimensional cell culture: a breakthrough in vivo. *International journal of molecular sciences* **2015**, *16*, 5517-5527, doi:10.3390/ijms16035517.

24. Sini, M.C.; Doneddu, V.; Paliogiannis, P.; Casula, M.; Colombino, M.; Manca, A.; Botti, G.; Ascierto, P.A.; Lissia, A.; Cossu, A.; et al. Genetic alterations in main candidate genes during melanoma progression. *Oncotarget* **2018**, *9*, 8531-8541, doi:10.18632/oncotarget.23989.

25. Olbryt, M.; Piglowski, W.; Rajczykowski, M.; Pfeifer, A.; Student, S.; Fiszer-Kierzkowska, A. Genetic Profiling of Advanced Melanoma: Candidate Mutations for Predicting Sensitivity and Resistance to Targeted Therapy. *Target Oncol* **2020**, *15*, 101-113, doi:10.1007/s11523-020-00695-0.

26. Huang, F.W.; Hodis, E.; Xu, M.J.; Kryukov, G.V.; Chin, L.; Garraway, L.A. Highly recurrent TERT promoter mutations in human melanoma. *Science (New York, N.Y.)* **2013**, *339*, 957-959, doi:10.1126/science.1229259.

27. Horn, S.; Figl, A.; Rachakonda, P.S.; Fischer, C.; Sucker, A.; Gast, A.; Kadel, S.; Moll, I.; Nagore, E.; Hemminki, K.; et al. TERT promoter mutations in familial and sporadic melanoma. *Science (New York, N.Y.)* **2013**, *339*, 959-961, doi:10.1126/science.1230062.

28. Palmieri, G.; Colombino, M.; Casula, M.; Sini, M.C.; Manca, A.; Pisano, M.; Paliogiannis, P.; Cossu, A. Molecular Landscape Profile of Melanoma. In *New Therapies in Advanced Cutaneous Malignancies*, Rutkowski, P., Mandalà, M., Eds.; Springer International Publishing: Cham, 2021; pp. 31-55.

29. Hayward, N.K.; Wilmott, J.S.; Waddell, N.; Johansson, P.A.; Field, M.A.; Nones, K.; Patch, A.M.; Kakavand, H.; Alexandrov, L.B.; Burke, H.; et al. Whole-genome landscapes of major melanoma subtypes. *Nature* **2017**, *545*, 175-180, doi:10.1038/nature22071.

30. Yingjuan, W.; Li, Z.; Wei, C.; Xiaoyuan, W. Identification of prognostic genes and construction of a novel gene signature in the skin melanoma based on the tumor microenvironment. *Medicine (Baltimore)* **2021**, *100*, e26017, doi:10.1097/MD.0000000000026017.

31. Grzywa, T.M.; Paskal, W.; Włodarski, P.K. Intratumor and Intertumor Heterogeneity in Melanoma. *Transl Oncol* **2017**, *10*, 956-975, doi:10.1016/j.tranon.2017.09.007.

32. Schadendorf, D.; Fisher, D.E.; Garbe, C.; Gershenwald, J.E.; Grob, J.J.; Halpern, A.; Herlyn, M.; Marchetti, M.A.; McArthur, G.; Ribas, A.; et al. Melanoma. *Nat Rev Dis Primers* **2015**, *1*, 15003, doi:10.1038/nrdp.2015.3.

33. Mozūraitienė, J.; Bielskienė, K.; Atkočius, V.; Labeikytė, D. Molecular alterations in signal pathways of melanoma and new personalized treatment strategies: Targeting of Notch. *Medicina* **2015**, *51*, 133-145, doi:https://doi.org/10.1016/j.medici.2015.06.002.

34. Rossi, A.; Roberto, M.; Panebianco, M.; Botticelli, A.; Mazzuca, F.; Marchetti, P. Drug resistance of BRAF-mutant melanoma: Review of up-to-date mechanisms of action and promising targeted agents. *Eur J Pharmacol* **2019**, *862*, 172621, doi:10.1016/j.ejphar.2019.172621.

35. Teixido, C.; Castillo, P.; Martinez-Vila, C.; Arance, A.; Alos, L. Molecular Markers and Targets in Melanoma. *Cells* **2021**, *10*, 2320, doi:10.3390/cells10092320.

36. Motwani, J.; Eccles, M.R. Genetic and Genomic Pathways of Melanoma Development, Invasion and Metastasis. *Genes (Basel)* **2021**, *12*, 1543, doi:10.3390/genes12101543.

37. Motwani, J.; Eccles, M.R. Genetic and Genomic Pathways of Melanoma Development, Invasion and Metastasis. *Genes* **2021**, *12*, 1543.

38. Harbst, K.; Jönsson, G. The Genetic Evolution of Melanoma. In *Melanoma*; Springer, Cham: 2018; pp. 105-114.

39. Paluncic, J.; Kovacevic, Z.; Jansson, P.J.; Kalinowski, D.; Merlot, A.M.; Huang, M.L.; Lok, H.C.; Sahni, S.; Lane, D.J.; Richardson, D.R. Roads to melanoma: Key pathways and emerging players in melanoma progression and oncogenic signaling. *Biochim Biophys Acta* **2016**, *1863*, 770-784, doi:10.1016/j.bbamcr.2016.01.025.

40. Kiuru, M.; Busam, K.J. The NF1 gene in tumor syndromes and melanoma. *Lab Invest* **2017**, *97*, 146-157, doi:10.1038/labinvest.2016.142.

41. Nissan, M.H.; Pratilas, C.A.; Jones, A.M.; Ramirez, R.; Won, H.; Liu, C.; Tiwari, S.; Kong, L.; Hanrahan, A.J.; Yao, Z.; et al. Loss of NF1 in Cutaneous Melanoma Is Associated with RAS Activation and MEK Dependence. *Cancer research* **2014**, *74*, 2340, doi:10.1158/0008-5472.CAN-13-2625.

42. Czarnecka, A.M.; Bartnik, E.; Fiedorowicz, M.; Rutkowski, P. Targeted Therapy in Melanoma and Mechanisms of Resistance. *Int J Mol Sci* **2020**, *21*, 4576, doi:10.3390/ijms21134576.

43. Heppt, M.V.; Siepmann, T.; Engel, J.; Schubert-Fritschle, G.; Eckel, R.; Mirlach, L.; Kirchner, T.; Jung, A.; Gesierich, A.; Ruzicka, T.; et al. Prognostic significance of BRAF and NRAS mutations in melanoma: a German study from routine care. *BMC Cancer* **2017**, *17*, 536, doi:10.1186/s12885-017-3529-5.

44. Raaijmakers, M.I.; Widmer, D.S.; Narechania, A.; Eichhoff, O.; Freiberger, S.N.; Wenzina, J.; Cheng, P.F.; Mihic-Probst, D.; Desalle, R.; Dummer, R.; et al. Co-existence of BRAF and NRAS driver mutations in the same melanoma cells results in heterogeneity of targeted therapy resistance. *Oncotarget* **2016**, *7*, 77163-77174, doi:10.18632/oncotarget.12848.

45. Bansal, R.; Nikiforov, M.A. Pathways of oncogene-induced senescence in human melanocytic cells. *Cell Cycle* **2010**, *9*, 2782-2788, doi:10.4161/cc.9.14.12551.

46. Davies, M.A. The role of the PI3K-AKT pathway in melanoma. *Cancer J* **2012**, *18*, 142-147, doi:10.1097/PPO.0b013e31824d448c.

47. Siroy, A.E.; Davies, M.A.; Lazar, A.J. The PI3K-AKT Pathway in Melanoma. In *Genetics of Melanoma*, Torres-Cabala, C.A., Curry, J.L., Eds.; Springer New York: New York, NY, 2016; pp. 165-180.

48. Parkman, G.L.; Foth, M.; Kircher, D.A.; Holmen, S.L.; McMahon, M. The role of PI3'-lipid signalling in melanoma initiation, progression and maintenance. *Exp Dermatol* **2022**, *31*, 43-56, doi:10.1111/exd.14489.

49. Kudchadkar, R. Novel Targeted Therapies for the Treatment of Metastatic Melanoma. *Ochsner Journal* **2010**, *10*, 117.

50. Kasakovski, D.; Skrygan, M.; Gambichler, T.; Susok, L. Advances in Targeting Cutaneous Melanoma. *Cancers (Basel)* **2021**, *13*, 2090, doi:10.3390/cancers13092090.

51. Lee, K.A.; Nathan, P. Cutaneous Melanoma - A Review of Systemic Therapies. *Acta Derm Venereol* **2020**, *100*, adv00141, doi:10.2340/00015555-3496.

52. Flaherty, K.T. Targeting metastatic melanoma. *Annu Rev Med* **2012**, *63*, 171-183, doi:10.1146/annurev-med-050410-105655.

53. Jenkins, R.W.; Fisher, D.E. Treatment of Advanced Melanoma in 2020 and Beyond. *J Invest Dermatol* **2021**, *141*, 23-31, doi:10.1016/j.jid.2020.03.943.

54. Steininger, J.; Gellrich, F.F.; Schulz, A.; Westphal, D.; Beissert, S.; Meier, F. Systemic Therapy of Metastatic Melanoma: On the Road to Cure. *Cancers (Basel)* **2021**, *13*, 1430, doi:10.3390/cancers13061430.

55. Steininger, J.; Gellrich, F.F.; Schulz, A.; Westphal, D.; Beissert, S.; Meier, F. Systemic Therapy of Metastatic Melanoma: On the Road to Cure. *Cancers (Basel)* **2021**, *13*, doi:10.3390/cancers13061430.

56. Chanda, M.; Cohen, M.S. Advances in the discovery and development of melanoma drug therapies. *Expert Opin Drug Discov* **2021**, *16*, 1319-1347, doi:10.1080/17460441.2021.1942834.

57. Schadendorf, D.; van Akkooi, A.C.J.; Berking, C.; Griewank, K.G.; Gutzmer, R.; Hauschild, A.; Stang, A.; Roesch, A.; Ugurel, S. Melanoma. *Lancet* **2018**, *392*, 971-984, doi:10.1016/S0140-6736(18)31559-9.

58. Ballantyne, A.D.; Garnock-Jones, K.P. Dabrafenib: first global approval. *Drugs* **2013**, *73*, 1367-1376, doi:10.1007/s40265-013-0095-2.

59. Ottaviano, M.; Giunta, E.F.; Tortora, M.; Curvietto, M.; Attademo, L.; Bosso, D.; Cardalesi, C.; Rosanova, M.; De Placido, P.; Pietroluongo, E.; et al. BRAF Gene and Melanoma: Back to the Future. *Int J Mol Sci* **2021**, *22*, 3474, doi:10.3390/ijms22073474.

60. Mackiewicz, J.; Mackiewicz, A. BRAF and MEK inhibitors in the era of immunotherapy in melanoma patients. *Contemp Oncol (Pozn)* **2018**, *22*, 68-72, doi:10.5114/wo.2018.73890.

61. Pelster, M.S.; Amaria, R.N. Combined targeted therapy and immunotherapy in melanoma: a review of the impact on the tumor microenvironment and outcomes of early clinical trials. *Ther Adv Med Oncol* **2019**, *11*, 1758835919830826, doi:10.1177/1758835919830826.

62. Livingstone, E.; Zimmer, L.; Vaubel, J.; Schadendorf, D. BRAF, MEK and KIT inhibitors for melanoma: adverse events and their management. *Chin Clin Oncol* **2014**, *3*, 29, doi:10.3978/j.issn.2304-3865.2014.03.03.

63. Rizos, H.; Menzies, A.M.; Pupo, G.M.; Carlino, M.S.; Fung, C.; Hyman, J.; Haydu, L.E.; Mijatov, B.; Becker, T.M.; Boyd, S.C.; et al. BRAF inhibitor resistance mechanisms in metastatic melanoma: spectrum and clinical impact. *Clin Cancer Res* **2014**, *20*, 1965-1977, doi:10.1158/1078-0432.CCR-13-3122.

64. Flaherty, K.T.; Robert, C.; Hersey, P.; Nathan, P.; Garbe, C.; Milhem, M.; Demidov, L.V.; Hassel, J.C.; Rutkowski, P.; Mohr, P.; et al. Improved survival with MEK inhibition in BRAF-mutated melanoma. *N Engl J Med* **2012**, *367*, 107-114, doi:10.1056/NEJMoa1203421.

65. Ascierto, P.A.; Schadendorf, D.; Berking, C.; Agarwala, S.S.; van Herpen, C.M.; Queirolo, P.; Blank, C.U.; Hauschild, A.; Beck, J.T.; St-Pierre, A.; et al. MEK162 for patients with advanced melanoma harbouring NRAS or Val600 BRAF mutations: a non-randomised, open-label phase 2 study. *Lancet Oncol* **2013**, *14*, 249-256, doi:10.1016/S1470-2045(13)70024-X.

66. Cheng, Y.; Tian, H. Current Development Status of MEK Inhibitors. *Molecules* **2017**, *22*, doi:10.3390/molecules22101551.

67. Chesnokov, M.S.; Khan, I.; Park, Y.; Ezell, J.; Mehta, G.; Yousif, A.; Hong, L.J.; Buckanovich, R.J.; Takahashi, A.; Chefetz, I. The MEK1/2 Pathway as a Therapeutic Target in High-Grade Serous Ovarian Carcinoma. *Cancers (Basel)* **2021**, *13*, doi:10.3390/cancers13061369.

68. Shirley, M. Encorafenib and Binimetinib: First Global Approvals. *Drugs* **2018**, *78*, 1277-1284, doi:10.1007/s40265-018-0963-x.

69. Heinzerling, L.; Eigentler, T.K.; Fluck, M.; Hassel, J.C.; Heller-Schenck, D.; Leipe, J.; Pauschinger, M.; Vogel, A.; Zimmer, L.; Gutzmer, R. Tolerability of BRAF/MEK inhibitor combinations: adverse event evaluation and management. *ESMO Open* **2019**, *4*, e000491, doi:10.1136/esmoopen-2019-000491.

70. Nguyen, K.; Hignett, E.; Khachemoune, A. Current and emerging treatment options for metastatic melanoma: a focused review. *Dermatol Online J* **2020**, *26*.

71. Zaremba, A.; Zimmer, L.; Griewank, K.G.; Ugurel, S.; Roesch, A.; Schadendorf, D.; Livingstone, E. [Immunotherapy for malignant melanoma]. *Internist (Berl)* **2020**, *61*, 669-675, doi:10.1007/s00108-020-00812-1.

72. Sharma, P.; Allison, J.P. The future of immune checkpoint therapy. *Science* **2015**, *348*, 56-61, doi:10.1126/science.aaa8172.

73. Janssen, L.M.E.; Ramsay, E.E.; Logsdon, C.D.; Overwijk, W.W. The immune system in cancer metastasis: friend or foe? *J Immunother Cancer* **2017**, *5*, 79, doi:10.1186/s40425-017-0283-9.

74. Feng, Z.; Yu, Q.; Zhang, T.; Tie, W.; Li, J.; Zhou, X. Updates on mechanistic insights and targeting of tumour metastasis. *J Cell Mol Med* **2020**, *24*, 2076-2086, doi:10.1111/jcmm.14931.

75. Gata, V.A.; Lisencu, C.I.; Vlad, C.I.; Piciu, D.; Irimie, A.; Achimas-Cadariu, P. Tumor infiltrating lymphocytes as a prognostic factor in malignant melanoma. Review of the literature. *J BUON* **2017**, *22*, 592-598.

76. Hodi, F.S.; O'Day, S.J.; McDermott, D.F.; Weber, R.W.; Sosman, J.A.; Haanen, J.B.; Gonzalez, R.; Robert, C.; Schadendorf, D.; Hassel, J.C.; et al. Improved survival with ipilimumab in patients with metastatic melanoma. *N Engl J Med* **2010**, *363*, 711-723, doi:10.1056/NEJMoa1003466.

77. Karimkhani, C.; Reddy, B.Y.; Dellavalle, R.P.; Sundararajan, S. Novel therapies for unresectable and metastatic melanoma. *BMJ* **2017**, *359*, j5174, doi:10.1136/bmj.j5174.

78. Van Allen, E.M.; Miao, D.; Schilling, B.; Shukla, S.A.; Blank, C.; Zimmer, L.; Sucker, A.; Hillen, U.; Foppen, M.H.G.; Goldinger, S.M.; et al. Genomic correlates of response to CTLA-4 blockade in metastatic melanoma. *Science* **2015**, *350*, 207-211, doi:10.1126/science.aad0095.

79. Wolchok, J.D.; Chiarion-Sileni, V.; Gonzalez, R.; Rutkowski, P.; Grob, J.J.; Cowey, C.L.; Lao, C.D.; Wagstaff, J.; Schadendorf, D.; Ferrucci, P.F.; et al. Overall Survival with Combined Nivolumab and Ipilimumab in Advanced Melanoma. *N Engl J Med* **2017**, *377*, 1345-1356, doi:10.1056/NEJMoa1709684.

80. Amaral, T.; Sinnberg, T.; Meier, F.; Krepler, C.; Levesque, M.; Niessner, H.; Garbe, C. The mitogen-activated protein kinase pathway in melanoma part I - Activation and primary resistance mechanisms to BRAF inhibition. *European journal of cancer (Oxford, England : 1990)* **2017**, *73*, 85-92, doi:10.1016/j.ejca.2016.12.010.

81. Villanueva, J.; Infante, J.R.; Krepler, C.; Reyes-Uribe, P.; Samanta, M.; Chen, H.Y.; Li, B.; Swoboda, R.K.; Wilson, M.; Vultur, A.; et al. Concurrent MEK2 mutation and BRAF amplification confer resistance to BRAF and MEK inhibitors in melanoma. *Cell reports* **2013**, *4*, 1090-1099, doi:10.1016/j.celrep.2013.08.023.

82. Dulgar, O.; Kutuk, T.; Eroglu, Z. Mechanisms of Resistance to BRAF-Targeted Melanoma Therapies. *American Journal of Clinical Dermatology* **2021**, *22*, 1-10, doi:10.1007/s40257-020-00572-6.

83. Kwong, L.N.; Davies, M.A. Targeted therapy for melanoma: rational combinatorial approaches. *Oncogene* **2014**, *33*, 1-9, doi:10.1038/onc.2013.34.

84. Solit, D.B.; Rosen, N. Resistance to BRAF inhibition in melanomas. *The New England journal of medicine* **2011**, *364*, 772-774, doi:10.1056/NEJMcibr1013704.

85. Tian, Y.; Guo, W. A Review of the Molecular Pathways Involved in Resistance to BRAF Inhibitors in Patients with Advanced-Stage Melanoma. *Med Sci Monit* **2020**, *26*, e920957-e920957, doi:10.12659/MSM.920957.

86. Saei, A.; Palafox, M.; Benoukraf, T.; Kumari, N.; Jaynes, P.W.; Iyengar, P.V.; Muñoz-Couselo, E.; Nuciforo, P.; Cortés, J.; Nötzel, C.; et al. Loss of USP28-mediated BRAF degradation drives resistance to RAF cancer therapies. *The Journal of experimental medicine* **2018**, *215*, 1913-1928, doi:10.1084/jem.20171960.

87. Cabanos, H.F.; Hata, A.N. Emerging Insights into Targeted Therapy-Tolerant Persister Cells in Cancer. *Cancers (Basel)* **2021**, *13*, doi:10.3390/cancers13112666.

88. Saei, A.; Eichhorn, P.J.A. Adaptive Responses as Mechanisms of Resistance to BRAF Inhibitors in Melanoma. **2019**, *11*, 1176.

89. Proietti, I.; Skroza, N.; Bernardini, N.; Tolino, E.; Balduzzi, V.; Marchesiello, A.; Michelini, S.; Volpe, S.; Mambrin, A.; Mangino, G.; et al. Mechanisms of Acquired BRAF Inhibitor Resistance in Melanoma: A Systematic Review. **2020**, *12*, 2801.

90. Fontoura, J.C.; Viezzer, C.; dos Santos, F.G.; Ligabue, R.A.; Weinlich, R.; Puga, R.D.; Antonow, D.; Severino, P.; Bonorino, C. Comparison of 2D and 3D cell culture models for cell growth, gene expression and drug resistance. *Materials Science and Engineering: C* **2020**, *107*, 110264, doi:https://doi.org/10.1016/j.msec.2019.110264.

91. Baker, B.M.; Chen, C.S. Deconstructing the third dimension – how 3D culture microenvironments alter cellular cues. *Journal of Cell Science* **2012**, *125*, 3015-3024, doi:10.1242/jcs.079509 %J Journal of Cell Science.

92. Fontana, F.; Raimondi, M.; Marzagalli, M.; Sommariva, M.; Gagliano, N.; Limonta, P. Three-Dimensional Cell Cultures as an In Vitro Tool for Prostate Cancer Modeling and Drug Discovery. **2020**, *21*, 6806.

93. Westhouse, R.A. Safety assessment considerations and strategies for targeted small molecule cancer therapeutics in drug discovery. *Toxicologic pathology* **2010**, *38*, 165-168, doi:10.1177/0192623309354341.

94. Chaicharoenaudomrung, N.; Kunhorm, P.; Noisa, P. Three-dimensional cell culture systems as an in vitro platform for cancer and stem cell modeling. *World journal of stem cells* **2019**, *11*, 1065-1083, doi:10.4252/wjsc.v11.i12.1065.

95. Jensen, C.; Teng, Y. Is It Time to Start Transitioning From 2D to 3D Cell Culture? *Front Mol Biosci* **2020**, *7*, 33-33, doi:10.3389/fmolb.2020.00033.

96. Rebecca, V.W.; Somasundaram, R.; Herlyn, M. Pre-clinical modeling of cutaneous melanoma. *Nature Communications* **2020**, *11*, 2858, doi:10.1038/s41467-020-15546-9.

97. Yoshida, G.J. Applications of patient-derived tumor xenograft models and tumor organoids. *J Hematol Oncol* **2020**, *13*, 4, doi:10.1186/s13045-019-0829-z.

98. Brassart-Pasco, S.; Brézillon, S.; Brassart, B.; Ramont, L.; Oudart, J.-B.; Monboisse, J.C. Tumor Microenvironment: Extracellular Matrix Alterations Influence Tumor Progression. *Front Oncol* **2020**, *10*, doi:10.3389/fonc.2020.00397.

99. Amaral, R.; Zimmermann, M.; Ma, A.-H.; Zhang, H.; Swiech, K.; Pan, C.-X. A Simple Three-Dimensional In Vitro Culture Mimicking the In Vivo-Like Cell Behavior of Bladder Patient-Derived Xenograft Models. *Cancers* **2020**, *12*, 1304, doi:10.3390/cancers12051304.

100. Zhang, Z.; Wang, H.; Ding, Q.; Xing, Y.; Xu, Z.; Lu, C.; Luo, D.; Xu, L.; Xia, W.; Zhou, C.; et al. Establishment of patient-derived tumor spheroids for non-small cell lung cancer. *PLoS One* **2018**, *13*, e0194016, doi:10.1371/journal.pone.0194016.

101. Szasz, I.; Koroknai, V.; Kiss, T.; Vizkeleti, L.; Adany, R.; Balazs, M. Molecular alterations associated with acquired resistance to BRAFV600E targeted therapy in melanoma cells. *Melanoma Res* **2019**, *29*, 390-400, doi:10.1097/CMR.0000000000000588.

102. Patel, V.; Szász, I.; Koroknai, V.; Kiss, T.; Balázs, M. Molecular Alterations Associated with Acquired Drug Resistance during Combined Treatment with Encorafenib and Binimetinib in Melanoma Cell Lines. *Cancers* **2021**, *13*, 6058.

103. Koroknai, V.; Ecsedi, S.; Vizkeleti, L.; Kiss, T.; Szasz, I.; Lukacs, A.; Papp, O.; Adany, R.; Balazs, M. Genomic profiling of invasive melanoma cell lines by array comparative genomic hybridization. *Melanoma Res* **2016**, *26*, 100-107, doi:10.1097/CMR.0000000000000227.

104. Toth, B.B.; Arianti, R.; Shaw, A.; Vamos, A.; Vereb, Z.; Poliska, S.; Gyory, F.; Bacso, Z.; Fesus, L.; Kristof, E. FTO Intronic SNP Strongly Influences Human Neck Adipocyte Browning Determined by Tissue and PPARgamma Specific Regulation: A Transcriptome Analysis. *Cells* **2020**, *9*, 987, doi:10.3390/cells9040987.

105. Vizkeleti, L.; Kiss, T.; Koroknai, V.; Ecsedi, S.; Papp, O.; Szasz, I.; Adany, R.; Balazs, M. Altered integrin expression patterns shown by microarray in human cutaneous melanoma. *Melanoma research* **2017**, *27*, 180-188, doi:10.1097/cmr.0000000000000322.

106. Ahn, J.H.; Hwang, S.H.; Cho, H.S.; Lee, M. Differential Gene Expression Common to Acquired and Intrinsic Resistance to BRAF Inhibitor Revealed by RNA-Seq Analysis. *Biomol Ther (Seoul)* **2019**, *27*, 302-310, doi:10.4062/biomolther.2018.133.

107. Wan, P.T.; Garnett, M.J.; Roe, S.M.; Lee, S.; Niculescu-Duvaz, D.; Good, V.M.; Jones, C.M.; Marshall, C.J.; Springer, C.J.; Barford, D.; et al. Mechanism of activation of the RAF-ERK signaling pathway by oncogenic mutations of B-RAF. *Cell* **2004**, *116*, 855-867, doi:10.1016/s0092-8674(04)00215-6.

108. Moreira, A.; Heinzerling, L.; Bhardwaj, N.; Friedlander, P. Current Melanoma Treatments: Where Do We Stand? *Cancers (Basel)* **2021**, *13*, doi:10.3390/cancers13020221.

109. Subbiah, V.; Baik, C.; Kirkwood, J.M. Clinical Development of BRAF plus MEK Inhibitor Combinations. *Trends in Cancer* **2020**, *6*, 797-810, doi:https://doi.org/10.1016/j.trecan.2020.05.009.

110. Trojaniello, C.; Festino, L.; Vanella, V.; Ascierto, P.A. Encorafenib in combination with binimetinib for unresectable or metastatic melanoma with BRAF mutations. *Expert Rev Clin Pharmacol* **2019**, *12*, 259-266, doi:10.1080/17512433.2019.1570847.

111. Delord, J.P.; Robert, C.; Nyakas, M.; McArthur, G.A.; Kudchakar, R.; Mahipal, A.; Yamada, Y.; Sullivan, R.; Arance, A.; Kefford, R.F.; et al. Phase I Dose-Escalation and -Expansion Study of the BRAF Inhibitor Encorafenib (LGX818) in Metastatic BRAF-Mutant Melanoma. *Clin Cancer Res* **2017**, *23*, 5339-5348, doi:10.1158/1078-0432.CCR-16-2923.

112. Dummer, R.; Ascierto, P.A.; Gogas, H.J.; Arance, A.; Mandala, M.; Liszkay, G.; Garbe, C.; Schadendorf, D.; Krajsova, I.; Gutzmer, R.; et al. Encorafenib plus binimetinib versus vemurafenib or encorafenib in patients with BRAF-mutant melanoma (COLUMBUS): a multicentre, open-label, randomised phase 3 trial. *Lancet Oncol* **2018**, *19*, 603-615, doi:10.1016/S1470-2045(18)30142-6.

113. Patel, H.; Yacoub, N.; Mishra, R.; White, A.; Long, Y.; Alanazi, S.; Garrett, J.T. Current Advances in the Treatment of BRAF-Mutant Melanoma. *Cancers (Basel)* **2020**, *12*, doi:10.3390/cancers12020482.

114. Long, G.V.; Eroglu, Z.; Infante, J.; Patel, S.; Daud, A.; Johnson, D.B.; Gonzalez, R.; Kefford, R.; Hamid, O.; Schuchter, L.; et al. Long-Term Outcomes in Patients With BRAF V600-Mutant Metastatic Melanoma Who Received Dabrafenib Combined With Trametinib. *J Clin Oncol* **2018**, *36*, 667-673, doi:10.1200/JCO.2017.74.1025.

115. Lugowska, I.; Teterycz, P.; Rutkowski, P. Immunotherapy of melanoma. *Contemp Oncol (Pozn)* **2018**, *22*, 61-67, doi:10.5114/wo.2018.73889.

116. Czarnecka, A.M.; Bartnik, E.; Fiedorowicz, M.; Rutkowski, P. Targeted Therapy in Melanoma and Mechanisms of Resistance. *Int J Mol Sci* **2020**, *21*, doi:10.3390/ijms21134576.

117. Kapałczyńska, M.; Kolenda, T.; Przybyła, W.; Zajączkowska, M.; Teresiak, A.; Filas, V.; Ibbs, M.; Bliźniak, R.; Łuczewski, Ł.; Lamperska, K. 2D and 3D cell cultures – a comparison of different types of cancer cell cultures. *Archives of Medical Science* **2018**, doi:10.5114/aoms.2016.63743.

118. Kapalczynska, M.; Kolenda, T.; Przybyla, W.; Zajaczkowska, M.; Teresiak, A.; Filas, V.; Ibbs, M.; Blizniak, R.; Luczewski, L.; Lamperska, K. 2D and 3D cell cultures - a comparison of different types of cancer cell cultures. *Arch Med Sci* **2018**, *14*, 910-919, doi:10.5114/aoms.2016.63743.

119. Antoni, D.; Burckel, H.; Josset, E.; Noel, G. Three-dimensional cell culture: a breakthrough in vivo. *Int J Mol Sci* **2015**, *16*, 5517-5527, doi:10.3390/ijms16035517.

120. Birgersdotter, A.; Sandberg, R.; Ernberg, I. Gene expression perturbation in vitro--a growing case for three-dimensional (3D) culture systems. *Semin Cancer Biol* **2005**, *15*, 405-412, doi:10.1016/j.semcancer.2005.06.009.

121. Fontoura, J.C.; Viezzer, C.; dos Santos, F.G.; Ligabue, R.A.; Weinlich, R.; Puga, R.D.; Antonow, D.; Severino, P.; Bonorino, C. Comparison of 2D and 3D cell culture models for cell growth, gene expression and drug resistance. *Materials Science and Engineering C* **2020**, *107*, 110264-110264, doi:10.1016/j.msec.2019.110264.

122. Fontoura, J.C.; Viezzer, C.; Dos Santos, F.G.; Ligabue, R.A.; Weinlich, R.; Puga, R.D.; Antonow, D.; Severino, P.; Bonorino, C. Comparison of 2D and 3D cell culture models for cell growth, gene expression and drug resistance. *Mater Sci Eng C Mater Biol Appl* **2020**, *107*, 110264, doi:10.1016/j.msec.2019.110264.

123. Ravi, M. Applications of three-dimensional cell cultures in the early stages of drug discovery, focusing on gene expressions, drug metabolism, and susceptibility. *Critical Reviews in Eukaryotic Gene Expression* **2017**, doi:10.1615/CritRevEukaryotGeneExpr.2017018935.

124. Ravi, M. Applications of Three-Dimensional Cell Cultures in the Early Stages of Drug Discovery, Focusing on Gene Expressions, Drug Metabolism, and Susceptibility. *Crit Rev Eukaryot Gene Expr* **2017**, *27*, 53-62, doi:10.1615/CritRevEukaryotGeneExpr.2017018935.

125. Castiaux, A.D.; Spence, D.M.; Martin, R.S. Review of 3D Cell Culture with Analysis in Microfluidic Systems. *Anal Methods* **2019**, *11*, 4220-4232, doi:10.1039/c9ay01328h.

126. Ghosh, S.; Spagnoli, G.C.; Martin, I.; Ploegert, S.; Demougin, P.; Heberer, M.; Reschner, A. Three-dimensional culture of melanoma cells profoundly affects gene expression profile: a high density oligonucleotide array study. *J Cell Physiol* **2005**, *204*, 522-531, doi:10.1002/jcp.20320.

127. Lee, M.A.; Bergdorf, K.N.; Phifer, C.J.; Jones, C.Y.; Byon, S.Y.; Sawyer, L.M.; Bauer, J.A.; Weiss, V.L. Novel three dimensional cultures provide insights into thyroid cancer behavior. *Endocrine-Related Cancer* **2019**, doi:10.1530/ERC-19-0374.

128. Ryan, S.L.; Baird, A.M.; Vaz, G.; Urquhart, A.J.; Senge, M.; Richard, D.J.; O'Byrne, K.J.; Davies, A.M. Drug Discovery Approaches Utilizing Three-Dimensional Cell Culture. *Assay Drug Dev Technol* **2016**, *14*, 19-28, doi:10.1089/adt.2015.670.

129. Breslin, S.; O'Driscoll, L. The relevance of using 3D cell cultures, in addition to 2D monolayer cultures, when evaluating breast cancer drug sensitivity and resistance. *Oncotarget* **2016**, doi:10.18632/oncotarget.9935.

130. Ryabaya, O.; Prokofieva, A.; Akasov, R.; Khochenkov, D.; Emelyanova, M.; Burov, S.; Markvicheva, E.; Inshakov, A.; Stepanova, E. Metformin increases antitumor activity of MEK inhibitor binimetinib in 2D and 3D models of human metastatic melanoma cells. *Biomedicine and Pharmacotherapy* **2019**, doi:10.1016/j.biopha.2018.11.109.

131. Ahn, J.H.; Hwang, S.H.; Cho, H.S.; Lee, M. Differential gene expression common to acquired and intrinsic resistance to BRAF inhibitor revealed by RNA-seq analysis. *Biomolecules and Therapeutics* **2019**, doi:10.4062/biomolther.2018.133.

132. Qiu, T.; Wang, H.; Wang, Y.; Zhang, Y.; Hui, Q.; Tao, K. Identification of genes associated with melanoma metastasis. *Kaohsiung Journal of Medical Sciences* **2015**, doi:10.1016/j.kjms.2015.10.002.

133. Lim, S.Y.; Yuzhalin, A.E.; Gordon-Weeks, A.N.; Muschel, R.J. Targeting the CCL2-CCR2 signaling axis in cancer metastasis. *Oncotarget* **2016**, doi:10.18632/oncotarget.7376.

134. Schmit, T.L.; Zhong, W.; Setaluri, V.; Spiegelman, V.S.; Ahmad, N. Targeted depletion of polo-like kinase (Plk) 1 through lentiviral shrna or a small-molecule inhibitor causes mitotic catastrophe and induction of apoptosis in human melanoma cells. *Journal of Investigative Dermatology* **2009**, doi:10.1038/jid.2009.172.

135. Vergani, E.; Di Guardo, L.; Dugo, M.; Rigoletto, S.; Tragni, G.; Ruggeri, R.; Perrone, F.; Tamborini, E.; Gloghini, A.; Arienti, F.; et al. Overcoming melanoma resistance to vemurafenib by targeting CCL2-induced miR-34a, miR-100 and miR-125b. *Oncotarget* **2016**, *7*, 4428-4441, doi:10.18632/oncotarget.6599.

136. Jansen, J.; Vieten, P.; Pagliari, F.; Hanley, R.; Marafioti, M.G.; Tirinato, L.; Seco, J. A Novel Analysis Method for Evaluating the Interplay of Oxygen and Ionizing Radiation at the Gene Level. *Front Genet* **2021**, *12*, 597635, doi:10.3389/fgene.2021.597635.

137. Su, S.; Chhabra, G.; Ndiaye, M.A.; Singh, C.K.; Ye, T.; Huang, W.; Dewey, C.N.; Setaluri, V.; Ahmad, N. PLK1 and NOTCH Positively Correlate in Melanoma and Their Combined Inhibition Results in Synergistic Modulations of Key Melanoma Pathways. *Mol Cancer Ther* **2021**, *20*, 161-172, doi:10.1158/1535-7163.MCT-20-0654.

138. Kazanietz, M.G.; Caloca, M.J. The Rac GTPase in Cancer: From Old Concepts to New Paradigms. *Cancer Res* **2017**, *77*, 5445-5451, doi:10.1158/0008-5472.CAN-17-1456.

139. Eckert, R.L.; Adhikary, G.; Young, C.A.; Jans, R.; Crish, J.F.; Xu, W.; Rorke, E.A. AP1 Transcription Factors in Epidermal Differentiation and Skin Cancer. *Journal of Skin Cancer* **2013**, doi:10.1155/2013/537028.

140. Bhandari, A.; Xia, E.; Zhou, Y.; Guan, Y.; Xiang, J.; Kong, L.; Wang, Y.; Yang, F.; Wang, O.; Zhang, X. ITGA7 functions as a tumor suppressor and regulates migration and invasion in breast cancer. *Cancer Management and Research* **2018**, *10*, 969-976, doi:10.2147/CMAR.S160379.

141. Argast, G.M.; Croy, C.H.; Couts, K.L.; Zhang, Z.; Litman, E.; Chan, D.C.; Ahn, N.G. Plexin B1 is repressed by oncogenic B-Raf signaling and functions as a tumor suppressor in melanoma cells. *Oncogene* **2009**, doi:10.1038/onc.2009.133.

142. Ch'ng, E.S.; Kumanogoh, A. Roles of Sema4D and Plexin-B1 in tumor progression. *Mol Cancer* **2010**, *9*, 251, doi:10.1186/1476-4598-9-251.

143. Mastrantonio, R.; You, H.; Tamagnone, L. Semaphorins as emerging clinical biomarkers and therapeutic targets in cancer. *Theranostics* **2021**, *11*, 3262-3277, doi:10.7150/thno.54023.

144. Denk, A.E.; Braig, S.; Schubert, T.; Boserhof, A.K. Slit3 inhibits activator protein 1-mediated migration of malignant melanoma cells. *International Journal of Molecular Medicine* **2011**, doi:10.3892/ijmm.2011.742.

145. Dave, B.; Granados-Principal, S.; Zhu, R.; Benz, S.; Rabizadeh, S.; Soon-Shiong, P.; Yu, K.D.; Shao, Z.; Li, X.; Gilcrease, M.; et al. Targeting RPL39 and MLF2 reduces tumor initiation and metastasis in breast cancer by inhibiting nitric oxide synthase signaling. *Proceedings of the National Academy of Sciences of the United States of America* **2014**, doi:10.1073/pnas.1320769111.

146. Wang, Y.; Hu, S.; Gabisi, A.M.; Er, J.A.V.; Pope, A.; Burstein, G.; Schardon, C.L.; Cardounel, A.J.; Ekmekcioglu, S.; Fast, W. Developing an irreversible inhibitor of human DDAH-1, an enzyme upregulated in melanoma. *ChemMedChem* **2014**, doi:10.1002/cmdc.201300557.

147. Cheng, W.C.; Tsui, Y.C.; Ragusa, S.; Koelzer, V.H.; Mina, M.; Franco, F.; Läubli, H.; Tschumi, B.; Speiser, D.; Romero, P.; et al. Uncoupling protein 2 reprograms the tumor microenvironment

to support the anti-tumor immune cycle. *Nature Immunology* **2019**, doi:10.1038/s41590-018-0290-0.

148. Arimura, Y.; Ikura, M.; Fujita, R.; Noda, M.; Kobayashi, W.; Horikoshi, N.; Sun, J.; Shi, L.; Kusakabe, M.; Harata, M.; et al. Cancer-associated mutations of histones H2B, H3.1 and H2A.Z.1 affect the structure and stability of the nucleosome. *Nucleic Acids Research* **2018**, doi:10.1093/nar/gky661.

149. Xin, H.; Lei, M.; Zhang, Z.; Li, J.; Zhang, H.; Luo, X.; Wang, A.; Deng, F. Suppression of IGF1R in Melanoma Cells by an Adenovirus-Mediated One-Step Knockdown System. *Molecular Therapy - Nucleic Acids* **2018**, doi:10.1016/j.omtn.2018.08.004.

150. Eriksson, J.; Le Joncour, V.; Nummela, P.; Jahkola, T.; Virolainen, S.; Laakkonen, P.; Saksela, O.; Hölttä, E. Gene expression analyses of primary melanomas reveal CTHRC1 as an important player in melanoma progression. *Oncotarget* **2016**, doi:10.18632/oncotarget.7604.

151. Igci, Y.Z.; Bozgeyik, E.; Borazan, E.; Pala, E.; Suner, A.; Ulasli, M.; Gurses, S.A.; Yumrutas, O.; Balik, A.A.; Igci, M. Expression profiling of SCN8A and NDUFC2 genes in colorectal carcinoma. *Experimental Oncology* **2015**, doi:10.31768/2312-8852.2015.37(1):77-80.

152. Carrithers, M.D.; Chatterjee, G.; Carrithers, L.M.; Offoha, R.; Iheagwara, U.; Rahner, C.; Graham, M.; Waxman, S.G. Regulation of podosome formation in macrophages by a splice variant of the sodium channel SCN8A. *J Biol Chem* **2009**, *284*, 8114-8126, doi:10.1074/jbc.M801892200.

153. Huang, J.M.; Hornyak, T.J. Polycomb group proteins - epigenetic repressors with emerging roles in melanocytes and melanoma. *Pigment Cell and Melanoma Research* **2015**, doi:10.1111/pcmr.12341.

154. Chen, J.; Peng, C.; Lei, L.; Zhang, J.; Zeng, W.; Chen, X. Nuclear Envelope-distributed CD147 interacts with and inhibits the transcriptional function of RING1 and promotes melanoma cell motility. *PLoS ONE* **2017**, doi:10.1371/journal.pone.0183689.

155. Paoli, P.; Giannoni, E.; Chiarugi, P. Anoikis molecular pathways and its role in cancer progression. *Biochim Biophys Acta* **2013**, *1833*, 3481-3498, doi:10.1016/j.bbamcr.2013.06.026.

156. Kruiswijk, F.; Hasenfuss, S.C.; Sivapatham, R.; Baar, M.P.; Putavet, D.; Naipal, K.A.T.; Van Den Broek, N.J.F.; Kruit, W.; Van Der Spek, P.J.; Van Gent, D.C.; et al. Targeted inhibition of metastatic melanoma through interference with Pin1-FOXM1 signaling. *Oncogene* **2016**, doi:10.1038/onc.2015.282.

157. Abourbih, D.A.; Di Cesare, S.; Orellana, M.E.; Antecka, E.; Martins, C.; Petruccelli, L.A.; Burnier, M.N. Lysyl oxidase expression and inhibition in uveal melanoma. *Melanoma Research* **2010**, doi:10.1097/CMR.0b013e328336edfe.

158. Romano, E.; Rufo, N.; Korf, H.; Mathieu, C.; Garg, A.D.; Agostinis, P. BNIP3 modulates the interface between B16-F10 melanoma cells and immune cells. *Oncotarget* **2018**, doi:10.18632/oncotarget.24815.

159. Maes, H.; Van Eygen, S.; Krysko, D.V.; Vandenabeele, P.; Nys, K.; Rillaerts, K.; Garg, A.D.; Verfaillie, T.; Agostinis, P. BNIP3 supports melanoma cell migration and vasculogenic mimicry by orchestrating the actin cytoskeleton. *Cell Death and Disease* **2014**, doi:10.1038/cddis.2014.94.

160. Kukkula, A.; Ojala, V.K.; Mendez, L.M.; Sistonen, L.; Elenius, K.; Sundvall, M. Therapeutic Potential of Targeting the SUMO Pathway in Cancer. *Cancers (Basel)* **2021**, *13*, 4402, doi:10.3390/cancers13174402.

161. Sarogni, P.; Palumbo, O.; Servadio, A.; Astigiano, S.; D'Alessio, B.; Gatti, V.; Cukrov, D.; Baldari, S.; Pallotta, M.M.; Aretini, P.; et al. Overexpression of the cohesin-core subunit SMC1A contributes to colorectal cancer development. *Journal of Experimental and Clinical Cancer Research* **2019**, doi:10.1186/s13046-019-1116-0.

162. Li, P.; Guo, M.; Sun, B. Integration of multi-omics data to mine cancer-related gene modules. *J Bioinform Comput Biol* **2019**, *17*, 1950038, doi:10.1142/S0219720019500380.

163. Yang, Y.; Liu, X.; Li, R.; Zhang, M.; Wang, H.; Qu, Y. Kinesin family member 3A inhibits the carcinogenesis of non-small cell lung cancer and prolongs survival. *Oncol Lett* **2020**, *20*, 348, doi:10.3892/ol.2020.12211.

164. Szász, I.; Koroknai, V.; Kiss, T.; Vízkeleti, L.; Ádány, R.; Balázs, M. Molecular alterations associated with acquired resistance to BRAFV600E targeted therapy in melanoma cells. *Melanoma Research* **2019**, doi:10.1097/cmr.0000000000000588.

165. Kakadia, S.; Yarlagadda, N.; Awad, R.; Kundranda, M.; Niu, J.; Naraev, B.; Mina, L.; Dragovich, T.; Gimbel, M.; Mahmoud, F. Mechanisms of resistance to BRAF and MEK inhibitors and clinical update of US Food and Drug Administration-approved targeted therapy in advanced melanoma. *Onco Targets Ther* **2018**, *11*, 7095-7107, doi:10.2147/OTT.S182721.

166. Czarnecka, A.M.; Bartnik, E.; Fiedorowicz, M.; Rutkowski, P. Targeted Therapy in Melanoma and Mechanisms of Resistance. *Int J Mol Sci* **2020**, *21*, 4576, doi:10.3390/ijms21134576.

167. Ziogas, D.C.; Konstantinou, F.; Bouros, S.; Theochari, M.; Gogas, H. Combining BRAF/MEK Inhibitors with Immunotherapy in the Treatment of Metastatic Melanoma. *Am J Clin Dermatol* **2021**, *22*, 301-314, doi:10.1007/s40257-021-00593-9.

168. McClure, E.; Patel, A.; Carr, M.J.; Sun, J.; Zager, J.S. The combination of encorafenib and binimetinib for the treatment of patients with BRAF-mutated advanced, unresectable, or metastatic melanoma: an update. *Expert Review of Precision Medicine and Drug Development* **2021**, *6*, 19-29, doi:10.1080/23808993.2021.1847639.

169. Haugh, A.M.; Salama, A.K.S.; Johnson, D.B. Advanced Melanoma: Resistance Mechanisms to Current Therapies. *Hematol Oncol Clin North Am* **2021**, *35*, 111-128, doi:10.1016/j.hoc.2020.09.005.

170. Dratkiewicz, E.; Simiczyjew, A.; Pietraszek-Gremplewicz, K.; Mazurkiewicz, J.; Nowak, D. Characterization of Melanoma Cell Lines Resistant to Vemurafenib and Evaluation of Their Responsiveness to EGFR- and MET-Inhibitor Treatment. *Int J Mol Sci* **2019**, *21*, 113, doi:10.3390/ijms21010113.

171. Pouliquen, D.L.; Boissard, A.; Coqueret, O.; Guette, C. Biomarkers of tumor invasiveness in proteomics (Review). *Int J Oncol* **2020**, *57*, 409-432, doi:10.3892/ijo.2020.5075.

172. Yu, C.F.; Chen, F.H.; Lu, M.H.; Hong, J.H.; Chiang, C.S. Dual roles of tumour cells-derived matrix metalloproteinase 2 on brain tumour growth and invasion. *Br J Cancer* **2017**, *117*, 1828-1836, doi:10.1038/bjc.2017.362.

173. Das Thakur, M.; Salangsang, F.; Landman, A.S.; Sellers, W.R.; Pryer, N.K.; Levesque, M.P.; Dummer, R.; McMahon, M.; Stuart, D.D. Modelling vemurafenib resistance in melanoma

reveals a strategy to forestall drug resistance. *Nature* **2013**, *494*, 251-255, doi:10.1038/nature11814.

174. Tetu, P.; Vercellino, L.; Reger de Moura, C.; Baroudjian, B.; Dumaz, N.; Mourah, S.; Lebbe, C. Mitogen-activated protein kinase blockade in melanoma: intermittent versus continuous therapy, from preclinical to clinical data. *Curr Opin Oncol* **2021**, *33*, 127-132, doi:10.1097/CCO.0000000000000706.

175. Algazi, A.P.; Othus, M.; Daud, A.I.; Lo, R.S.; Mehnert, J.M.; Truong, T.G.; Conry, R.; Kendra, K.; Doolittle, G.C.; Clark, J.I.; et al. Continuous versus intermittent BRAF and MEK inhibition in patients with BRAF-mutated melanoma: a randomized phase 2 trial. *Nat Med* **2020**, *26*, 1564-1568, doi:10.1038/s41591-020-1060-8.

176. Kong, X.; Kuilman, T.; Shahrabi, A.; Boshuizen, J.; Kemper, K.; Song, J.Y.; Niessen, H.W.M.; Rozeman, E.A.; Geukes Foppen, M.H.; Blank, C.U.; et al. Cancer drug addiction is relayed by an ERK2-dependent phenotype switch. *Nature* **2017**, *550*, 270-274, doi:10.1038/nature24037.

177. Proietti, I.; Skroza, N.; Bernardini, N.; Tolino, E.; Balduzzi, V.; Marchesiello, A.; Michelini, S.; Volpe, S.; Mambrin, A.; Mangino, G.; et al. Mechanisms of Acquired BRAF Inhibitor Resistance in Melanoma: A Systematic Review. *Cancers (Basel)* **2020**, *12*, doi:10.3390/cancers12102801.

178. Mourad-Zeidan, A.A.; Melnikova, V.O.; Wang, H.; Raz, A.; Bar-Eli, M. Expression profiling of Galectin-3-depleted melanoma cells reveals its major role in melanoma cell plasticity and vasculogenic mimicry. *Am J Pathol* **2008**, *173*, 1839-1852, doi:10.2353/ajpath.2008.080380.

179. Braeuer, R.R.; Shoshan, E.; Kamiya, T.; Bar-Eli, M. The sweet and bitter sides of galectins in melanoma progression. *Pigment Cell Melanoma Res* **2012**, *25*, 592-601, doi:10.1111/j.1755-148X.2012.01026.x.

180. Capone, E.; Iacobelli, S.; Sala, G. Role of galectin 3 binding protein in cancer progression: a potential novel therapeutic target. *J Transl Med* **2021**, *19*, 405, doi:10.1186/s12967-021-03085-w.

181. Sato, S.; Kato, J.; Sawada, M.; Horimoto, K.; Okura, M.; Hida, T.; Uhara, H. Usefulness of neuron-specific enolase as a serum marker of metastatic melanoma. **2020**, *47*, 1141-1148, doi:https://doi.org/10.1111/1346-8138.15502.

182. Berthier-Vergnes, O.; El Kharbili, M.; de la Fouchardiere, A.; Pointecouteau, T.; Verrando, P.; Wierinckx, A.; Lachuer, J.; Le Naour, F.; Lamartine, J. Gene expression profiles of human melanoma cells with different invasive potential reveal TSPAN8 as a novel mediator of invasion. *Br J Cancer* **2011**, *104*, 155-165, doi:10.1038/sj.bjc.6605994.

183. Yang, J.; Antin, P.; Berx, G.; Blanpain, C.; Brabletz, T.; Bronner, M.; Campbell, K.; Cano, A.; Casanova, J.; Christofori, G.; et al. Guidelines and definitions for research on epithelial-mesenchymal transition. *Nat Rev Mol Cell Biol* **2020**, *21*, 341-352, doi:10.1038/s41580-020-0237-9.

184. Molnar, E.; Garay, T.; Donia, M.; Baranyi, M.; Rittler, D.; Berger, W.; Timar, J.; Grusch, M.; Hegedus, B. Long-Term Vemurafenib Exposure Induced Alterations of Cell Phenotypes in Melanoma: Increased Cell Migration and Its Association with EGFR Expression. *Int J Mol Sci* **2019**, *20*, doi:10.3390/ijms20184484.

185. Settleman, J.; Neto, J.M.F.; Bernards, R. Thinking Differently about Cancer Treatment Regimens. *Cancer Discov* **2021**, *11*, 1016-1023, doi:10.1158/2159-8290.CD-20-1187.

186. Dooley, A.J.; Gupta, A.; Bhattacharyya, M.; Middleton, M.R. Intermittent dosing with vemurafenib in BRAF V600E-mutant melanoma: review of a case series. *Ther Adv Med Oncol* **2014**, *6*, 262-266, doi:10.1177/1758834014548187.

187. Jain, T.; Bryce, A. Intermittent BRAF Inhibition Can Achieve Prolonged Disease Control in BRAF Mutant Melanoma. *Cureus* **2015**, *7*, e410, doi:10.7759/cureus.410.

188. Dooley, A.J.; Gupta, A.; Middleton, M.R. Ongoing Response in BRAF V600E-Mutant Melanoma After Cessation of Intermittent Vemurafenib Therapy: A Case Report. *Target Oncol* **2016**, *11*, 557-563, doi:10.1007/s11523-015-0410-9.

189. Bradley, C.A. Targeted therapies: Understanding tumour drug addiction. *Nat Rev Cancer* **2017**, *17*, 634-635, doi:10.1038/nrc.2017.98.

190. Hong, A.; Moriceau, G.; Sun, L.; Lomeli, S.; Piva, M.; Damoiseaux, R.; Holmen, S.L.; Sharpless, N.E.; Hugo, W.; Lo, R.S. Exploiting Drug Addiction Mechanisms to Select against MAPKi-Resistant Melanoma. *Cancer Discov* **2018**, *8*, 74-93, doi:10.1158/2159-8290.CD-17-0682.

191. Chi, Y.; Xue, J.; Huang, S.; Xiu, B.; Su, Y.; Wang, W.; Guo, R.; Wang, L.; Li, L.; Shao, Z.; et al. CapG promotes resistance to paclitaxel in breast cancer through transactivation of PIK3R1/P50. *Theranostics* **2019**, *9*, 6840-6855, doi:10.7150/thno.36338.

192. Zhe, N.; Wang, J.; Chen, S.; Lin, X.; Chai, Q.; Zhang, Y.; Zhao, J.; Fang, Q. Heme oxygenase-1 plays a crucial role in chemoresistance in acute myeloid leukemia. *Hematology* **2015**, *20*, 384-391, doi:10.1179/1607845414Y.0000000212.

193. Singh, N.; Krishnakumar, S.; Kanwar, R.K.; Cheung, C.H.; Kanwar, J.R. Clinical aspects for survivin: a crucial molecule for targeting drug-resistant cancers. *Drug Discov Today* **2015**, *20*, 578-587, doi:10.1016/j.drudis.2014.11.013.

194. Zhao, K.; Lu, Y.; Chen, Y.; Cheng, J.; Zhang, W. RNA sequencing data of Vemurafenib-resistant melanoma cells and parental cells. *Data Brief* **2020**, *30*, 105610-105610, doi:10.1016/j.dib.2020.105610.

195. Anastas, J.N.; Kulikauskas, R.M.; Tamir, T.; Rizos, H.; Long, G.V.; von Euw, E.M.; Yang, P.-T.; Chen, H.-W.; Haydu, L.; Toroni, R.A.; et al. WNT5A enhances resistance of melanoma cells to targeted BRAF inhibitors. *The Journal of Clinical Investigation* **2014**, *124*, 2877-2890, doi:10.1172/JCI70156.

196. Zhu, X.; Yan, S.; Xiao, S.; Xue, M. Knockdown of ALPK2 inhibits the development and progression of Ovarian Cancer. *Cancer Cell Int* **2020**, *20*, 267-267, doi:10.1186/s12935-020-01347-z.

197. Junnila, S.; Kokkola, A.; Karjalainen-Lindsberg, M.L.; Puolakkainen, P.; Monni, O. Genome-wide gene copy number and expression analysis of primary gastric tumors and gastric cancer cell lines. *BMC Cancer* **2010**, *10*, 73, doi:10.1186/1471-2407-10-73.

198. Su, H.; Lin, F.; Deng, X.; Shen, L.; Fang, Y.; Fei, Z.; Zhao, L.; Zhang, X.; Pan, H.; Xie, D.; et al. Profiling and bioinformatics analyses reveal differential circular RNA expression in radioresistant esophageal cancer cells. *J Transl Med* **2016**, *14*, 225, doi:10.1186/s12967-016-0977-7.

199. Robey, R.W.; Pluchino, K.M.; Hall, M.D.; Fojo, A.T.; Bates, S.E.; Gottesman, M.M. Revisiting the role of ABC transporters in multidrug-resistant cancer. *Nature Reviews Cancer* **2018**, *18*, 452-464, doi:10.1038/s41568-018-0005-8.

200. Tun, H.W.; Marlow, L.A.; von Roemeling, C.A.; Cooper, S.J.; Kreinest, P.; Wu, K.; Luxon, B.A.; Sinha, M.; Anastasiadis, P.Z.; Copland, J.A. Pathway signature and cellular differentiation in clear cell renal cell carcinoma. *PLoS One* **2010**, *5*, e10696-e10696, doi:10.1371/journal.pone.0010696.

201. Sinnberg, T.; Levesque, M.P.; Krochmann, J.; Cheng, P.F.; Ikenberg, K.; Meraz-Torres, F.; Niessner, H.; Garbe, C.; Busch, C. Wnt-signaling enhances neural crest migration of melanoma cells and induces an invasive phenotype. *Molecular Cancer* **2018**, *17*, 59, doi:10.1186/s12943-018-0773-5.

202. Shathasivam, P.; Kollara, A.; Spybey, T.; Park, S.; Clarke, B.; Ringuette, M.J.; Brown, T.J. VEPH1 expression decreases vascularisation in ovarian cancer xenografts and inhibits VEGFA and IL8 expression through inhibition of AKT activation. *British Journal of Cancer* **2017**, *116*, 1065-1076, doi:10.1038/bjc.2017.51.

203. Feng, H.; Jia, X.M.; Gao, N.N.; Tang, H.; Huang, W.; Ning, N. Overexpressed VEPH1 inhibits epithelial-mesenchymal transition, invasion, and migration of human cutaneous melanoma cells through inactivating the TGF-beta signaling pathway. *Cell Cycle* **2019**, *18*, 2860-2875, doi:10.1080/15384101.2019.1638191.

204. Zhang, M.; Zhang, Y.Y.; Chen, Y.; Wang, J.; Wang, Q.; Lu, H. TGF-beta Signaling and Resistance to Cancer Therapy. *Front Cell Dev Biol* **2021**, *9*, 786728, doi:10.3389/fcell.2021.786728.

205. Chen, D.; Lu, T.; Tan, J.; Li, H.; Wang, Q.; Wei, L. Long Non-coding RNAs as Communicators and Mediators Between the Tumor Microenvironment and Cancer Cells. **2019**, *9*, doi:10.3389/fonc.2019.00739.

206. Liu, F.; Xing, L.; Zhang, X.; Zhang, X. A Four-Pseudogene Classifier Identified by Machine Learning Serves as a Novel Prognostic Marker for Survival of Osteosarcoma. *Genes (Basel)* **2019**, *10*, doi:10.3390/genes10060414.

207. Wang, Y.; Wang, Z.; Xu, J.; Li, J.; Li, S.; Zhang, M.; Yang, D. Systematic identification of non-coding pharmacogenomic landscape in cancer. *Nat Commun* **2018**, *9*, 3192, doi:10.1038/s41467-018-05495-9.

208. Dolcino, M.; Pelosi, A.; Fiore, P.F.; Patuzzo, G.; Tinazzi, E.; Lunardi, C.; Puccetti, A. Long Non-Coding RNAs Play a Role in the Pathogenesis of Psoriatic Arthritis by Regulating MicroRNAs and Genes Involved in Inflammation and Metabolic Syndrome. *Front Immunol* **2018**, *9*, 1533, doi:10.3389/fimmu.2018.01533.

209. Zhang, L.; Forst, C.V.; Gordon, A.; Gussin, G.; Geber, A.B.; Fernandez, P.J.; Ding, T.; Lashua, L.; Wang, M.; Balmaseda, A.; et al. Characterization of antibiotic resistance and host-microbiome interactions in the human upper respiratory tract during influenza infection. *Microbiome* **2020**, *8*, 39, doi:10.1186/s40168-020-00803-2.

210. Alonso-Marañón, J.; Villanueva, A.; Piulats, J.M.; Martínez-Iniesta, M.; Solé, L.; Martín-Liberal, J.; Segura, S.; Pujol, R.M.; Iglesias, M.; Bigas, A.; et al. Combination of chemotherapy with BRAF inhibitors results in effective eradication of malignant melanoma by preventing ATM-dependent DNA repair. *Oncogene* **2021**, *40*, 5042-5048, doi:10.1038/s41388-021-01879-2.

211. Michielin, O.; van Akkooi, A.C.J.; Ascierto, P.A.; Dummer, R.; Keilholz, U.; clinicalguidelines@esmo.org, E.G.C.E.a. Cutaneous melanoma: ESMO Clinical Practice Guidelines for diagnosis, treatment and follow-updagger. *Ann Oncol* **2019**, *30*, 1884-1901, doi:10.1093/annonc/mdz411.

212. Michielin, O.; Atkins, M.B.; Koon, H.B.; Dummer, R.; Ascierto, P.A. Evolving impact of long-term survival results on metastatic melanoma treatment. *J Immunother Cancer* **2020**, *8*, e000948, doi:10.1136/jitc-2020-000948.

213. Matheis, F.; Heppt, M.V.; Graf, S.A.; Duwell, P.; Kammerbauer, C.; Aigner, A.; Besch, R.; Berking, C. A Bifunctional Approach of Immunostimulation and uPAR Inhibition Shows Potent Antitumor Activity in Melanoma. *J Invest Dermatol* **2016**, *136*, 2475-2484, doi:10.1016/j.jid.2016.07.026.

214. Mahmoodi Chalbatani, G.; Dana, H.; Gharagouzloo, E.; Grijalvo, S.; Eritja, R.; Logsdon, C.D.; Memari, F.; Miri, S.R.; Rad, M.R.; Marmari, V. Small interfering RNAs (siRNAs) in cancer therapy: a nano-based approach. *Int J Nanomedicine* **2019**, *14*, 3111-3128, doi:10.2147/IJN.S200253.

215. Wang, L.; Leite de Oliveira, R.; Huijberts, S.; Bosdriesz, E.; Pencheva, N.; Brunen, D.; Bosma, A.; Song, J.Y.; Zevenhoven, J.; Los-de Vries, G.T.; et al. An Acquired Vulnerability of Drug-Resistant Melanoma with Therapeutic Potential. *Cell* **2018**, *173*, 1413-1425 e1414, doi:10.1016/j.cell.2018.04.012.

Publications related to the dissertation

UNIVERSITY of DEBRECEN

UNIVERSITY AND NATIONAL LIBRARY
UNIVERSITY OF DEBRECEN
H-4002 Egyetem tér 1, Debrecen
Phone: +3652/410-443, email: publikaciok@lib.unideb.hu

Registry number: DEENK/533/2021.PL
Subject: PhD Publication List

Candidate: Vikas Patel
Doctoral School: Doctoral School of Health Sciences

List of publications related to the dissertation

1. **Patel, V.**, Szász, I., Koroknai, V., Kiss, T., Balázs, M.: Molecular Alterations Associated with Acquired Drug Resistance during Combined Treatment with Encorafenib and Binimetinib in Melanoma Cell Lines.
   Cancers (Basel). 13 (23), 1-22, 2021.
   DOI: http://dx.doi.org/10.3390/cancers13236058
   IF: 6.639 (2020)

2. Koroknai, V., **Patel, V.**, Szász, I., Ádány, R., Balázs, M.: Gene Expression Signature of BRAF Inhibitor Resistant Melanoma Spheroids.
   Pathol. Oncol. Res. 26 (4), 2557-2566, 2020.
   DOI: http://dx.doi.org/10.1007/s12253-020-00837-9
   IF: 3.201

UNIVERSITY of DEBRECEN

UNIVERSITY AND NATIONAL LIBRARY
UNIVERSITY OF DEBRECEN
H-4002 Egyetem tér 1, Debrecen
Phone: +3652/410-443, email: publikaciok@lib.unideb.hu

List of other publications

3. Szász, I., Koroknai, V., **Patel, V.**, Hajdú, T., Kiss, T., Ádány, R., Balázs, M.: Cell Proliferation Is Strongly Associated with the Treatment Conditions of an ER Stress Inducer New Anti-Melanoma Drug in Melanoma Cell Lines.
Biomedicines. 9 (2), 1-19, 2021.
DOI: http://dx.doi.org/10.3390/biomedicines9020096
IF: 6.081 (2020)

Total IF of journals (all publications): 15,921
Total IF of journals (publications related to the dissertation): 9,84

The Candidate's publication data submitted to the iDEa Tudóstér have been validated by DEENK on the basis of the Journal Citation Report (Impact Factor) database.

17 December, 2021

DEBRECENI EGYETEM Egyetemi és Nemzeti Könyvtár

Keywords

malignant melanoma, *BRAF*^{V600E}, 2D and 3D cell culture, spheroids, gene expression analysis, *BRAF*^{V600E} mutation, drug resistance, melanoma cell lines, BRAF and MEK inhibitors, encorafenib and binimetinib, MAPK pathways, proteome profiler, RNA-seq, signalling pathways in cancer

Acknowledgements

First and foremost, I would like to express my heartfelt and sincere gratitude to my supervisor, Prof. Dr. Margit Balazs PhD, DSc, for providing me with the opportunity to immerse myself in the fascinating world of melanoma research, and for helping and guiding me with vast knowledge and tolerant patience in my dissertation work.

Moreover, I would like to express my gratitude to Prof. Dr. Róza Ádány, PhD, DSc, Head of Doctoral School of Health Sciences, Department of Public Health and Epidemiology, for providing me with this excellent opportunity for scientific work and for all of her help over the years.

I also would like to extend my gratitude to Dr. Istvan Szasz, Dr. Viktória Koroknai, Timea Kiss, and Krisztina Jámbor for their constant generosity and criticism during my experiments.

My gratitude is also extended to all departmental personnel for their academic and administrative support throughout these years of study.

Last but certainly not least, I am really grateful for the love, encouragement, and support of my family, without which I could not have progressed this far.

Financial supports

This research was supported by Stipendium Hungaricum Scholarship Programme, and my research was also co-financed by the National Research Development and Innovation Fund (grant number K-112327), by the European Regional Development Fund (GINOP-2.3.2-15-2016-00005), by the ÚNKP-19-3 New National Excellence Program of the Ministry for Innovation and Technology as well as by the Hungarian Academy of Sciences (MTA11010 and TK2016-78).

This work was carried out at the Department of Public Health and Epidemiology, Faculty of Medicine, University of Debrecen, Debrecen, Hungary, during 2017- 2022.

Appendix/Supplementary material

Because the large size of the following Supplementary Tables those are attached as separate files

Supplementary Table 2:

List of genes which are differentially expressed in cell lines derived from sensitive melanoma spheroid comparing to sensitive monolayer cultures (N=1049). Genes are sorted by fold change (upregulated if fold change >1; downregulated if fold change < 1)

Supplementary Table 3:

Significantly upregulated genes in sensitive melanoma spheroid compared to sensitive monolayer grouped by molecular pathways

Supplementary Table 8:

List of differentially expressed genes between BRAFi/MEKi sensitive and resistant melanoma cell lines

Supplementary Table 1A.

Primer sequences for the validation of Affymetrix gene expression data using RT-qPCR

Gene	Primer sequence (5'-3')[1]	Amplicon size (bp)[2]
GAPDH*	F: AGCCACATCGCTCAGACAC	66
	R: GCCCAATACGACCAAATCC	
HIST1H2BB	F: ATGCCTGAACCCTCTAAGTCT	98
	R: CTGCGCTTACGCTTCTTACCA	
DCUN1D1	F: AGGATCATTGGACAGGAAGAAGT	102
	R: TGCCAGGTCATCACAGAACTG	
CMSS1	F: TAGCAGCAGACGCTTGGTG	83
	R: TGTGAGTCAAATCATTGGCCTT	
SMC3	F: AACATAATGTGATTGTGGGCAGA	244
	R: TCCTTTTTGGCACCAATAACTCT	
ZNF639	F: AAGACTCTACACCCTTCTCGTT	163
	R: ACGTCTCGGTATCAGAATCATCA	
IKBIP	F: GCTCATCTAAAGCGTCTACAGG	102
	R: AAGCGTCGTCAGACTGTTGTT	
SCN8A	F: CCTTTCACCCCTGAGTCACTG	131
	R: AGGTCGCTGTTTGGCTTGG	
ABHD4	F: TCCCCTCCGACCAACTAACC	109
	R: AGCTACTCGAAGAACAGCCAA	

*[1]F: forward, R: reverse; [2]bp: base pair and *House keeping gene.*

Supplementary Table 1B.

Primer sequences for the validation of RNA seq data using RT-qPCR

Gene	Primer sequence (5′-3′)[1]	Amplicon size (bp)[2]
CXCL12	F: ATTCTCAACACTCCAAACTGTGC	88
	R: ACTTTAGCTTCGGGTCAATGC	
COL5A1	F: GCCCGGATGTCGCTTACAG	80
	R: AAATGCAGACGCAGGGTACAG	
ALPK2	F: TGCTGTCTATCAAATCTCGGCT	75
	R: GAGCACTCAACCTCAACGGA	
ABCC3	F: TGGGGTGAAGTTTCGTACTGG	77
	R: CACGTTTGACTGAGTTGGTGATA	
CHST15	F: TCGTGTGGACAGTAAGCAGAT	155
	R: TGTAAGAAGCCATTACCAAGGTC	
DMRT2	F: TTTAGAAGGCTATCGCCCCAT	132
	R: TCCAGCATAATGTTCTCCAACTC	
MRGPRX4	F: GTCCCAGTCTTCGGTACAAAAC	119
	R: CCTGTCAGTCCGACAAGGG	
TRIM51	F: GGCCCTGTTTGTACCTCAACT	81
	R: TTCTCTGCCGCGTTGTCTTC	
VEPH1	F: TTGAAGACAGCCTTACAGAAGC	86
	R: TGCCTGGTCATTGTTATTGGTTT	
GJB1	F: GCGTGAACCGGCATTCTACT	167
	R: TTGGTCATAGCAAACGCTGTT	
GAPDH*	F: AGCCACATCGCTCAGACAC	66
	R: GCCCAATACGACCAAATCC	

*[1]F: forward, R: reverse; [2]bp: base pair and *House keeping gene.*

Supplementary Table 4
Significantly Downregulated genes in sensitive melanoma spheroid compared to sensitive monolayer grouped by molecular pathways

Pathway identifier	Pathway name	P-Value	FDR Value	Genes included (at least 5)
R-HSA-3371453	Regulation of HSF1-mediated heat shock response	0.006094953	0.617858	HSPH1, RPS19BP1, HSPA1L, HSBP1, MRPL18, ATM
R-HSA-9024446	NR1H2 and NR1H3-mediated signaling	0.007506727	0.617858	RXRB, SCD, APOC1, APOD, APOE
R-HSA-3371556	Cellular response to heat stress	0.008494393	0.617858	HSPH1, RPS19BP1, HSPA1L, HSBP1, MRPL18, ATM
R-HSA-1989781	PPARA activates gene expression	0.023110549	0.617858	RXRB, HMGCS1, ACOX1, ACSL1, HMGCR, NR1D1, MED7, MED13L
R-HSA-400206	Regulation of lipid metabolism by Peroxisome proliferator-activated receptor alpha (PPARalpha)	0.025026582	0.617858	RXRB, HMGCS1, ACOX1, ACSL1, HMGCR, NR1D1, MED7, MED13L
R-HSA-191273	Cholesterol biosynthesis	0.025949409	0.617858	IDI1, HMGCS1, DHCR24, MSMO1, HMGCR, ACAT2
R-HSA-2262752	Cellular responses to stress	0.030486666	0.617858	DCTN6, DYNC1H1, CEBPB, HSPA1L, RING1, RPS19BP1, ANAPC16, HSBP1, EPAS1, MRPL18, UBE2D3, FOS, PHC3, HSPH1, RHEB, RPS6KA2, ATP6V1B2, ATM, TPP1, PSMF1, RPS27A, ATP6V0D1, ATP6V1D
R-HSA-9006936	Signaling by TGF-beta family members	0.039820988	0.617858	PPP1R15A, SMAD2, BMPR2, UBE2D3, RPS27A, BMPR1B, JUNB, BMPR1A
R-HSA-8953897	Cellular responses to external stimuli	0.043376647	0.617858	DCTN6, DYNC1H1, CEBPB, HSPA1L, RING1, RPS19BP1, ANAPC16, HSBP1, EPAS1, MRPL18, UBE2D3, FOS, PHC3, HSPH1, RHEB, RPS6KA2, ATP6V1B2, ATM, TPP1, PSMF1, RPS27A, ATP6V0D1, ATP6V1D
R-HSA-6785807	Interleukin-4 and Interleukin-13 signaling	0.044013241	0.617858	IRF4, PIM1, BCL2, HMOX1, FOS, PTGS2, JUNB
R-HSA-5633008	TP53 Regulates Transcription of Cell Death Genes	0.049116436	0.617858	PPP1R13B, TP53INP1, ATM, NDRG1, ZNF420

Supplementary Table 5
List of genes which are differentially expressed in cell lines derived from resistant melanoma spheroid comparing to resistant monolayer cultures (N=297). Genes are sorted by fold change (upregulated if fold change >1; downregulated if fold change < 1)

UPREGULATED GENES

No.	Gene symbol	Description	Fold change
1	ACTG2	actin gamma 2, smooth muscle	8.799
2	PKP2	plakophilin 2	3.961
3	RPS9	ribosomal protein S9	3.367
4	LCP1	lymphocyte cytosolic protein 1	3.041
5	REXO1L1P	REXO1 like 1, pseudogene	2.798
6	NLGN4Y	neuroligin 4 Y-linked	2.794
7	RASGRP3	RAS guanyl releasing protein 3	2.764
8	TSHZ2	teashirt zinc finger homeobox 2	2.753
9	NAP1L3	nucleosome assembly protein 1 like 3	2.741
10	APBB3	amyloid beta precursor protein binding family B member 3	2.666
11	SCN8A	sodium voltage-gated channel alpha subunit 8	2.664
12	DEFB124	defensin beta 124	2.625
13	AGAP9	ArfGAP with GTPase domain, ankyrin repeat and PH domain 9	2.574
14	TGIF1	TGFB induced factor homeobox 1	2.499
15	HLA-F	major histocompatibility complex, class I, F	2.469
16	LENG8	leukocyte receptor cluster member 8	2.459
17	LOC388022		2.448
18	ZNF257	zinc finger protein 257	2.442
19	MOG	myelin oligodendrocyte glycoprotein	2.428
20	PIGF	phosphatidylinositol glycan anchor biosynthesis class F	2.423
21	ELP5	elongator acetyltransferase complex subunit 5	2.302
22	ADHFE1	alcohol dehydrogenase iron containing 1	2.276
23	SLAMF8	SLAM family member 8	2.254
24	PCDHB2	protocadherin beta 2	2.250
25	TBX18	T-box transcription factor 18	2.219
26	PSMB6	proteasome 20S subunit beta 6	2.191
27	SRGN	serglycin	2.190
28	RING1	ring finger protein 1	2.170
29	CCNL2		2.121
30	SLCO2B1	solute carrier organic anion transporter family member 2B1	2.120
31	GSTM4	glutathione S-transferase mu 4	2.101
32	CCNL2	cyclin L2	2.090
33	THY1	Thy-1 cell surface antigen	2.084
34	DCUN1D3	defective in cullin neddylation 1 domain containing 3	2.084
35	PLCB4	phospholipase C beta 4	2.068
36	MBD3L5	methyl-CpG binding domain protein 3 like 5	2.067
37	TMEM47	transmembrane protein 47	2.048

No.	Gene symbol	Description	Fold change
38	PDCD1LG2	programmed cell death 1 ligand 2	2.041
39	DDAH1	dimethylarginine dimethylaminohydrolase 1	2.040
40	UCP2	uncoupling protein 2	2.036
41	LINC00173	long intergenic non-protein coding RNA 173	2.020
42	NOX4	NADPH oxidase 4	2.001
43	TMEM255B	transmembrane protein 255B	1.999
44	SLC25A27	solute carrier family 25 member 27	1.993
45	LHFP		1.974
46	MLF2	myeloid leukemia factor 2	1.968
47	MANBAL	mannosidase beta like	1.948
48	HIST1H2BM		1.942
49	ABHD4	abhydrolase domain containing 4	1.899
50	STRADB	STE20 related adaptor beta	1.892
51	ARRDC1-AS1	ARRDC1 antisense RNA 1	1.888
52	LCE2C	late cornified envelope 2C	1.882
53	GINS1	GINS complex subunit 1	1.870
54	SPIN4	spindlin family member 4	1.847
55	LRRFIP1	LRR binding FLII interacting protein 1	1.846
56	NDUFS3	NADH:ubiquinone oxidoreductase core subunit S3	1.845
57	SPIN1	spindlin 1	1.843
58	VAMP7	vesicle associated membrane protein 7	1.821
59	DPY19L2P1	DPY19L2 pseudogene 1	1.814
60	ATP6V0A1	ATPase H+ transporting V0 subunit a1	1.801
61	WSB1	WD repeat and SOCS box containing 1	1.768
62	AHSA2		1.745
63	XCL1	X-C motif chemokine ligand 1	1.727
64	PRKAB2	protein kinase AMP-activated non-catalytic subunit beta 2	1.724
65	LOC642533		1.697
66	CD22	CD22 molecule	1.684
67	CYB5R2	cytochrome b5 reductase 2	1.656
68	MRAP2	melanocortin 2 receptor accessory protein 2	1.654
69	CALCOCO1	calcium binding and coiled-coil domain 1	1.653
70	POTEF	POTE ankyrin domain family member F	1.649
71	ELOVL1	ELOVL fatty acid elongase 1	1.582
72	TXLNGY	taxilin gamma pseudogene, Y-linked	1.580

DOWNREGULATED GENES

	Gene symbol	Description	Fold change
1	VTRNA1-1	vault RNA 1-1	0.059
2	RNU4-1	RNA, U4 small nuclear 1	0.068
3	RNU4-2	RNA, U4 small nuclear 2	0.080
4	SNORA38B	small nucleolar RNA, H/ACA box 38B	0.146
5	SCARNA6	small Cajal body-specific RNA 6	0.147
6	RAC1	Rac family small GTPase 1	0.150
7	SNORA20	small nucleolar RNA, H/ACA box 20	0.151
8	GLUD1	glutamate dehydrogenase 1	0.189
9	BGN	biglycan	0.202
10	BCHE	butyrylcholinesterase	0.204
11	SNORA7B	small nucleolar RNA, H/ACA box 7B	0.206
12	C7orf69	chromosome 7 open reading frame 69	0.229
14	RPPH1	ribonuclease P RNA component H1	0.252
15	SCARNA5	small Cajal body-specific RNA 5	0.256
16	RNU5B-1	RNA, U5B small nuclear 1	0.259
17	SNORD15B	small nucleolar RNA, C/D box 15B	0.273
18	RNU5E-1	RNA, U5E small nuclear 1	0.299
20	RPL13	ribosomal protein L13	0.300
21	SNORA49	small nucleolar RNA, H/ACA box 49	0.305
22	RNU4ATAC	RNA, U4atac small nuclear (U12-dependent splicing)	0.306
23	SNORA23	small nucleolar RNA, H/ACA box 23	0.308
24	RPS12	ribosomal protein S12	0.308
25	USMG5		0.309
26	TMEM203	transmembrane protein 203	0.309
27	SCARNA10	small Cajal body-specific RNA 10	0.318
28	BNIP3	BCL2 interacting protein 3	0.322
29	PTGS2	prostaglandin-endoperoxide synthase 2	0.326
30	RPL24	ribosomal protein L24	0.331
31	SNORA80E	small nucleolar RNA, H/ACA box 80E	0.331
32	RAP1B	RAP1B, member of RAS oncogene family	0.333
33	SNORA60	small nucleolar RNA, H/ACA box 60	0.337
34	KLHDC10	kelch domain containing 10	0.345
35	ATL3	atlastin GTPase 3	0.347
36	RPL23P8	ribosomal protein L23 pseudogene 8	0.347
37	SFTA2	surfactant associated 2	0.349
38	SCG2	secretogranin II	0.349
39	RPS27	ribosomal protein S27	0.357
40	AEBP1	AE binding protein 1	0.357
41	SNORA22	small nucleolar RNA, H/ACA box 22	0.366
42	RPL39L	ribosomal protein L39 like	0.366
43	RNU11	RNA, U11 small nuclear	0.368

	Gene symbol	Description	Fold change
44	ACAA1	acetyl-CoA acyltransferase 1	0.369
45	SNORA2A	small nucleolar RNA, H/ACA box 2A	0.370
46	SNORD105	small nucleolar RNA, C/D box 105	0.375
47	RPS7	ribosomal protein S7	0.382
48	EVI2A	ecotropic viral integration site 2A	0.387
49	TBCA	tubulin folding cofactor A	0.387
50	SNORD46	small nucleolar RNA, C/D box 46	0.389
51	RAB23	RAB23, member RAS oncogene family	0.390
52	ZBTB38	zinc finger and BTB domain containing 38	0.395
53	FAM175A		0.396
54	COX7B	cytochrome c oxidase subunit 7B	0.400
55	ARHGAP24	Rho GTPase activating protein 24	0.403
56	TXN	thioredoxin	0.406
57	KRCC1	lysine rich coiled-coil 1	0.406
58	HERC4	HECT and RLD domain containing E3 ubiquitin protein ligase 4	0.410
59	ZNF518A	zinc finger protein 518A	0.412
60	IGF1R	insulin like growth factor 1 receptor	0.416
61	SNORD94	small nucleolar RNA, C/D box 94	0.417
62	BBS12	Bardet-Biedl syndrome 12	0.419
63	STAG1	stromal antigen 1	0.424
64	FANCF	FA complementation group F	0.429
65	RPS27A	ribosomal protein S27a	0.430
66	RPS24	ribosomal protein S24	0.430
67	SNRPE	small nuclear ribonucleoprotein polypeptide E	0.430
68	SKIL	SKI like proto-oncogene	0.432
69	DNAH14	dynein axonemal heavy chain 14	0.436
70	DDIT4	DNA damage inducible transcript 4	0.439
71	LSM14B	LSM family member 14B	0.445
72	RPL10A	ribosomal protein L10a	0.445
73	TNS3	tensin 3	0.445
74	RPS6	ribosomal protein S6	0.447
75	ASCC1	activating signal cointegrator 1 complex subunit 1	0.447
76	SCARNA7	small Cajal body-specific RNA 7	0.448
77	MMP16	matrix metallopeptidase 16	0.448
78	NME7	NME/NM23 family member 7	0.449
79	PUS7	pseudouridine synthase 7	0.450
80	CHCHD1	coiled-coil-helix-coiled-coil-helix domain containing 1	0.450
81	POP5	POP5 homolog, ribonuclease P/MRP subunit	0.451
82	IFIT2	interferon induced protein with tetratricopeptide repeats 2	0.451
83	NPM1	nucleophosmin 1	0.451
84	SLC29A4	solute carrier family 29 member 4	0.453

	Gene symbol	Description	Fold change
85	RPL23AP32	ribosomal protein L23a pseudogene 32	0.456
86	ADSS		0.457
87	C5	complement C5	0.457
88	MRTO4	MRT4 homolog, ribosome maturation factor	0.458
89	LBH	LBH regulator of WNT signaling pathway	0.469
90	SLIT3	slit guidance ligand 3	0.469
91	THAP2	THAP domain containing 2	0.471
92	STK19	serine/threonine kinase 19	0.473
93	OCR1		0.474
94	DCUN1D1	defective in cullin neddylation 1 domain containing 1	0.475
95	GIMAP2	GTPase, IMAP family member 2	0.475
96	DHRS7	dehydrogenase/reductase 7	0.476
97	WDR78	WD repeat domain 78	0.477
98	PPP3CB	protein phosphatase 3 catalytic subunit beta	0.480
99	BLVRA	biliverdin reductase A	0.482
100	ADCK2	aarF domain containing kinase 2	0.482
101	RRP15	ribosomal RNA processing 15 homolog	0.484
102	RPS4Y1	ribosomal protein S4 Y-linked 1	0.485
103	EHHADH	enoyl-CoA hydratase and 3-hydroxyacyl CoA dehydrogenase	0.485
104	ZNF770	zinc finger protein 770	0.488
105	MRPS33	mitochondrial ribosomal protein S33	0.488
106	MRPL36	mitochondrial ribosomal protein L36	0.489
107	THNSL1	threonine synthase like 1	0.490
108	GDF15	growth differentiation factor 15	0.490
109	PFDN6	prefoldin subunit 6	0.491
110	CEP19	centrosomal protein 19	0.492
111	IARS2	isoleucyl-tRNA synthetase 2, mitochondrial	0.493
112	MERTK	MER proto-oncogene, tyrosine kinase	0.494
113	SLMO2		0.495
114	CENPBD1P1	CENPB DNA-binding domains containing 1 pseudogene 1	0.496
115	OARD1	O-acyl-ADP-ribose deacylase 1	0.496
116	PINK1-AS	PINK1 antisense RNA	0.496
117	ZNF271		0.497
118	PSMB7	proteasome 20S subunit beta 7	0.497
119	FAM35A		0.499
120	IFT81	intraflagellar transport 81	0.505
121	JPX	JPX transcript, XIST activator	0.505
122	VTRNA1-3	vault RNA 1-3	0.507
123	LOC100132167		0.509
124	MRPL24	mitochondrial ribosomal protein L24	0.509
125	MRPL1	mitochondrial ribosomal protein L1	0.511

	Gene symbol	Description	Fold change
126	HIST1H2BB		0.516
127	IKBIP	IKBKB interacting protein	0.521
128	ZNF654	zinc finger protein 654	0.524
129	CCDC58	coiled-coil domain containing 58	0.525
130	MRPS23	mitochondrial ribosomal protein S23	0.525
131	P4HA1	prolyl 4-hydroxylase subunit alpha 1	0.526
132	CSPG4	chondroitin sulfate proteoglycan 4	0.526
133	TOR1AIP2	torsin 1A interacting protein 2	0.526
134	BEND6	BEN domain containing 6	0.530
135	MRPS36	mitochondrial ribosomal protein S36	0.534
136	MOCOS	molybdenum cofactor sulfurase	0.535
137	LTBP1	latent transforming growth factor beta binding protein 1	0.535
138	CD82	CD82 molecule	0.536
139	KDM4C	lysine demethylase 4C	0.538
140	THAP5	THAP domain containing 5	0.538
141	MRPS22	mitochondrial ribosomal protein S22	0.539
142	VEGFA	vascular endothelial growth factor A	0.539
143	IL1RAP	interleukin 1 receptor accessory protein	0.542
144	HOXB7	homeobox B7	0.542
145	ST6GALNAC3	ST6 N-acetylgalactosaminide alpha-2,6-sialyltransferase 3	0.543
146	GRB10	growth factor receptor bound protein 10	0.543
147	EIF3E	eukaryotic translation initiation factor 3 subunit E	0.546
148	CLSTN1	calsyntenin 1	0.546
149	HRSP12		0.548
150	EVI5	ecotropic viral integration site 5	0.549
151	EVI2B	ecotropic viral integration site 2B	0.549
152	CENPF	centromere protein F	0.549
153	YEATS2	YEATS domain containing 2	0.549
154	PFDN5	prefoldin subunit 5	0.551
155	S100A6	S100 calcium binding protein A6	0.551
156	NHP2	NHP2 ribonucleoprotein	0.551
157	CHMP1B	charged multivesicular body protein 1B	0.553
158	RNF130	ring finger protein 130	0.555
159	HLTF	helicase like transcription factor	0.555
160	PPAPDC2		0.556
161	PREX1	phosphatidylinositol-3,4,5-trisphosphate dependent Rac exchange factor 1	0.556
162	SERTAD4	SERTA domain containing 4	0.557
163	GCLM	glutamate-cysteine ligase modifier subunit	0.557
164	HIST1H1C		0.559
165	TMED9	transmembrane p24 trafficking protein 9	0.561
166	FLOT1	flotillin 1	0.562

	Gene symbol	Description	Fold change
167	FAM129A		0.564
168	LPCAT1	lysophosphatidylcholine acyltransferase 1	0.566
169	ZDHHC21	zinc finger DHHC-type palmitoyltransferase 21	0.566
170	PRSS23	serine protease 23	0.567
171	KIAA1586	KIAA1586	0.569
172	EDF1	endothelial differentiation related factor 1	0.569
173	IGSF3	immunoglobulin superfamily member 3	0.569
174	GPD2	glycerol-3-phosphate dehydrogenase 2	0.569
176	PIGN	phosphatidylinositol glycan anchor biosynthesis class N	0.571
177	REEP3	receptor accessory protein 3	0.572
178	MIPEP	mitochondrial intermediate peptidase	0.574
179	DNAJC11	DnaJ heat shock protein family (Hsp40) member C11	0.574
180	RRP36	ribosomal RNA processing 36	0.574
181	ERMP1	endoplasmic reticulum metallopeptidase 1	0.574
182	GFM1	G elongation factor mitochondrial 1	0.575
183	C8orf48	chromosome 8 open reading frame 48	0.576
184	DPH5	diphthamide biosynthesis 5	0.577
185	NIP7	nucleolar pre-rRNA processing protein NIP7	0.580
186	SNORD104	small nucleolar RNA, C/D box 104	0.581
187	RPL39	ribosomal protein L39	0.587
188	MRPL15	mitochondrial ribosomal protein L15	0.588
189	MRPS18A	mitochondrial ribosomal protein S18A	0.588
190	ZNF639	zinc finger protein 639	0.589
191	ROR1	receptor tyrosine kinase like orphan receptor 1	0.589
192	HNRNPF	heterogeneous nuclear ribonucleoprotein F	0.592
193	DMXL1	Dmx like 1	0.592
194	TMEM67	transmembrane protein 67	0.594
195	C18orf32	chromosome 18 open reading frame 32	0.596
196	TUBD1	tubulin delta 1	0.596
197	NDUFS4	NADH:ubiquinone oxidoreductase subunit S4	0.596
198	GPAM	glycerol-3-phosphate acyltransferase, mitochondrial	0.596
199	ATP5A1		0.597
200	CMSS1	cms1 ribosomal small subunit homolog	0.597
201	NSUN3	NOP2/Sun RNA methyltransferase 3	0.599
202	MRPS10	mitochondrial ribosomal protein S10	0.600
203	MDC1	mediator of DNA damage checkpoint 1	0.600
204	PCDHA5	protocadherin alpha 5	0.601
205	EIF2A	eukaryotic translation initiation factor 2A	0.601
206	PRKXP1	PRKX pseudogene 1	0.601
207	ARPC1A	actin related protein 2/3 complex subunit 1A	0.602
208	ZNF322	zinc finger protein 322	0.607
209	IGFBP3	insulin like growth factor binding protein 3	0.609

	Gene symbol	Description	Fold change
210	POLR1E	RNA polymerase I subunit E	0.611
211	ALCAM	activated leukocyte cell adhesion molecule	0.611
212	CARF	calcium responsive transcription factor	0.612
213	PPA1	inorganic pyrophosphatase 1	0.613
214	HEATR1	HEAT repeat containing 1	0.614
215	IFT57	intraflagellar transport 57	0.615
216	CTSL	cathepsin L	0.617
217	AHNAK	AHNAK nucleoprotein	0.618
218	LOXL2	lysyl oxidase like 2	0.620
219	SMC3	structural maintenance of chromosomes 3	0.621
221	ZNF605	zinc finger protein 605	0.623
222	ATR	ATR serine/threonine kinase	0.624
223	TRMT10C	tRNA methyltransferase 10C, mitochondrial RNase P subunit	0.629
224	DNAAF2	dynein axonemal assembly factor 2	0.629
225	UTP14A	UTP14A small subunit processome component	0.630

Supplementary Table 6.
Significantly downregulated genes in resistant melanoma spheroid compare to resistant monolayer grouped by molecular pathways

Pathway identifier	Pathway name	P-Value	FDR Value	Genes included (at least 5)
R-HSA-72766	Translation	2.30E-13	2.00E-10	GFM1, MRPS36, MRPS33, MRPS10, MRPL36, MRPL15, RPS4Y1, RPL10A, MRPL1, RPL13, IARS2, RPS27A, CHCHD1, RPL39, RPS12, EIF2A, RPL39L, RPS7, MRPS22, MRPS23, RPS6, MRPS18A, MRPL24, RPS27, PPA1, RPL24, EIF3E, RPS24
R-HSA-72706	GTP hydrolysis and joining of the 60S ribosomal subunit	1.02E-09	2.96E-07	RPL39L, RPS7, RPS6, RPS4Y1, RPL10A, RPS27, RPL24, RPL13, EIF3E, RPS27A, RPL39, RPS24, EIF2A, RPS12
R-HSA-156827	L13a-mediated translational silencing of Ceruloplasmin expression	1.02E-09	2.96E-07	RPL39L, RPS7, RPS6, RPS4Y1, RPL10A, RPS27, RPL24, RPL13, EIF3E, RPS27A, RPL39, RPS24, EIF2A, RPS12
R-HSA-72689	Formation of a pool of free 40S subunits	1.56E-09	3.38E-07	RPL39L, RPS7, RPS6, RPS4Y1, RPL10A, RPS27, RPL24, RPL13, EIF3E, RPS27A, RPL39, RPS24, RPS12
R-HSA-72613	Eukaryotic Translation Initiation	3.13E-09	4.53E-07	RPL39L, RPS7, RPS6, RPS4Y1, RPL10A, RPS27, RPL24, RPL13, EIF3E, RPS27A, RPL39, RPS24, EIF2A, RPS12
R-HSA-72737	Cap-dependent Translation Initiation	3.13E-09	4.53E-07	RPL39L, RPS7, RPS6, RPS4Y1, RPL10A, RPS27, RPL24, RPL13, EIF3E, RPS27A, RPL39, RPS24, EIF2A, RPS12
R-HSA-156902	Peptide chain elongation	4.31E-09	5.34E-07	RPL39L, RPS27, RPS7, RPS6, RPL24, RPL13, RPS4Y1, RPL10A, RPS27A, RPL39, RPS24, RPS12
R-HSA-975956	Nonsense Mediated Decay (NMD) independent of the Exon Junction Complex (EJC)	7.12E-09	7.68E-07	RPL39L, RPS27, RPS7, RPS6, RPL24, RPL13, RPS4Y1, RPL10A, RPS27A, RPL39, RPS24, RPS12
R-HSA-156842	Eukaryotic Translation Elongation	8.04E-09	7.72E-07	RPL39L, RPS27, RPS7, RPS6, RPL24, RPL13, RPS4Y1, RPL10A, RPS27A, RPL39, RPS24, RPS12
R-HSA-8868773	rRNA processing in the nucleus and cytosol	1.15E-08	9.98E-07	RPL39L, RPS7, NIP7, RPS6, HEATR1, RPS4Y1, RPL10A, RPS27, NHP2, RRP36, RPL24, RPL13, RPS27A, UTP14A, RPL39, RPS24, RPS12
R-HSA-72764	Eukaryotic Translation Termination	1.29E-08	1.02E-06	RPL39L, RPS27, RPS7, RPS6, RPL24, RPL13, RPS4Y1, RPL10A, RPS27A, RPL39, RPS24, RPS12
R-HSA-6791226	Major pathway of rRNA processing in the nucleolus and cytosol	1.62E-08	1.17E-06	RPL39L, RPS7, NIP7, RPS6, HEATR1, RPS4Y1, RPL10A, RPS27, RRP36, RPL24, RPL13, RPS27A, UTP14A, RPL39, RPS24, RPS12

Pathway identifier	Pathway name	P-Value	FDR Value	Genes included (at least 5)
R-HSA-5389840	Mitochondrial translation elongation	2.54E-08	1.67E-06	GFM1, MRPL1, MRPS36, MRPS22, MRPS33, MRPS23, MRPS10, MRPS18A, MRPL36, MRPL15, CHCHD1, MRPL24
R-HSA-2408557	Selenocysteine synthesis	2.83E-08	1.71E-06	RPL39L, RPS27, RPS7, RPS6, RPL24, RPL13, RPS4Y1, RPL10A, RPS27A, RPL39, RPS24, RPS12
R-HSA-192823	Viral mRNA Translation	3.15E-08	1.71E-06	RPL39L, RPS27, RPS7, RPS6, RPL24, RPL13, RPS4Y1, RPL10A, RPS27A, RPL39, RPS24, RPS12
R-HSA-72312	rRNA processing	3.16E-08	1.71E-06	RPL39L, TRMT10C, RPS7, NIP7, RPS6, HEATR1, RPS4Y1, RPL10A, RPS27, NHP2, RRP36, RPL24, RPL13, RPS27A, UTP14A, RPL39, RPS24
R-HSA-1799339	SRP-dependent cotranslational protein targeting to membrane	5.31E-08	2.71E-06	RPL39L, RPS27, RPS7, RPS6, RPL24, RPL13, RPS4Y1, RPL10A, RPS27A, RPL39, RPS24, RPS12
R-HSA-5368287	Mitochondrial translation	6.46E-08	3.10E-06	GFM1, MRPL1, MRPS36, MRPS22, MRPS33, MRPS23, MRPS10, MRPS18A, MRPL36, MRPL15, CHCHD1, MRPL24
R-HSA-72695	Formation of the ternary complex, and subsequently, the 43S complex	7.59E-08	3.41E-06	RPS27, RPS7, RPS6, EIF3E, RPS4Y1, RPS27A, RPS24, EIF2A, RPS12
R-HSA-927802	Nonsense-Mediated Decay (NMD)	8.73E-08	3.58E-06	RPL39L, RPS27, RPS7, RPS6, RPL24, RPL13, RPS4Y1, RPL10A, RPS27A, RPL39, RPS24, RPS12
R-HSA-975957	Nonsense Mediated Decay (NMD) enhanced by the Exon Junction Complex	8.73E-08	3.58E-06	RPL39L, RPS27, RPS7, RPS6, RPL24, RPL13, RPS4Y1, RPL10A, RPS27A, RPL39, RPS24, RPS12
R-HSA-5419276	Mitochondrial translation termination	2.05E-07	7.99E-06	MRPL1, MRPS36, MRPS22, MRPS33, MRPS23, MRPS10, MRPS18A, MRPL36, MRPL15, CHCHD1, MRPL24
R-HSA-5368286	Mitochondrial translation initiation	2.55E-07	9.45E-06	MRPL1, MRPS36, MRPS22, MRPS33, MRPS23, MRPS10, MRPS18A, MRPL36, MRPL15, CHCHD1, MRPL24
R-HSA-72649	Translation initiation complex formation	2.66E-07	9.59E-06	RPS27, RPS7, RPS6, EIF3E, RPS4Y1, RPS27A, RPS24, EIF2A, RPS12
R-HSA-72702	Ribosomal scanning and start codon recognition	3.55E-07	1.21E-05	RPS27, RPS7, RPS6, EIF3E, RPS4Y1, RPS27A, RPS24, EIF2A, RPS12
R-HSA-376176	Signaling by ROBO receptors	3.93E-07	1.30E-05	RPL39L, RPS7, RPS6, RPS4Y1, RPL10A, PSMB7, PPP3CB, RPS27, RPL24, RPL13, SLIT3, RAC1, RPS27A, RPL39, RPS24, RPS12
R-HSA-72662	Activation of the mRNA upon binding of the cap-binding complex and eIFs, and subsequent binding to 43S	4.68E-07	1.50E-05	RPS27, RPS7, RPS6, EIF3E, RPS4Y1, RPS27A, RPS24, EIF2A, RPS12

Pathway identifier	Pathway name	P-Value	FDR Value	Genes included (at least 5)
R-HSA-9010553	Regulation of expression of SLITs and ROBOs	1.65E-06	5.11E-05	RPL39L, RPS7, RPS6, RPS4Y1, RPL10A, PSMB7, RPS27, RPL24, RPL13, RPS27A, RPL39, RPS24, RPS12
R-HSA-168273	Influenza Viral RNA Transcription and Replication	4.83E-06	1.45E-04	RPL39L, RPS27, RPS7, RPS6, RPL24, RPL13, RPS4Y1, RPL10A, RPS27A, RPL39, RPS24, RPS12
R-HSA-2408522	Selenoamino acid metabolism	7.04E-06	2.04E-04	RPL39L, RPS27, RPS7, RPS6, RPL24, RPL13, RPS4Y1, RPL10A, RPS27A, RPL39, RPS24, RPS12
R-HSA-168255	Influenza Life Cycle	1.07E-05	3.00E-04	RPL39L, RPS27, RPS7, RPS6, RPL24, RPL13, RPS4Y1, RPL10A, RPS27A, RPL39, RPS24, RPS12
R-HSA-168254	Influenza Infection	2.00E-05	5.39E-04	RPL39L, RPS27, RPS7, RPS6, RPL24, RPL13, RPS4Y1, RPL10A, RPS27A, RPL39, RPS24, RPS12
R-HSA-8953854	Metabolism of RNA	4.77E-04	0.012393	POP5, NIP7, HEATR1, RPS4Y1, RPL10A, RNU11, PSMB7, RPPH1, RRP36, RPL13, RPS27A, RPL39, RNU4ATAC, UTP14A, RPS12, RPL39L, TRMT10C, RPS7, RPS6, PUS7, RPS27, HNRNPF, NHP2, RPL24, SNRPE, RPS24
R-HSA-6790901	rRNA modification in the nucleus and cytosol	0.001998693	0.047969	RPS7, RPS6, HEATR1, NHP2, RRP36, UTP14A
R-HSA-422475	Axon guidance	0.002322366	0.055737	RPL39L, RPS7, RPS6, ARPC1A, RPS4Y1, RPL10A, PSMB7, PPP3CB, RPS27, ALCAM, GRB10, RPL24, RPL13, SLIT3, RAC1, RPS27A, RPL39, RPS24, RPS12
R-HSA-5663205	Infectious disease	0.004661982	0.107226	RPL39L, NPM1, RPS7, RPS6, RPS4Y1, RPL10A, PSMB7, RPS27, RPL24, RPL13, RAC1, RPS27A, RPL39, RPS24, ATR, RPS12
R-HSA-5693607	Processing of DNA double-strand break ends	0.006266444	0.131595	MDC1, FAM175A, RPS27A, HIST1H2BB, ATR
R-HSA-392499	Metabolism of proteins	0.007341968	0.146839	MDC1, GFM1, PIGN, MRPS10, MRPL36, RPL10A, SMC3, PRSS23, MRPL1, CHCHD1, RPL39, RPS12, EIF2A, TMED9, RPS7, MRPS22, IGFBP3, MRPS23, RPS6, MRPS18A, PPA1, RPL24, ST6GALNAC3, HIST1H2BB, SCG2, PFDN5, PFDN6, MRPS36, MRPS33, DCUN1D1, MRPL15, TXN, RPS4Y1, LTBP1, PSMB7, RAB23, HLTF, RPL13, DPH5, IARS2, RPS27A, RPL39L, BCHE, NPM1, TBCA, MRPL24, STAG1, RPS27, FAM175A, EIF3E, RPS24
R-HSA-69481	G2/M Checkpoints	0.022827267	0.328794	MDC1, PSMB7, FAM175A, RPS27A, HIST1H2BB, ATR

Pathway identifier	Pathway name	P-Value	FDR Value	Genes included (at least 5)
R-HSA-5693567	HDR through Homologous Recombination (HRR)	0.026095622	0.34649	MDC1, FAM175A, RPS27A, HIST1H2BB, ATR
R-HSA-5693538	Homology Directed Repair	0.031766266	0.381195	MDC1, FAM175A, RPS27A, HIST1H2BB, ATR

Supplementary Table 7
List of common altered gene (N=46) between BRAFi sensitive spheroid and resistant spheroid.

No.	Gene symbol	Description	Fold-change (in sensitive spheroids[1])	Fold-change (in resistant spheroid[2])
1	DEFB124	defensin beta 124	1.45	2.63
2	MBD3L5	methyl-CpG binding domain protein 3 like 5	1.90	2.07
3	DDAH1	dimethylarginine dimethylaminohydrolase 1	3.82	2.04
4	UCP2	uncoupling protein 2	2.86	2.04
5	MLF2	myeloid leukemia factor 2	1.32	1.97
6	HIST1H2BM		12.91	1.94
8	SNORA20	small nucleolar RNA, H/ACA box 20	0.31	0.15
9	FAM21C		0.53	0.25
10	RPPH1	ribonuclease P RNA component H1	0.53	0.25
11	SNORD15B	small nucleolar RNA, C/D box 15B	0.33	0.27
12	USMG5		0.39	0.30
13	SNORA49	small nucleolar RNA, H/ACA box 49	0.66	0.31
14	SCARNA10	small Cajal body-specific RNA 10	0.59	0.32
15	PTGS2	prostaglandin-endoperoxide synthase 2	0.22	0.33
16	RPL24	ribosomal protein L24	0.58	0.33
17	KLHDC10	kelch domain containing 10	0.39	0.35
18	SNORD105	small nucleolar RNA, C/D box 105	0.64	0.38
19	EVI2A	ecotropic viral integration site 2A	0.72	0.39
20	SNORD46	small nucleolar RNA, C/D box 46	0.33	0.39
21	IGF1R	insulin like growth factor 1 receptor	0.64	0.42
22	BBS12	Bardet-Biedl syndrome 12	0.66	0.42
23	RPS27A	ribosomal protein S27a	0.53	0.43
24	LSM14B	LSM family member 14B	0.35	0.45
25	MMP16	matrix metallopeptidase 16	0.79	0.45
26	WDR78	WD repeat domain 78	0.24	0.48
27	PFDN6	prefoldin subunit 6	0.51	0.49
28	CENPBD1P1	CENPB DNA-binding domains containing 1 pseudogene 1	0.31	0.50
29	OARD1	O-acyl-ADP-ribose deacylase 1	0.40	0.50
30	FAM35A		0.63	0.50
31	P4HA1	prolyl 4-hydroxylase subunit alpha 1	0.91	0.53
32	CSPG4	chondroitin sulfate proteoglycan 4	0.76	0.53
33	MRPS22	mitochondrial ribosomal protein S22	0.63	0.54
34	ST6GALNAC3	ST6 N-acetylgalactosaminide alpha-2,6-sialyltransferase 3	0.59	0.54

No.	Gene symbol	Description	Fold-change (in sensitive spheroids[1])	Fold-change (in resistant spheroid[2])
35	PFDN5	prefoldin subunit 5	0.49	0.55
36	S100A6	S100 calcium binding protein A6	0.81	0.55
37	CHMP1B	charged multivesicular body protein 1B	0.21	0.55
38	FLOT1	flotillin 1	0.53	0.56
39	SNORD104	small nucleolar RNA, C/D box 104	0.30	0.58
40	DMXL1	Dmx like 1	0.51	0.59
41	MRPS10	mitochondrial ribosomal protein S10	0.77	0.60
42	PRKXP1	PRKX pseudogene 1	0.42	0.60
43	ARPC1A	actin related protein 2/3 complex subunit 1A	0.83	0.60
44	ZNF322	zinc finger protein 322	0.50	0.61
45	CARF	calcium responsive transcription factor	0.56	0.61
46	CEP19	dynein axonemal assembly factor 2	0.73	0.63

[1]*Comparison of gene expression between sensitive spheroids and sensitive monolayer cultures.*
[2]*Comparison of gene expression between resistant spheroids and resistant monolayer cultures.*

Supplementary Figure 1.

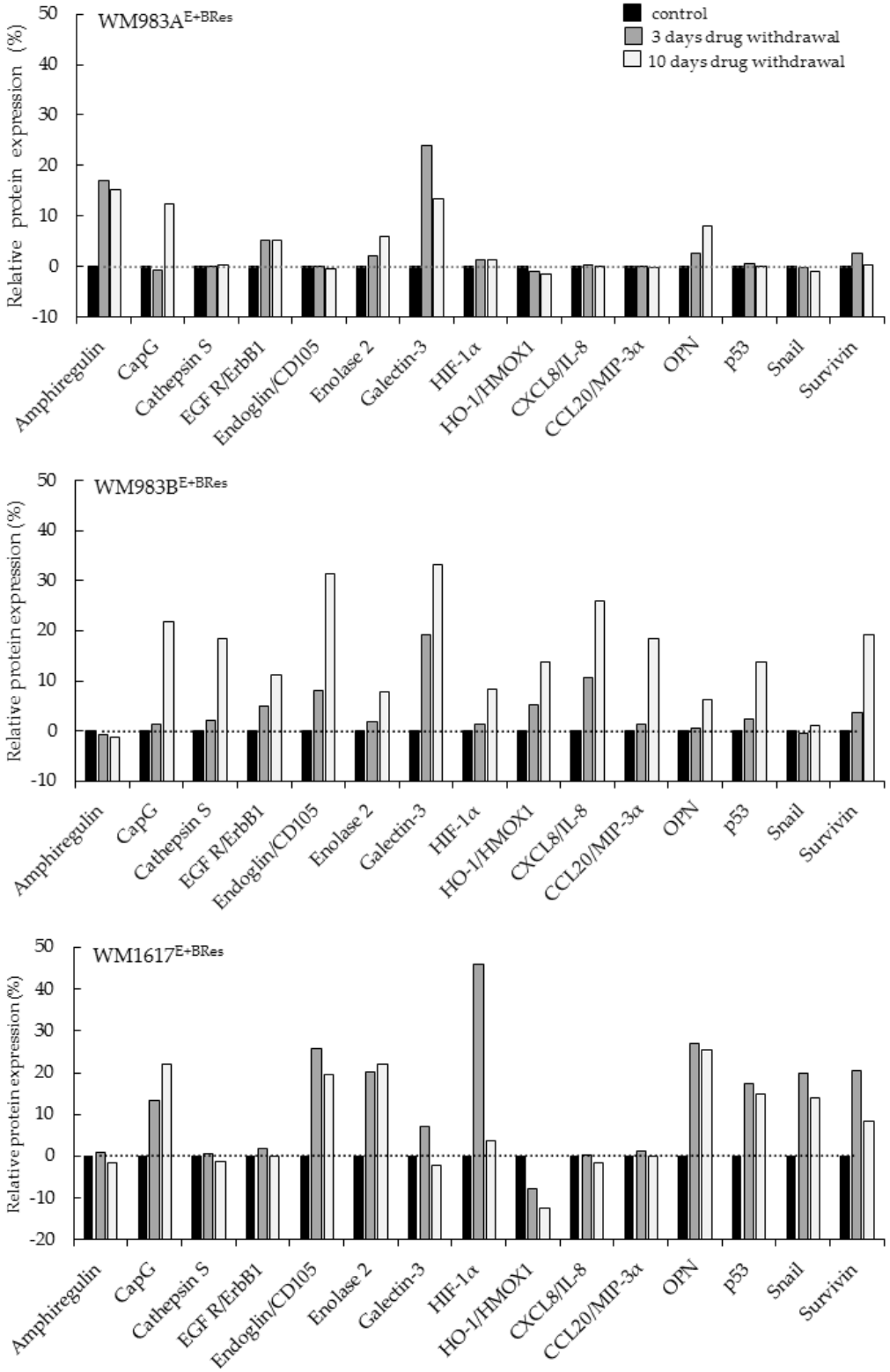

Supplementary Figure 1. Protein expression changes after drug holiday in the resistant melanoma cell lines. Control cells were grown in the presence of 200 nmol/l BRAFi/MEKi mixture (black columns). Drug withdrawal for 3 days (cells grown in the presence DMSO: dark grey columns), drug withdrawal for 10 days drug withdrawal (cells grown in the presence DMSO: light grey columns).

Supplementary table 10.

List of downregulated genes expressed in BRAFi/MEKi resistant cell lines. The top 30 genes are displayed for each cell line.

WM983A^{E+BRes}		WM983B^{E+BRes}		WM278^{E+BRes}		WM1617^{E+BRes}		WM902B^{E+BRes}	
Gene Symbol	Fold change	Gene Symbol	Fold change	Gene Symbol	Fold change	Gene Symbol	Fold change	Gene Symbol	Fold change
PDLIM4	-43,57	CTD-2207A17.1	-23,90	IL1RL1	-18,62	RP11-334J6.7	-20,71	MMP8	-55,22
LPL	-34,14	ITCH	-19,65	NGEF	-17,41	RP11-265N6.1	-19,48	PCDH1	-28,57
CD74	-30,95	RP11-334J6.7	-18,64	MMP1	-14,54	RP11-63M22.2	-17,43	NPPC	-24,13
TF	-28,59	ART3	-12,82	DSCAM	-14,49	RP5-956O18.3	-14,68	ADGRG6	-23,48
SORCS1	-27,90	DMRT2	-12,75	LA16c-390E6.5	-14,34	MAGEA10	-12,34	TGFA	-23,16
ENPP2	-27,83	CTC-250I14.6	-10,94	MRGPRX4	-13,06	AC005301.9	-12,04	FXYD3	-22,50
ADAMTS4	-25,30	TRIM51	-10,74	IL37	-12,84	CACNA2D1	-11,11	SOX10	-22,12
EFS	-23,60	GJA5	-10,43	RP11-59D5__B.2	-12,20	LINC00112	-11,04	GLDC	-21,95
MTND6P22	-22,95	RP11-78A19.3	-9,72	ANO1	-11,26	RP11-294J22.6	-10,60	GJB1	-20,66
EXTL1	-22,20	C15orf54	-9,72	EGR3	-10,27	SAGE1	-10,27	ERBB3	-20,59
CD200	-21,90	TYRP1	-9,69	ESM1	-9,98	RORB	-10,23	RHOJ	-19,90
NTM	-21,90	AP000479.1	-9,12	TRHDE-AS1	-9,85	RP11-229P13.23	-9,64	COL9A3	-18,96
QPRT	-21,85	ALDH1A1	-9,10	ITIH5	-9,30	RP3-468K18.7	-9,49	KCNQ5	-18,58
BAALC	-21,26	LINC01198	-9,06	IRX4	-9,10	CDK14	-9,47	EGR3	-17,18
PPARGC1A	-20,47	ITGB8	-9,05	RP3-430N8.11	-8,85	AC006011.4	-8,96	GRIK2	-16,98
TYRP1	-20,20	GALC	-9,02	TRHDE	-8,39	BCL11A	-8,35	KIAA1549L	-16,47
SIGLEC15	-19,81	MGAM2	-8,76	SLC24A3	-7,95	TEX15	-8,20	HILS1	-16,17
SERPINB2	-19,74	NPPC	-8,74	STC1	-7,68	CT45A10	-8,13	DCT	-15,58
RP11-459E5.1	-18,97	LAYN	-8,63	BTBD11	-7,57	RP11-557C18.3	-7,94	S100B	-15,55
MGAM	-18,13	ICOS	-8,57	GFPT2	-7,02	RP11-334E6.10	-7,91	CTD-2207A17.1	-15,08
NOV	-17,98	CTB-31O20.6	-8,57	AC100802.3	-6,81	COL4A5	-7,58	RNF43	-15,05
DNAJC15	-17,78	COL14A1	-8,49	MRGPRX3	-6,79	EEF1G	-7,40	FAM78B	-14,92
PLCB1	-17,18	RP11-143A12.3	-8,45	HTR7	-6,67	LACTB2-AS1	-7,31	NGFR	-14,91

WM983A^{E+BRes}		WM983B^{E+BRes}		WM278^{E+BRes}		WM1617^{E+BRes}		WM902B^{E+BRes}	
Gene Symbol	**Fold change**	**Gene Symbol**	**Fold change**	**Gene Symbol**	**Fold change**	**Gene Symbol**	**Fold change**	**Gene Symbol**	**Fold change**
RNF128	-17,13	FSTL5	-8,36	RP11-264B14.2	-6,65	LINC01050	-7,27	NFATC2	-14,90
ACAN	-17,07	SHISA9	-8,08	KCNN4	-6,56	CLVS1	-7,08	FREM1	-14,82
CACNA1E	-16,92	RP11-732A19.2	-8,01	LCN2	-6,51	RP11-629N8.5	-7,02	LINC00473	-14,66
C15orf54	-16,90	RP11-120K24.5	-7,85	IGF2BP2-AS1	-6,50	SLC47A1	-6,99	SLC5A4	-14,58
COL22A1	-16,88	SLC18A1	-7,72	SOX8	-6,48	NOX4	-6,91	PMEL	-14,40
SLITRK2	-16,87	TENM3	-7,68	COL4A6	-6,32	EPHA5	-6,86	SLC6A15	-14,08
ABCB4	-16,75	GJB1	-7,58	AJAP1	-6,26	PNLIPRP3	-6,72	MLANA	-14,05

Supplementary table 11.

List of upregulated genes expressed in BRAFi/MEKi resistant cell lines. The top 30 genes are displayed for each cell line

WM983A^{E+BRes}		WM983B^{E+BRes}		WM278^{E+BRes}		WM1617^{E+BRes}		WM902B^{E+BRes}	
Gene Symbol	Fold change	Gene Symbol	Fold change	Gene Symbol	Fold change	Gene Symbol	Fold change	Gene Symbol	Fold change
ALDH3A1	193,05	POSTN	39,73	CRYAB	23,88	REG3G	5,98	CXCL12	65,46
UCHL1	129,53	COL5A1	26,04	RP11-334J6.7	23,28	LHFPL5	5,37	CXCL14	59,9
SPINT2	81,32	TMEM178B	24,15	PAPPA-AS1	21,97	ZNF681	5,05	GLDN	37,06
CXCL5	77,05	FPR3	24,05	CXCL12	21,95	MOXD1	4,77	SOST	35,79
AKR1C3	69,68	CXCL12	22,94	LRRTM4	21,2	SLC2A4	4,57	VCAM1	34,83
WNT7B	65,54	PTGIR	21,5	PRUNE2	21,12	DLX3	4,49	C1S	34,03
MGST1	62,7	ADM	20,43	IL34	20,56	KYNU	4,49	CARD16	33,87
EREG	61,08	SUCNR1	19,75	NXF3	18,92	DUOX2	4,33	FAM65C	33,69
AKR1B10	59,47	LYPD6B	19,54	MPPED2	16,53	RP5-894A10.6	3,99	SLCO2B1	32,31
CPLX2	58,83	C7orf69	19,32	SV2B	15,76	LRP2	3,95	FENDRR	30,96
AKR1B10P1	57,43	SPNS3	18,61	IL32	15,45	MT1G	3,87	OLR1	30,86
AKR1B15	54,76	FENDRR	18,42	CACNA1C	14,9	RP11-680G24.6	3,8	F2RL2	30,85
CLDN2	52,8	RP11-134F2.8	17,96	CPXM2	14,72	DUOXA1	3,71	LBP	27,3
CA12	51,93	IL3RA	17,84	FAM65C	13,62	AL078471.5	3,71	PLXDC2	27,1
CYP24A1	51,58	WDR86	17,56	RP11-626G11.3	12,68	RP1-305B16.3	3,7	TNFRSF11B	26,96
PPP1R14A	48,56	EPHB2	17,38	GABBR1	11,99	TAS2R5	3,69	PAMR1	26,01
RSPO3	48,14	CPA4	16,92	UBD	11,91	RP11-317M11.1	3,59	PTGER3	25,41
MALL	46,6	GPR78	15,86	XAF1	11,59	RPL10P8	3,59	XAF1	24,37
IGFBP4	44,53	SARDH	15,73	MATN2	11,31	LRRTM1	3,47	IFI44L	23,81
EDN1	42,64	RP11-301G19.1	15,72	RP11-805J14.5	10,27	BAGE2	3,37	PLEKHA6	23,53
AKR1C2	41,25	FLNC	15,67	CXCR4	10,27	CST7	3,34	SLA	23
CTB-102L5.4	40,99	PLEKHA6	15,5	RP11-567I13.1	10,04	ZNF257	3,26	WFDC1	22,46

BIRC3	40,5	CPZ	15,5	PALM	9,97	AP000439.1	3,21	TRIM22	21,83
WM983A^{E+BRes}		WM983B^{E+BRes}		WM278^{E+BRes}		WM1617^{E+BRes}		WM902B^{E+BRes}	
Gene Symbol	Fold change	Gene Symbol	Fold change	Gene Symbol	Fold change	Gene Symbol	Fold change	Gene Symbol	Fold change
ALDH2	39,59	BMP5	15,21	SLCO2B1	9,91	CD207	3,19	WISP1	21,81
TNS4	38,99	COL1A1	14,87	CHRNA6	9,62	IGFBP5	3,15	DCLK1	21,78
ADD2	37,66	ZNF467	14,86	CHI3L2	9,6	MMP13	3,11	COL5A1	21,59
GCNT3	36,95	VCAM1	14,61	IDO1	9,55	LINC01060	3,1	TMEM119	21,26
C19orf33	36,48	SOX9	14,27	SEC14L5	9,45	IGFN1	3,07	CLIC2	21,12
SFN	36,01	SAMD11	13,85	FRG2DP	9,21	TPTE	3,05	FOXF1	21,03
BIRC2	34,26	CACNA1G	13,7	CRTAC1	9,2	MRPS33	3,05	SCUBE1	20,48